Optimierung der Therapie von chronischer myeloischer Leukämie mit Hilfe eines dynamischen Modells normaler und leukämischer Stammzellorganisation

Dissertation

zur Erlangung des akademischen Grades

Dr. rer. med.

an der Medizinischen Fakultät

der Universität Leipzig

eingereicht von:

Dipl.-Inf. Matthias Horn

geboren am 5. März 1980 in Leipzig

angefertigt am:

Institut für Medizinische Informatik, Statistik und Epidemiologie

Universität Leipzig

Betreuer:

Prof. Dr. Ingo Röder

Beschluss über die Verleihung des Doktorgrades vom: 21. Oktober 2014

Danksagung

Die vorliegende Arbeit wurde am Institut für Medizinische Informatik, Statistik und Epidemiologie (IMISE) der Universität Leipzig unter der Betreuung von Herrn Prof. Dr. Ingo Röder angefertigt, dem ich hiermit für die engagierte Begleitung und geduldige Unterstützung bei der Bearbeitung des Dissertationsthemas herzlich danken möchte. Auch nach seiner Berufung zum Direktor des Instituts für Medizinische Informatik und Biometrie (IMB) in Dresden war er stets mit unschätzbaren Hinweisen und methodischen Ratschlägen zur Stelle.

Ich bedanke mich bei Herrn Prof. Dr. Markus Löffler, der als Direktor des IMISE trotz seines dicht gefüllten Terminkalenders immer ein offenes Ohr für meine Fragen hatte und mir somit das Gefühl vermittelte, dass ihm das Thema der Dissertation am Herzen liegt. Das von ihm (gemeinsam mit Herrn Röder) konzipierte mathematische Hämatopoese-Modell legte überhaupt erst den Grundstein für die Bearbeitung des Themas.

Weiterhin möchte ich mich bei Herrn Dr. Ingmar Glauche für wertvolle Anregungen und konstruktive Diskussionen betreffs der mathematischen Modellierung bedanken.

Ebenfalls gilt mein Dank Herrn Prof. Dr. Andreas Hochhaus, Herrn Prof. Dr. Martin Müller, Herrn Prof. Dr. Rüdiger Hehlmann sowie Herrn PD Dr. Thoralf Lange für die freundliche Überlassung von klinischen Patientendaten sowie für Erläuterungen zur Biologie der CML.

Bedanken möchte ich mich ferner bei Herrn Lars Thielecke für programmiertechnische Unterstützung bei der Erweiterung des Computerprogramms und zahlreiche Tests desselben.

Ich danke meinen Eltern, Wolfgang Horn und Reinhild Horn, für vielfältige Unterstützung.

Ein ganz besonderer Dank gilt meiner Frau Katrin Horn, die mir für meine Arbeit stets den Rücken frei hielt und dadurch wesentlich zu deren erfolgreichen Abschluss beitrug.

Schließlich möchte ich meine Kinder Pascal Alexander und Isabell Marie um Entschuldigung bitten, dass ihr Papa gelegentlich nicht so viel Zeit für sie übrig hatte wie gewünscht.

Bibliographische Beschreibung

Horn, Matthias

Optimierung der Therapie von chronischer myeloischer Leukämie mit Hilfe eines dynamischen Modells normaler und leukämischer Stammzellorganisation

Universität Leipzig, Dissertation

124 Seiten, 61 Literaturangaben, 13 Abbildungen

Referat:

Unter Verwendung eines mathematischen Hämatopoese-Modells werden verschiedene Fragen adressiert, die im Zusammenhang mit einer möglichen Optimierung der gegenwärtigen Therapie chronischer myeloischer Leukämie (CML) stehen. Es handelt sich um ein agentenbasiertes Modell, das heißt, jede Zelle wird als einzelnes Objekt repräsentiert und gemäß festgelegter Regeln im Computer simuliert. Es werden proliferative von ruhenden Stammzellen unterschieden, wobei sich der Proliferationszustand reversibel ändern kann. Das Modell basiert auf der Annahme, dass sich normale und maligne Stammzellen in einem Wettbewerb um gemeinsame Ressourcen befinden, wobei der CML-Klon einen kompetitiven Vorteil besitzt.

Es ist ungeklärt, ob Tyrosinkinaseinhibitoren wie Imatinib (IM) in der Lage sind, die Erkrankung in jedem Fall zu heilen. Es gibt Evidenz, dass residuale leukämische Stammzellen im Knochenmark persistieren, welche in einem Ruhezustand (G_0-Phase des Zellzyklus) von IM nicht eradiziert werden können. Proliferativ aktive Zellen sind der IM-Wirkung hingegen ausgesetzt. Das Modell sagt voraus, unter welchen Bedingungen eine Kombinationsstrategie von IM mit stammzellaktivierenden Substanzen Synergieeffekte hervorbringen könnte.

Ein verwandtes Problem ist die Frage, in welchen Fällen nach Reduktion der Tumorlast auf ein mittels hochsensitiver Messmethoden undetektierbares Niveau ein Therapieabbruch gerechtfertigt ist. Basierend auf dem dynamischen Modell wird in dieser Arbeit ein Prädiktor vorgeschlagen, der vorhersagt, ob ein Patient nach Abbruch der Therapie einen molekularen Rückfall zu erwarten hat. Zusätzlich wird approximativ ein modellunabhängiger Prädiktor angegeben, der die Vorhersage nur auf Basis klinisch messbarer Größen gestattet.

Inhaltsverzeichnis

Abbildungsverzeichnis

Abkürzungsverzeichnis

ABL	Abelson murine leukemia viral oncogene homolog (Gen auf Chromosom 9)
ABM	agentenbasiertes Modell
AML	akute myeloische Leukämie
Ara-C	Arabinofuranosylcytidin (auch bekannt als Cytarabin)
ATP	Adenosintriphosphat
BCR	breakpoint cluster region (Gen auf Chromosom 22)
BCR-ABL	Fusionsgen aus *BCR* und *ABL* auf dem Ph
CML	chronische myeloische Leukämie
DNA	Desoxyribonukleinsäure
FISH	Fluoreszenz-in-situ-Hybridisierung
G-CSF	Granulozyten-Kolonie stimulierender Faktor
GUS	β-Glucuronidase (Gen auf Chromosom 7)
GvHD	Graft-versus-Host-Krankheit
HSC	hämatopoetische Stammzelle
HU	Hydroxyharnstoff (engl. Hydroxyurea)
IFN-α	Interferon-alpha
IM	Imatinibmesylat (kurz: Imatinib)
IRIS	International Randomized Study of Interferon-α vs. STI571
IS	Internationale Skala
LSC	leukämische Stammzelle
MMR	majore molekulare Remission
MR$^{(x)}$	molekulare Remission (oft mit Angabe der Log-Reduktion)
MRD	minimale Resterkrankung
ODE	gewöhnliche Differentialgleichungen
PCR	Polymerase-Kettenreaktion
Ph	Philadelphia-Chromosom
qRT-PCR	quantitative Echtzeit-Polymerase-Kettenreaktion
RNA	Ribonukleinsäure
STI571	Imatinib-Bezeichnung in der Entwicklungsphase
TKI	Tyrosinkinasehemmer

Every sentence that I utter must be understood

not as an affirmation, but as a question.

Niels Bohr

1. Einführung und Motivation

Chronische myeloische Leukämie (CML) ist eine Erkrankung des hämatopoetischen Systems, die durch eine Mutation in einer einzelnen hämatopoetischen Stammzelle verursacht wird (1). Im Gegensatz zu anderen Leukämien, beispielsweise akuter myeloischer Leukämie (AML) (2), sind CML-Tumorzellen zytogenetisch durch eine einzige chromosomale Aberration, das sogenannte „Philadelphia-Chromosom" gekennzeichnet. Damit wird das verkürzte Chromosom 22 bezeichnet, welches infolge einer Translokation das *BCR-ABL*-Fusionsgen trägt. Dabei handelt es sich um ein Onkogen, das in der Zelle transkribiert wird. Dadurch entsteht ein neues Protein, die BCR-ABL-Tyrosinkinase, welche zu einer unkontrollierten Vermehrung dieser Zelle beiträgt (1). Das BCR-ABL-Fusionsprotein kann in mehr als 90% aller CML-Patienten nachgewiesen werden (3). Basierend auf dieser Tatsache wurden spezielle Tyrosinkinasehemmer (TKI) entwickelt, beginnend im Jahr 1996 mit dem Präparat Imatinib (IM) (4). Man geht davon aus, dass diese Medikamente gezielt in Tumorzellen Apoptose induzieren, normale Zellen im Gegensatz zu chemotherapeutischen Interventionen jedoch kaum negativ beeinflusst werden (5). Durch diesen Einsatz von „zielgerichteter Therapie" („targeted therapy") wurde CML zu einer Modellerkrankung der Tumortherapie insgesamt (6).

Der Einsatz von TKIs führt zu einer massiv verbesserten Prognose der Patienten. So stieg beispielsweise das 5-Jahres-Überleben neudiagnostizierter CML-Patienten von ungefähr 60% (Interferon-α [IFN-α] als medikamentöse Therapie der Wahl in der prä-IM-Ära) (7) auf etwa 90% (IM) an (8). Auch hinsichtlich des Zurückdrängens der Erkrankung, zum Beispiel in Form des Erreichens einer vollständigen zytogenetischen Remission, konnten erhebliche Verbesserungen erzielt werden: Nach 18-monatiger Behandlung betrug der Anteil der Patienten etwa 15% (IFN-α plus niedrig dosiertes Ara-C) bzw. 75% (IM) (9).

Trotz des Erreichens vergleichsweise schneller und tiefer Remissionen mit Hilfe von Tyrosinkinasehemmern bei der Mehrzahl der Patienten ist es nach wie vor unklar, ob mit Hilfe dieser Medikamente eine vollständige „Heilung" der Erkrankung möglich ist. Unter Verwendung hochsensitiver Messmethoden wie quantitativer Echtzeit-Polymerase-Kettenreaktion (qRT-PCR) lassen sich bei vielen Patienten auch noch nach mehreren Behandlungsjahren geringe Tumorzellanteile in peripherem Blut oder Knochenmark detektieren (10). Selbst bei negativer PCR und anschließendem Abbruch der Behandlung kommt es bei einigen Patienten zu einem molekularen Rückfall (11), was darauf hindeutet, dass kleine Tumorklone unterhalb der PCR-Detektionsschwelle persistieren und nach Therapiestopp wieder expandieren können.

Die Ursachen der interindividuellen Heterogenität bezüglich Therapieansprechen sind weitestgehend unverstanden. Folglich ist eine Vorhersage des Langzeittherapieerfolgs bei kontinuierlicher IM-Therapie derzeit nicht möglich. Dies gilt auch für das individuelle Risiko eines molekularen Rückfalls nach Therapieabbruch, falls mittels PCR keine *BCR-ABL*-Transkripte mehr nachweisbar sind. Da es Evidenz dafür gibt, dass sich residuale Leukämiestammzellen (LSCs) in einem dormanten Zustand in so genannten Stammzellnischen, z.B. im Knochenmark, dem TKI-Einfluss entziehen (12), gibt es Bestrebungen, die Therapie mit Substanzen zu kombinieren, welche ruhende Stammzellen in den Zellzyklus aktivieren können (13). Eine Substanz, für die man (im Mausexperiment) stammzellaktivierendes Potenzial zeigen konnte, ist interessanterweise das früher oft als CML-Monotherapie eingesetzte IFN-α (14).

Es ist das Ziel dieser Arbeit mit Hilfe eines dynamischen Modells zur Beantwortung der vorgenannten offenen Fragen und damit zur Optimierung der gegenwärtigen CML-Behandlung beizutragen. Bei dem Modell handelt es sich um ein einzelzellbasiertes Modell der hämatopoetischen Stammzellorganisation. Das Modell wurde ursprünglich von Ingo Röder und Markus Löffler für die Hämatopoese der Maus entwickelt (15). Die Anwendbarkeit des Modells auf die humane Hämatopoese sowie speziell auf CML konnte von mir in meiner Diplomarbeit demonstriert werden (16; 17). Das Modell postuliert eine Dualität zwischen proliferativen und dormanten Stammzellen, welche ihren Zustand reversibel verändern können. Durch die Möglichkeit einzelnen Zellen verschiedene Parameterkonfigurationen zuzuordnen, ist das Modell zur Beschreibung klonaler Kompetitionsphänomene, zum Beispiel in Bezug auf die Kompetition normaler und maligner Zellen um gemeinsame Ressourcen, geeignet.

Die Arbeit ist wie folgt aufgebaut: Zunächst (Abschnitt 1.1) wird in die biologischen Grundlagen eingeführt. Anschließend (Abschnitt 1.2) werden die klinischen Daten vorgestellt, welche für die Modellanalysen zur Verfügung standen. In Abschnitt 1.3 wird das verwendete mathematische Modell erläutert, in 1.4 werden bereits anderweitig publizierte Vorarbeiten dargestellt. Im folgenden Kapitel 2 sind drei Publikationen zu finden, die im Rahmen der Dissertation unter meiner Mitwirkung entstanden. Als Hauptpublikation ist dabei das Anfang 2013 in Blood veröffentlichte Paper (Abschnitt 2.3) anzusehen. Letztere Arbeit wird um zusätzliche Ergebnisse ergänzt, welche im Paper keinen Platz fanden. Jede Publikation wird im entsprechenden Abschnitt kurz zusammengefasst, gefolgt vom formatierten Originalmanuskript (inklusive Supplement). Um die jeweiligen Eigenanteile deutlich zu kennzeichnen, dient Abschnitt 2.4. Die Dissertation wird in Kapitel 3 durch eine Diskussion der wichtigsten Ergebnisse und einen Zukunftsausblick abgeschlossen.

1.1 Biologische Grundlagen

1.1.1 Das humane hämatopoetische System

Hauptaufgabe des hämatopoetischen (blutbildenden) Systems ist die Produktion und Erhaltung (sowie im Falle einer Verletzung die Regeneration) sämtlicher Arten von funktionalen Blut- und Immunzellen. Man unterscheidet dabei verschiedene Linien: rote Blutkörperchen (Erythrozyten), Blutplättchen (Thrombozyten), sowie weiße Blutkörperchen (Leukozyten). Zu letzteren zählen die Immunzellen (lymphoide Linie), darunter T-Lymphozyten und B-Lymphozyten, sowie Granulozyten, Monozyten und Makrophagen. Aufgrund der begrenzen Lebensdauer dieser Zellen (Granulozyten leben weniger als einen Tag, Erythrozyten immerhin etwa vier Monate) muss der kontinuierliche Output dieser Zellen während der gesamten Lebenszeit des Organismus gewährleistet sein (18).

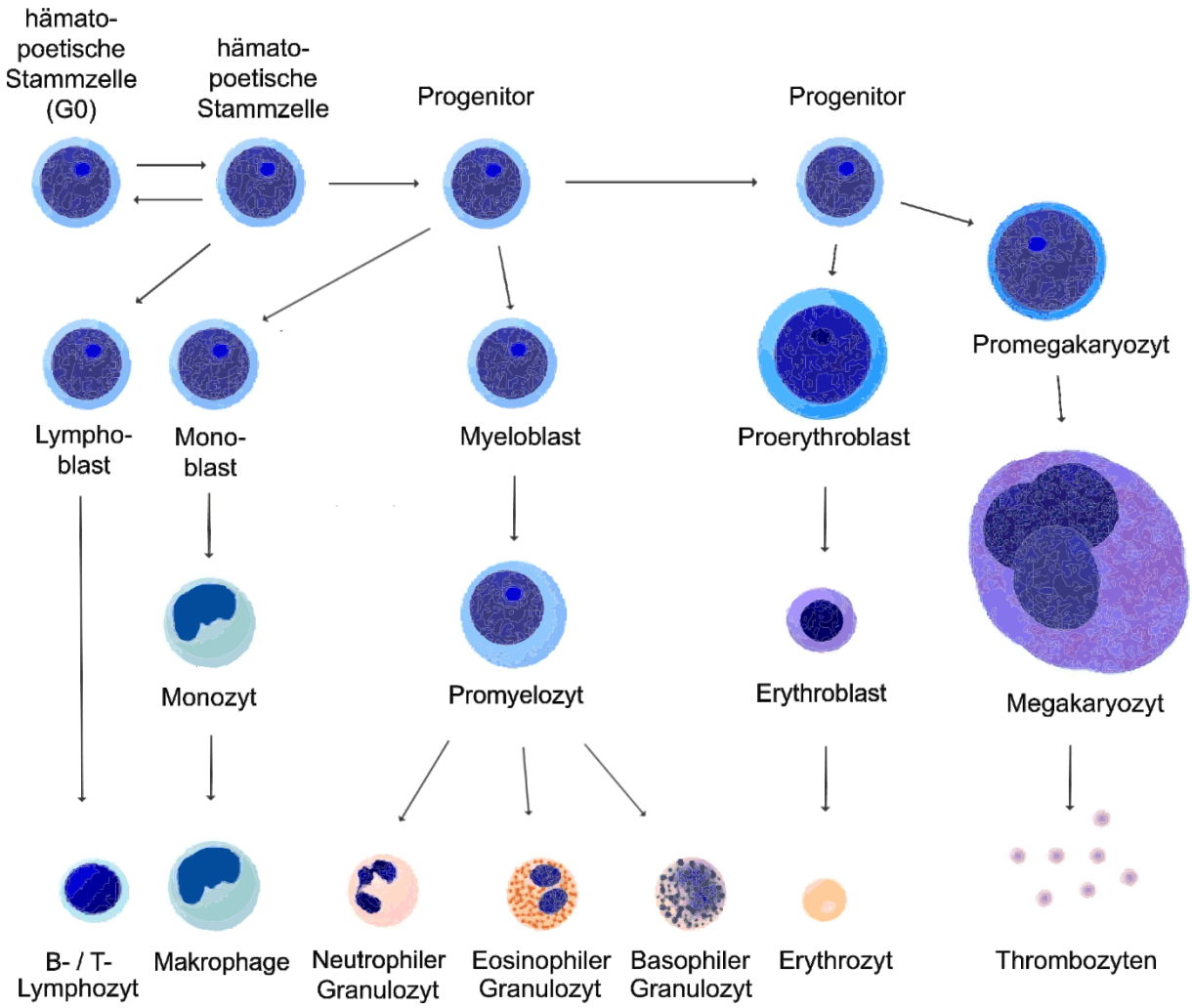

Abbildung 1: Schematische Darstellung der Hämatopoese. Ausgehend von den hämatopoetischen Stammzellen entwickeln sich über Zwischenstufen funktionale Blutzellen.

Die Hämatopoese findet vorwiegend im Knochenmark, aber auch im lymphatischen System oder in der Milz statt. Ausgangszellen für die Produktion sämtlicher funktionaler Blutzellen sind die hämatopoetischen Stammzellen (HSCs). Wie in Abbildung 1 schematisch dargestellt ist, entstehen ausgehend von diesen primitiven, undifferenzierten Zellen über mehrere Zwischenstufen (Progenitor- oder Vorläuferzellen) die entsprechenden Blutzellen (19). Ein hoher kurzfristiger Bedarf an funktionalen Zellen kann auch durch Amplifikation auf Ebene der Vorläuferzellen abgedeckt werden (20).

HSCs verfügen über alle Eigenschaften, die der funktionalen Definition adulter Stammzellen zugrunde liegen: Es handelt sich um eine heterogene Zellpopulation (z.B. in Bezug auf Zellzyklusaktivität oder Repopulationspotenzial) mit der Fähigkeit zu proliferieren, ein große Zahl differenzierter Zellen zu produzieren, ihre Population zu erhalten oder zu erneuern sowie nach Verletzung das hämatopoetische System vollständig zu regenerieren. Zur Ausnutzung des proliferativen und regenerativen Potenzials besteht darüber hinaus eine Abhängigkeit von geeigneten Mikroumgebungen (z.B. Stammzellnischen, vorwiegend im Knochenmark). Schließlich besteht in den vorgenannten Funktionen Flexibilität und Umkehrbarkeit, z.B. in Bezug auf Proliferationsaktivität und Differenzierungsstatus (21).

1.1.2 Chronische myeloische Leukämie (CML)

Chronische myeloische Leukämie (CML) ist eine klonale Störung der Hämatopoese. Die Erkrankung wird durch eine Mutation in einer einzelnen hämatopoetischen Stammzelle induziert, in deren Folge es zu einer malignen Expansion und Überproduktion von zum Teil unreifen myeloischen Blutzellen kommt. Zytogenetisch sind die malignen Zellen durch eine reziproke Translokation der Chromosomen 9 und 22 gekennzeichnet (siehe Abbildung 2). Das verkürzte Chromosom 22 wird „Philadelphia-Chromosom“ (Ph) genannt (22). Als Risikofaktor für das Auftreten der Aberration gilt die Exposition gegenüber ionisierender Strahlung oder bestimmten Chemikalien (23). Infolge der Translokation fusioniert das Gen *BCR* von Chromosom 22 mit *ABL* von Chromosom 9 und bildet das *BCR-ABL*-Onkogen. Bei dessen Genprodukt, dem Fusionsprotein BCR-ABL, handelt es sich um eine konstitutiv aktive Tyrosinkinase, deren Transkription für die CML-Pathogenese sowohl notwendig als auch hinreichend ist. Indem ATP an das Fusionsprotein bindet, werden Tyrosinreste phosphoryliert. Dies aktiviert Signaltransduktionswege, welche für übermäßige Proliferation, aber auch verminderte Apoptose und gestörte Bindung ans Knochenmarkstroma verantwortlich sind (1) (siehe hierzu auch Abbildung 3A).

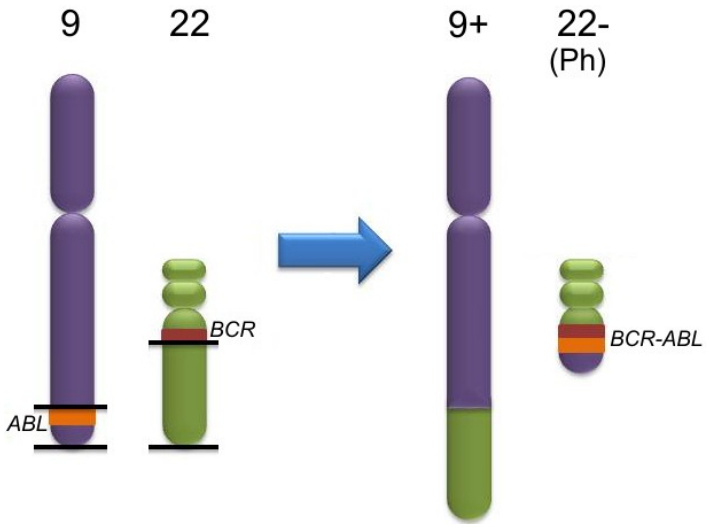

Abbildung 2: Entstehung des Philadelphia-Chromosoms. Durch eine reziproke Translokation der Chromosomen 9 und 22 entsteht das sogenannte Philadelphia-Chromosom (Ph). Auf diesem Chromosom befindet sich das onkogene *BCR-ABL*-Fusionsgen.

Ph-Positivität liegt bei etwa 90% der CML-Patienten vor. Aufgrund anderer, komplexerer chromosomaler Aberrationen ist in der Mehrzahl der fehlenden 10% das *BCR-ABL*-Onkogen dennoch nachweisbar (24). Diese Fälle unterscheiden sich im klinischen Verlauf nicht wesentlich von Ph-positiver CML und werden in dieser Arbeit nicht gesondert besprochen.

CML verläuft klinisch in der Regel in zwei oder drei Phasen. Die allermeisten Patienten werden in der sogenannten chronischen Phase diagnostiziert. Diese ist durch eine lange Latenzzeit von etwa fünf bis sieben Jahren und eine Koexistenz von normalen und malignen Zellen gekennzeichnet. Für diese Phase sind Milzvergrößerung (Splenomegalie) sowie die Überproduktion weißer Blutzellen (Leukozytose), mit oft mehr als 30.000 pro Mikroliter Blut, charakteristisch. Ebenso werden im peripheren Blut unreife Vorläuferzellen der myeloischen Linie (Myeloblasten) gefunden. An die chronische Phase schließt sich in der Regel die Akzelerationsphase an, in der sich die Zahl der Leukozyten pro Volumeneinheit weiter erhöht, die Milz weiter vergrößert und der Blastenanteil im peripheren Blut bereits bis zu 30% beträgt. Auch eine progrediente Thrombozytose und Anämie sind oft zu beobachten. An die Akzelerationsphase (manchmal auch direkt an die chronische Phase) schließt sich die Blastenkrise an. Bei dieser terminalen Phase der Erkrankung, welche unbehandelt innerhalb weniger Wochen tödlich verläuft, beträgt der Blastenanteil im peripheren Blut mehr als 30%. Das Erscheinungsbild in dieser Phase entspricht dem einer akuten Leukämie.

Auch wenn CML durch eine einzige chromosomale Aberration gekennzeichnet ist, kommt es im Verlauf der Erkrankung dennoch häufig zu klonaler Evolution. Von besonderer klinischer Relevanz sind hierbei Mutationen der *BCR-ABL*-Kinasedomäne, da sie zu Therapieresistenz führen können (25). Der Aminosäureaustausch im Onkoprotein ist für die jeweilige Mutation namensgebend, wobei die Position im Molekül und die Einbuchstaben-Abkürzungen der beteiligten Aminosäuren angegeben werden. So bedeutet T315I, dass Threonin an Position 315 durch Isoleucin ersetzt wird. In Folge des Selektionsdrucks tumorspezifischer Medikamente wie Tyrosinkinasehemmer expandieren die mutierten Klone unter Therapie. Es ist noch ungeklärt, ob die Sekundärmutationen stets (auf undetektierbarem Niveau) präexistieren oder teilweise erst während der Therapie entstehen (26).

1.1.3 Messungen der Tumorlast

Hauptmerkmal einer erfolgreichen CML-Therapie ist das Zurückdrängen der malignen Zellen zugunsten einer normalen Hämatopoese. Um den Therapieerfolg zu quantifizieren, gibt es verschiedene Möglichkeiten. Gelingt es, unter Therapie die Leukozytenzahl im peripheren Blut auf unter 10.000 pro Mikroliter zu senken, während gleichzeitig auch Thrombozytenzahl und Milzgröße wieder normale Werte aufweisen, spricht man von einer kompletten hämatologischen Remission. Eine partielle hämatologische Remission ist erreicht, wenn die Leukozytenzahl auf unter 20.000 pro Mikroliter Blut sinkt.

Eine andere Möglichkeit, die Tumorlast zu bestimmen, besteht in der Zytogenetik. Dabei werden mindestens 20 Knochenmarkzellen in der Metaphase lichtmikroskopisch auf das Vorhandensein des Philadelphia-Chromosoms untersucht und dabei der Anteil der malignen Zellen an der Gesamtanzahl der untersuchten Zellen bestimmt. Zum Diagnosezeitpunkt beträgt dieser Anteil fast immer 100%. Eine komplette zytogenetische Remission liegt vor, wenn keine einzige der untersuchten Zellen mehr Ph-positiv ist. Beträgt der Anteil der Tumorzellen maximal 35%, spricht man von einer partiellen zytogenetischen Remission.

Darüber hinaus existieren mehrere molekulare Methoden zur Bestimmung der Tumorlast, welche deutlich sensitiver als zytogenetische Untersuchungen sind, z.B. Fluoreszenz-in-situ-Hybridisierung (FISH), Southern Blot oder Western Blot. Für diese Arbeit wesentlich ist die Polymerase-Kettenreaktion (PCR). Mit diesem Assay lassen sich sehr kleine Mengen bestimmter Nukleotidsequenzen detektieren. Dabei wird im Allgemeinen ein kurzer, wohldefinierter Abschnitt eines DNA-Strangs amplifiziert, das heißt mit sogenannten Primern enzymatisch repliziert. Primer sind kurze artifizielle DNA-Segmente, welche komplementär zum

Anfang und zum Ende des zu vervielfältigenden DNA-Fragments sind. Zunächst werden die Wasserstoffbrückenbindungen zwischen beiden Strängen der DNA aufgelöst, so dass diese separiert vorliegen. Danach können sich die Primer an die Einzelstränge anlagern. Schließlich werden die fehlenden Nukleotide mit Hilfe der DNA-Polymerase aufgefüllt. Um die Sensitivität der Methode noch weiter zu erhöhen, kann eine sogenannte „Nested PCR" durchgeführt werden. Dabei werden im Wesentlichen zwei PCRs hintereinander geschaltet. Bei der CML handelt es sich bei dem zu amplifizierenden DNA-Abschnitt in der Regel um das *BCR-ABL*-Fusionsgen oder eine deren mutierten Varianten (27).

Da die Standard-PCR keine Quantifizierung der Tumorlast ermöglicht, wurden Methoden wie die quantitative Echtzeit-PCR (qRT-PCR) entwickelt, mit deren Hilfe die Menge eines bestimmten DNA- oder RNA-Moleküls innerhalb einer Probe bestimmt werden kann. Dabei werden in die DNA fluoreszierende Farbstoffe eingelagert, was als Interkalation bezeichnet wird. Je stärker die Fluoreszenz-Emission, das heißt, je mehr Licht von den Farbstoffen reflektiert wird, desto höher ist die Konzentration des entsprechenden genetischen Materials.

Der ermittelte Wert wird ausschließlich relativ zu einem im selben Assay gemessenen Kontrollgen angegeben, um eventuelle Schwankungen bei der Genauigkeit der DNA-Transkription oder der Qualität der Nukleinsäuren zu kompensieren. Bei der CML werden am häufigsten *BCR*, *ABL* oder *GUS* verwendet. Um die Ergebnisse verschiedener Labore vergleichen zu können, wird der gemessene Tumoranteil (z.B. *BCR-ABL/ABL*) in einem weiteren Normalisierungsschritt auf die sogenannte Internationale Skala (IS) umgerechnet (28). Hierbei wird der ermittelte Wert mit einem laborspezifischen Faktor multipliziert. Mit Hilfe der qRT-PCR lässt sich etwa eine CML-Zelle in einem Hintergrund von 10^5 Blutzellen detektieren (10; 29).

Bei einer Reduktion der Tumorlast um drei Logstufen ist von einer majoren molekularen Remission (MMR) die Rede. Noch tiefere Remissionen werden in der Form MR^x geschrieben, wobei „x" die Reduktion in Logstufen bezüglich Baseline-Level angibt. Bei $MR^{4,5}$ sinkt die Tumorlast z.B. um 4,5 Logstufen auf 0,0032% (nach IS). Sind mittels qRT-PCR keine *BCR-ABL*-Transkripte nachweisbar, spricht man von einer kompletten molekularen Remission.

Da die Sensitivität zwischen verschiedenen Assays unterschiedlich sein kann, geht einer qRT-PCR-Messung häufig eine Plasmid-Verdünnungsreihe voraus. Dabei wird die kleinste absolute Anzahl an *BCR-ABL*-Transkripten bestimmt, die gerade noch detektierbar ist. Falls bei der Messung der Tumorlast mit qRT-PCR keine *BCR-ABL*-Transkripte detektiert werden, kann zusätzlich eine Nested PCR durchgeführt werden. Da es sich hierbei um eine qualitative

Methode handelt, wird bei Detektion des Onkoproteins für die Berechnung des Tumoranteils der Zähler (*BCR-ABL*) durch die kleinste positive *BCR-ABL*-Kopienzahl aus der Verdünnungsreihe ersetzt. Damit wird der unbekannte wahre Wert durch eine obere Schranke approximiert. Im Fall einer negativen (oder nicht durchgeführten) Nested PCR wird der *BCR-ABL*-Transkriptlevel als null angenommen.

Die in dieser Arbeit verwendeten klinischen Daten der IRIS- und CML-IV-Studie (siehe Abschnitt 1.2) wurden ebenfalls in der vorgenannten Weise normalisiert. Der laborspezifische Faktor der zur Universität Heidelberg gehörenden medizinischen Fakultät Mannheim beträgt 0,878 für *BCR-ABL/ABL* < 10%, ansonsten 1. Messwerte mit sehr niedriger Sensitivität (absolute Anzahl der *ABL*-Transkripte < 1.000) wurden ebenso wie Werte mit einem Transkriptlevel von null für die mathematischen Anpassungen nicht berücksichtigt.

1.1.4. Therapie der CML

Unbehandelt ist CML eine tödliche Krankheit. Die derzeit einzige bekannte Heilungsmöglichkeit der Erkrankung besteht in der Transplantation von Knochenmark oder Stammzellen. Hierfür werden ein passender Spender (allogene Transplantation) oder nichtmaligne Stammzellen des Patienten (autologe Transplantation) benötigt. Häufig liegt beides nicht vor. Darüber hinaus ist die Prozedur mit einer erhöhten Frühmortalitätsrate bzw. Folgeerkrankungen wie chronischer Graft-versus-Host-Krankheit (GvHD) assoziiert. Es gibt jedoch medikamentöse Therapien, von denen die wichtigsten im Folgenden dargestellt werden.

Hydroxyharnstoff (HU)

Bei HU handelt es sich um ein Zytostatikum, das etwa ab den 60er Jahren des vorigen Jahrhunderts eingesetzt wurde. Es wirkt spezifisch auf Zellen in S-Phase, unabhängig von deren Genotyp. Durch Inhibition der Ribonukleotidreduktase blockiert das Medikament die DNA-Synthese. Dadurch wird die Proliferation der Zellen verhindert, was schließlich zu Apoptose führt (30). Bedingt durch diesen Mechanismus kann in den meisten Patienten eine schnelle hämatologische Remission induziert werden, allerdings werden zytogenetische Remissionen fast nie beobachtet. Das mediane Überleben unter HU-Monotherapie beträgt etwa viereinhalb Jahre (31). Auch heute wird HU noch vereinzelt eingesetzt, allerdings vorwiegend als Initialtherapie zur schnellen Reduktion der Leukozytenzahl.

Interferon-α (IFN-α)

IFN-α ist ein natürliches Zytokin, das von Zellen des Immunsystems, z.B. Monozyten oder Lymphozyten, als Reaktion auf das Vorhandensein von Tumorzellen oder Pathogenen produziert wird. Künstliches IFN-α wurde ab Mitte der 1980er Jahre als Therapie der chronischen Phase eingesetzt, teilweise in Kombination mit niedrig dosierten Zytostatika wie Ara-C. Die genaue Wirkungsweise des Medikaments ist dabei nicht abschließend geklärt. Sicher ist, dass IFN-α einen immunstimulierenden Effekt besitzt, indem es CML-Zellen für das Immunsystem „sichtbar" macht (32). Möglicherweise wird dadurch die gestörte Bindung an stromale Knochenmarkzellen normalisiert (33). Ebenso wird vermutet, dass IFN-α die Expression des *BCR-ABL*-Onkogens herunterreguliert (34). Wie in randomisierten Studien gezeigt, ist IFN-α-Monotherapie einer HU-Therapie überlegen, beispielsweise hinsichtlich Überleben, welches unter IFN-α im Median fünfeinhalb Jahre beträgt. Hämatologische Remissionen können in der Mehrzahl der Patienten induziert werden, oft jedoch langsamer als unter HU. Allerdings sind zytogenetische Remissionen zu beobachten, von denen etwa 10% komplett und stabil sind (7).

Als Folge der Beobachtung von Resistenzen gegenüber Tyrosinkinasehemmern (TKI; siehe nächster Abschnitt) hat IFN-α in den letzten Jahren wieder an Bedeutung gewonnen (35). Es gibt Evidenz für einen synergistischen Effekt des Medikaments in Kombination mit TKI, der zu einer Überlegenheit im Vergleich zu TKI-Monotherapie führt (36; 37). Als Ursache hierfür kommt neben der Immunstimulation noch ein zweiter Effekt in Frage: Im Mausexperiment konnte gezeigt werden, dass IFN-α ruhende (d.h. in G_0-Phase befindliche) hämatopoetische Stammzellen in den aktiven Zellzyklus aktivieren kann (14). Da angenommen wird, dass dormante LSCs für eine persistierende minimale Resterkrankung (MRD) unter TKI-Therapie verantwortlich sind (12), könnte eine Rolle für IFN-α darin bestehen, diese Zellen zu aktivieren, wodurch sie der TKI-Wirkung ausgesetzt werden. Für diese Überlegungen limitierend wirken sich jedoch die starken Nebenwirkungen der Kombinationstherapie aus. Darum wird in aktuellen Studien fast ausschließlich auf pegyliertes IFN-α, welches aufgrund einer längeren Halbwertszeit nur wöchentlich oder seltener verabreicht werden muss, zurückgegriffen.

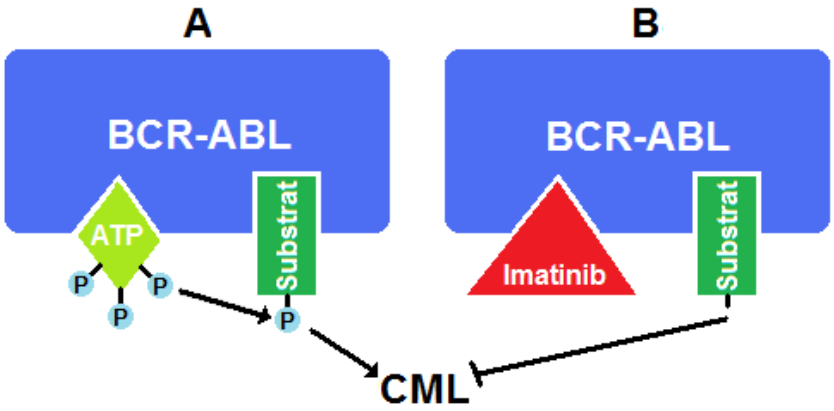

Abbildung 3: Molekularer Wirkmechanismus von Imatinib. A) CML-Mechanismus: Indem Substratmoleküle der BCR-ABL-Tyrosinkinase phosphoryliert werden, werden Signaltransduktionswege aktiviert, die für die CML-Pathogenese verantwortlich sind. B) Imatinib-Mechanismus: Indem Imatinib die ATP-Bindungstasche besetzt, können die Substratmoleküle nicht mehr phosphoryliert werden, wodurch die onkogenen Signalwege blockiert werden.

Tyrosinkinasehemmer (TKI)

Bei TKIs handelt es sich um Medikamente, die gezielt die BCR-ABL-Tyrosinkinase inhibieren. Das erste Medikament dieser Art war ab dem Ende der 1990er Jahre das zunächst als STI571 bezeichnete Imatinibmesylat (IM; kurz: Imatinib) (4). Der Wirkmechanismus, welcher in Abbildung 3 schematisch dargestellt ist, ist für alle bislang entwickelten TKIs im Wesentlichen identisch. Während in Abwesenheit des Medikaments ATP an das Onkoprotein binden und dadurch Substratmoleküle der BCR-ABL-Tyrosinkinase phosphorylieren kann (Abbildung 3A), blockiert IM die ATP-Bindungstasche und verhindert damit die Phosphorylierung des Substrats (Abbildung 3B). Das phosphorylierte Substratmolekül aktiviert onkogene Signaltransduktionswege, welche unter anderem eine unregulierte Proliferation, eine reduzierte Apoptoserate und eine gestörte Bindung ans Knochenmarkstroma bewirken (38). Obwohl diese Mechanismen auf molekularer Ebene gut verstanden sind, sind es die resultierenden dynamischen Effekte auf CML-Zellen nicht. Klar ist, dass IM selektiv auf *BCR-ABL*-positive Zellen wirkt und deren Proliferation hemmt (39). Strittig ist, ob IM in Leukämiezellen Apoptose induziert. Da man in diesen Zellen eine erhöhte Apoptoserate beobachtet (40), ist die Frage, ob es sich um einen direkten oder indirekten Effekt, z.B. durch Abschwächung der Apoptoseinhibition, handelt. Darüber hinaus gibt es Evidenz in Form von *in-vitro*-Experimenten, dass dormante LSCs von IM nicht

angegriffen werden (12). Ein Hinweis darauf ist auch, dass klinisch nach vielen Behandlungsjahren residuale CML-Zellen beobachtet werden (10) bzw. dass bei einigen Patienten in kompletter molekularer Remission nach Therapiestopp ein molekularer Rückfall auftritt (11).

Für IM-Monotherapie konnte eine signifikante Überlegenheit gegenüber IFN-α hinsichtlich Remissionen und Überleben demonstriert werden, auch in akzelerierter Phase und Blastenkrise (9). Bei fast allen Patienten können schnelle hämatologische und zytogenetische Remissionen induziert werden (41). Bereits nach 12-monatiger Therapie weisen etwa 40% der Patienten eine MMR auf (42). Der Abfall der *BCR-ABL*-Transkriptlevel unter IM-Therapie ist bei den meisten Patienten durch einen biphasischen Verlauf (auf der logarithmischen Skala) gekennzeichnet: Während ungefähr im ersten Therapiehalbjahr ein sehr steiler Abfall zu beobachten ist, kommt es in der Folge zu einem deutlichen Abschwächen der Tumorlastreduktion (43). Ein typischer Verlauf ist in Abbildung 4 zu sehen. Man geht davon aus, dass der steile initiale Abfall durch die schnelle Elimination proliferierender *BCR-ABL*-positiver Zellen erklärt wird, während die abgeschwächte zweite Phase Ausdruck der langsamen Elimination residualer LSCs ist (17). Hierfür ursächlich ist vermutlich, dass ruhende Knochenmarkzellen nur vergleichsweise selten in den Zyklus aktiviert werden (19).

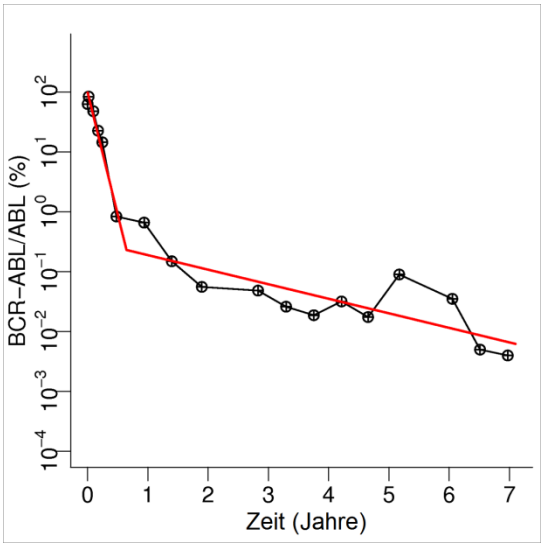

Abbildung 4: Biphasischer Abfall der *BCR-ABL*-Transkriptlevel unter IM-Monotherapie. Schwarze Kreise repräsentieren Datenpunkte (Messungen der Tumorlast mittels qRT-PCR) eines typischen Beispielpatienten. Die roten Linien entstammen einem biphasischen Regressionsmodell und dienen der Verdeutlichung der beobachteten Dynamik.

Trotz der erheblichen Verbesserungen in Bezug auf Ansprechen und Überleben im Vergleich zu früheren Standardtherapien, besteht ein wesentliches Problem der IM-Therapie im Auftreten von Resistenzen gegenüber dem Medikament. Die wichtigsten Resistenzmechanismen sind hierbei die Überexpression von *BCR-ABL* sowie Punktmutationen in der Kinasedomäne des Onkogens (44). Der letztgenannte Mechanismus, der ursächlich für etwa 40% der beobachteten Resistenzen ist, bewirkt eine Konformationsänderung der ATP-Bindungstasche, was eine Bindung des IM-Moleküls erschwert bzw. verhindert. Das Auftreten von IM-Resistenzen sowie IM-Unverträglichkeit führte zur Entwicklung sogenannter TKIs der zweiten Generation. Hierzu zählen Dasatinib und Nilotinib. Beide Medikamente sind inzwischen für CML-Behandlung zugelassen und werden voraussichtlich in Kürze IM als Therapie der Wahl bei *de-novo*-CML ablösen. Sie sind wirksam gegenüber den meisten IM-resistenten Klonen (außer T315I) und IM in randomisierten prospektiven Studien in Bezug auf das Erreichen kompletter zytogenetischer sowie majorer molekularer Remissionen signifikant überlegen (45; 46). Da auch bei Gabe von TKIs der zweiten Generation Resistenzen auftreten und insbesondere der aggressive Mutant T315I mit einer sehr schlechten Prognose assoziiert ist, befinden sich zur Zeit TKIs der dritten Generation in der klinischen Prüfung. Hierzu zählen Bosutinib und Ponatinib. Letztere Substanz inhibiert auch den T315I-Mutanten effektiv (47).

1.2 Klinische Patientendaten

Für die in diese Arbeit eingeschlossenen Publikationen standen Patientendaten in anonymisierter Form aus zwei verschiedenen CML-Studien zur Verfügung. Konkret handelt es sich bei den Daten um individuelle Zeitverläufe der mittels qRT-PCR gemessenen Tumorlast in Form des Quotienten *BCR-ABL* geteilt durch *ABL*. Wie im Abschnitt „Messungen der Tumorlast“ erläutert, wurde bei negativer PCR häufig zusätzlich eine hochsensitive qualitative PCR (Nested PCR) durchgeführt und bei positivem Ergebnis eine obere Schranke für den unbekannten wahren *BCR-ABL/ABL*-Wert angegeben.

1.2.1 IRIS-Studie

Bei der “International Randomized Study of IFN-α vs. STI571” (IRIS) handelt es sich um eine prospektive zweiarmige randomisierte Phase-III-Therapiestudie, deren Ziel in einem Vergleich von IFN-α (plus niedrig dosiertem Ara-C) und IM-Monotherapie bei neudiagnostizierten CML-Patienten lag (41). Primärer Endpunkt war Krankheitsprogression, die neben Tod jedweder Ursache den Übergang in akzelerierte Phase oder Blastenkrise sowie den Verlust zuvor erreichter Remissionen einschloss. Sekundäre Endpunkte waren das Erreichen kompletter hämatologischer und partieller bzw. kompletter zytogenetischer Remission sowie Sicherheit und Verträglichkeit. Die Gesamtanzahl der weltweit eingeschlossenen Patienten betrug 1.106, gleichverteilt auf beide Therapiearme (siehe Abbildung 5). Bereits in der ersten Zwischenauswertung nach 18 Monaten (9) zeigte sich die Überlegenheit von IM hinsichtlich Progressionsfreiheit und Erreichen von Remissionen so stark, dass in der Folge fast alle Patienten im IFN-α-Arm auf IM umgestellt wurden. IRIS wurde dadurch mit der Zeit zu einer reinen Beobachtungsstudie für IM-Therapie. Nach achtjährigem Follow-up betrug das ereignisfreie Überleben etwa 81%, Progressionsfreiheit lag sogar bei 92% der Patienten vor. Für eine Kohorte von 98 Patienten wurden zusätzlich die *BCR-ABL*-Transkriptlevel über die Zeit monitoriert. Von diesen Patienten erreichten während der Beobachtungszeit 86% eine MMR (48). Für diese Arbeit standen die Daten von 69 Patienten aus dem IM-Arm (400 mg/d) zur Verfügung, was der vollständigen deutschen IM-Kohorte entspricht.

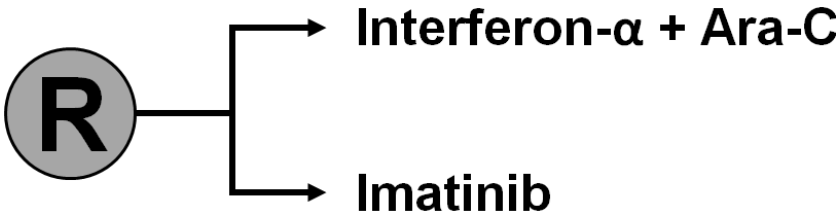

Abbildung 5: Design der IRIS-Studie. In der zweiarmigen Studie wurde IFN-α-Therapie (plus niedrig dosiertes Ara-C) mit IM-Monotherapie bei neudiagnostizierten CML-Patienten verglichen. Pro Arm wurden 553 Patienten randomisiert („R" bedeutet Randomisierung).

1.2.2 CML-IV-Studie

Bei der sogenannten CML-IV-Studie der Deutschen CML-Studiengruppe handelte es sich ursprünglich um eine prospektive vierarmige randomisierte Phase III-Therapiestudie. Dabei sollte IM-Monotherapie mit zwei verschiedenen Kombinationstherapien verglichen werden, darunter IM plus IFN-α sowie IM plus Ara-C. Der vierte Arm sah eine IM-Monotherapie nach IFN-α-Versagen vor. Während Patienten mit niedrigem und mittlerem Risiko die Standarddosis von 400 mg IM pro Tag erhielten, wurden Hochrisikopatienten mit 800 mg/d therapiert. Darüber hinaus sollte sich in jedem Arm nach etwaigem Therapieversagen eine allogene Stammzelltransplantation anschließen (siehe Abbildung 6). Es sollte erwähnt werden, dass in dieser Studie kein pegyliertes, sondern „normales" IFN-α zum Einsatz kommt.

Abbildung 6: Ursprüngliches Design der CML-IV-Studie. In dieser vierarmigen Studie sollte IM-Monotherapie (bzw. IM nach IFN-α-Versagen) mit einer Kombinationstherapie aus IM und IFN-α sowie IM und Ara-C verglichen werden. Bei Therapieversagen war in jedem Arm eine sich anschließende allogene Stammzelltransplantation vorgesehen.

Nach einer Pilotphase der Studie wurden die zwei Arme „Imatinib nach IFN-α-Versagen“ und „Imatinib plus Ara-C“ vorzeitig terminiert. Stattdessen konnten nun auch Patienten mit niedrigem und mittlerem Risiko 800 mg IM pro Tag erhalten, so dass für diese Dosierung ein eigener Arm eröffnet wurde. Das modifizierte dreiarmige Studiendesign findet sich in Abbildung 7. Primäre Endpunkte der Studie waren hämatologische Remission, komplette zytogenetische Remission, komplette oder majore MR (vor allem nach 12-monatiger Therapie) sowie progressionsfreies Überleben, wobei „Tod“ jede Todesursache einschließt und Progression als Übergang in akzelerierte Phase oder Blastenkrise definiert ist (49).

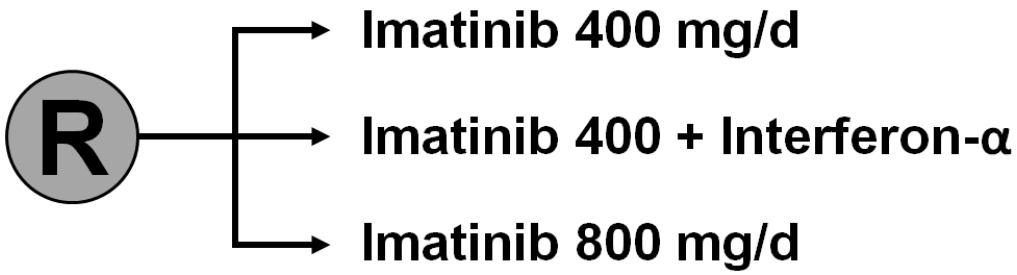

Abbildung 7: Modifiziertes Design der CML-IV-Studie. Bei neudiagnostizierten CML-Patienten werden IM 400 mg/d versus IM 800 mg/d versus IM 400 mg/d plus IFN-α verglichen.

Nach 5-jährigem Follow-up waren insgesamt 1.537 Patienten randomisiert. Bezüglich des Erreichens einer MMR nach 12 Therapiemonaten war der 800 mg-Arm (59%) dem 400 mg-Arm (44%) sowie der Kombinationstherapie (46%) signifikant überlegen. Eine Überlegenheit der hohen Dosis zeigt sich auch in Bezug auf das Erreichen einer kompletten zytogenetischen Remission. Hinsichtlich progressionsfreiem Überleben und Gesamtüberleben gab es keine signifikanten Unterschiede zwischen den drei Armen (49). Das Gesamtüberleben (alle Studienarme zusammen betrachtet) nach fünf Jahren ist kaum noch von einer vergleichbaren „gesunden“ Kohorte in der Normalbevölkerung unterscheidbar. Für diese Arbeit standen die Daten von insgesamt 280 Patienten aus dem 400 mg-Arm zur Verfügung. Durch Beschränkung auf diesen Arm ist eine Vergleichbarkeit mit den Daten der IRIS-Studie gewährleistet.

1.3 Mathematisches Stammzellmodell

Ursprungszelle der CML ist eine einzelne HSC, die durch eine genetische Aberration zu einer LSC entartet. Durch Proliferation dieser Zelle entsteht der maligne Klon, der sich in fortwährender Kompetition mit den normalen Zellen befindet, z.B. um gemeinsame Ressourcen oder freie Bindungsplätze an stromale Knochenmarkzellen. Da die klonalen Kompetitionsphänomene primär auf Stammzellebene reguliert werden, gleichzeitig aber hinsichtlich ihrer resultierenden zellulären Dynamik potenziell eine intuitiv nicht mehr fassbare Komplexität erreichen, stellt ein theoriebasierter Ansatz in Form eines dynamischen Stammzellmodells ein hilfreiches Werkzeug zur Erklärung der beobachteten Krankheits- und Therapieeffekte dar.

Das verwendete Modell wurde ursprünglich von Röder und Löffler für die Beschreibung der Hämatopoese in der Maus entwickelt (15). Da es keine Evidenz für wesentliche konzeptuelle Unterschiede der hämatopoetischen Stammzellorganisation zwischen Maus und Mensch gibt, habe ich das Modell im Rahmen meiner Diplomarbeit an humane Daten angepasst (16). Neben einer Beschreibung normaler Hämatopoese im Menschen ist das Modell auch im Stande, die Kompetition von normalen und malignen Zellen in der CML zu beschreiben, sowohl in der behandelten als auch unbehandelten Situation (17).

Bei dem Modell handelt es sich um ein agentenbasiertes Modell (ABM), das heißt, jede einzelne Stammzelle entspricht einem sogenannten Agenten. Die Zellen werden in einem stochastischen Prozess nach definierten Regeln simuliert. Die Zeit wird dabei diskretisiert betrachtet (Δt = 1 Stunde). Zu jedem dieser Zeitpunkte werden die Regeln angewendet und der Status aller Modellzellen aktualisiert. Normale und maligne Zellen befinden sich gleichzeitig im System und unterscheiden sich höchstens hinsichtlich ihrer Parameterwerte.

Die verwendete Modellklasse ist für klonale Kompetitionsphänomene besonders geeignet, da sich auch stochastische Fluktuationen im Falle sehr kleiner Zellzahlen beschreiben lassen. Sowohl bei der Entstehung der CML als auch bei MRD kompetieren oft sehr kleine leukämische Klone mit den normalen Zellen. Bei der Frage, ob solche Klone expandieren oder trotz kompetitiven Vorteils „aussterben“, spielen stochastische Effekte eine wesentliche Rolle. Möglicherweise sind diese Effekte dafür verantwortlich, dass *BCR-ABL*-positive Zellen temporär in sehr kleiner Zahl in gesunden Freiwilligen gefunden werden, ohne dass diese in der Folgezeit eine CML entwickeln (50). Eine solche Sichtweise würde beispielsweise bei einer mittelwertbasierten Modellierung unter Verwendung von ODEs verloren gehen.

1.3.1 Modellbeschreibung

Jedes Zellobjekt wird durch ein Tripel von Eigenschaften $\big(a(t), m(t), c(t)\big)$ beschrieben, wobei $m(t) \in \{\mathrm{A}, \Omega\}$ die Zugehörigkeit zu einer von zwei Signalumgebungen beschreibt. Während proliferative Zellen in Ω lokalisiert sind, befinden sich Stammzellen in Signalumgebung A in einem Ruhezustand, das heißt in G_0-Phase des Zellzyklus. Das A-Kompartiment kann als stromale Nische, z.B. im Knochenmark, interpretiert werden. Die Zellen können zwischen beiden Signalumgebungen reversibel wechseln. Die Variable $a(t) \in \{0\} \cup [a_{\min}, a_{\max}]$ stellt eine zellspezifische Affinität dar, die als Neigung sich an Signalumgebung A zu binden, interpretiert werden kann. Die dritte Eigenschaft $c(t) \in \{0,1,\dots,\tau_{\mathrm{c}}\}$ beschreibt die Position innerhalb des Zellzyklus, wobei τ_{c} die Zellzykluszeit bezeichnet.

Der Zellzyklus der proliferativen Zellen in Signalumgebung Ω ist als Sequenz von, in dieser Reihenfolge, G_1-Phase, S-Phase und G_2- bzw. M-Phase modelliert. Fixiert sind hierbei neben der Gesamtzykluszeit τ_{c} die Längen von S-Phase (τ_{S}) und kombinierter G_2/M-Phase ($\tau_{\mathrm{G_2/M}}$), so dass sich die Länge der G_1-Phase (und nach Konstruktion gleichzeitig der Beginn der S-Phase innerhalb des Zellzyklus) zu $\tau_{\mathrm{G_1}} = \tau_{\mathrm{c}} - \big(\tau_{\mathrm{S}} + \tau_{\mathrm{G_2/M}}\big)$ berechnet.

Um einen Aktualisierungsschritt aller Zellen innerhalb des Modells durchführen zu können, wird die Anzahl aller Zellen mit $a(t) > a_{\min}$ in A und Ω ($N_{\mathrm{A}}(t)$ und $N_{\Omega}(t)$) bestimmt. Nun wird für jede Zelle der neue Zustand $\big(a(t+1), m(t+1), c(t+1)\big)$ wie folgt berechnet:

Wenn sich eine Zelle in Signalumgebung A befindet, wechselt sie nach Ω oder bleibt in A mit Wahrscheinlichkeit ω bzw. $1-\omega$. Falls die Zelle in A bleibt, wird ihre Affinität $a(t)$ durch Multiplikation mit dem Regenerationskoeffizienten r ($r > 1$) erhöht ($a(t+1) = a(t) \cdot r$), solange $a(t+1)$ nicht die Regenerationsgrenze $a_{\max}$ erreicht hat. Dieser Vorgang lässt sich als Entdifferenzierungsschritt interpretieren. Falls die Zelle nach Ω wechselt ($m(t+1) = \Omega$), wird ihre Zellzyklusposition auf den Beginn der S-Phase gesetzt ($c(t+1) = \tau_{\mathrm{G_1}}$), unabhängig davon, an welcher Zyklusposition sich die Zelle vor dem Ruhezustand befand.

Wenn sich eine Zelle in Kompartiment Ω befindet, wechselt sie nach A oder bleibt in Ω mit Wahrscheinlichkeit α bzw. $1-\alpha$. Allerdings ist ein Wechsel in den Ruhezustand nur dann möglich, wenn sich die Zelle in der G_1-Phase befindet ($c(t) < \tau_{\mathrm{G_1}}$) und $a(t) > a_{\min}$ gilt. Wenn die Zelle nach A wechselt, wird nur $m(t+1) = \mathrm{A}$ gesetzt. Wenn die Zelle in Ω verbleibt, wird ihre Affinität $a(t)$ durch Multiplikation mit dem Differenzierungskoeffizienten $1/d$ ($d > 1$) verringert ($a(t+1) = a(t)/d$) und ihre Zellzyklusposition wird inkrementiert

($c(t+1) = c(t) + 1$). Dies lässt sich als Differenzierungsschritt (sukzessiver Verlust der Stammzelleigenschaft) interpretieren. Falls ein kompletter Zellzyklus abgeschlossen wurde ($c(t+1) = \tau_c$), wird $c(t+1) = 0$ gesetzt und durch Generierung eines neuen identischen Zellobjekts eine Zellteilung initiiert. Falls $a(t+1)$ die minimale Affinität $a_{\min}$ unterschreitet, wird $a(t+1) = 0$ gesetzt. Zellen mit dieser Eigenschaft werden im Modell als differenzierte Zellen bezeichnet und stehen im Gegensatz zu den Stammzellen, welche durch die Eigenschaft $a(t) > a_{\min}$ charakterisiert sind. Differenzierte Zellen können nicht mehr in Signalumgebung A regenerieren, sondern setzen ihre Entwicklung in Ω fort. Hierbei durchlaufen sie zunächst eine proliferative Phase (mit Zellzykluszeit $\tilde{\tau}_c$), deren Länge λ_p beträgt, gefolgt von einer finalen Reifungsphase (λ_m), in der nichtproliferative Progenitor- und reife Zellen zusammengefasst sind. Letztgenannte Zellpopulation lässt sich als Repräsentation des peripheren Blutes interpretieren und wird im Modell zur Bestimmung der *BCR-ABL*/*ABL*-Werte verwendet. Eine schematische Darstellung des Modells findet sich in Abbildung 8.

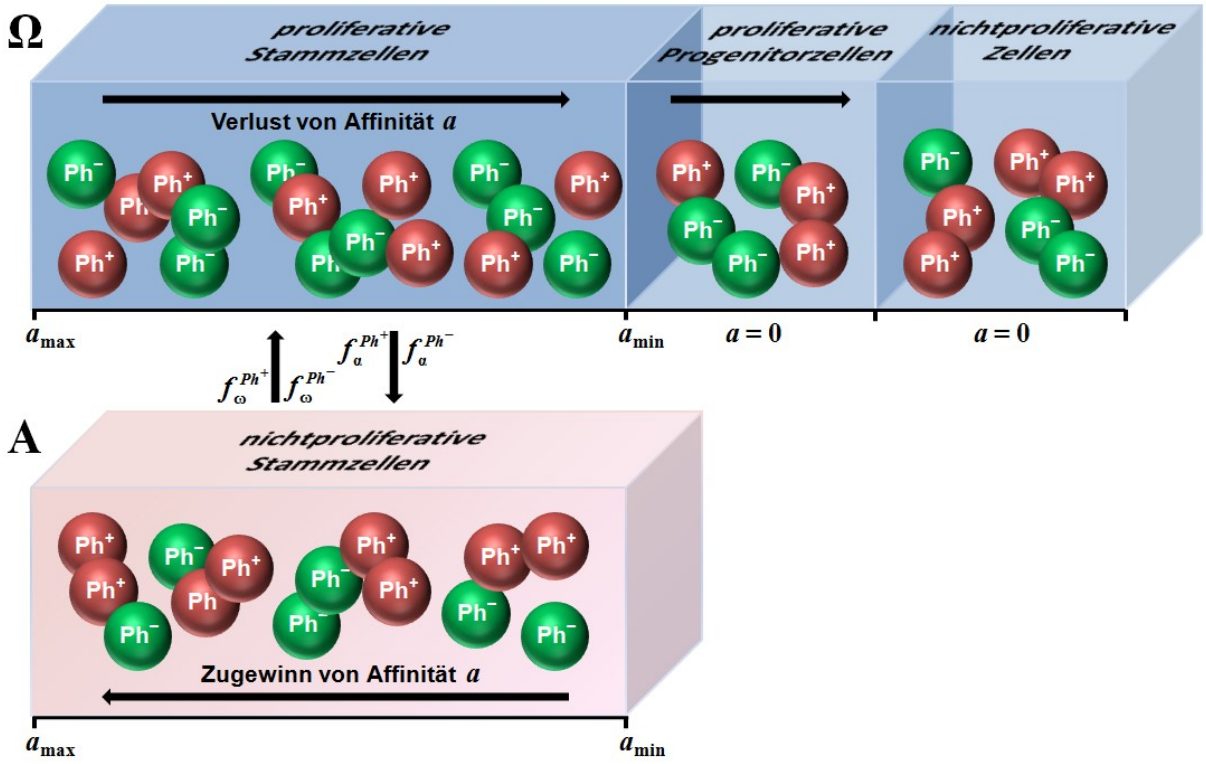

Abbildung 8: Schematische Darstellung des Stammzellmodells. Es werden proliferative (in Signalumgebung Ω) und nichtproliferative Stammzellen (in A) unterschieden. Normale (Ph^-) und maligne (Ph^+) Zellen kompetieren um gemeinsame Ressourcen. Zellen können zwischen A und Ω reversibel wechseln, abhängig von den Transitionscharakteristiken $\boldsymbol{f}_\alpha$ und $\boldsymbol{f}_\omega$.

Die Transitionswahrscheinlichkeiten α und ω hängen von der Affinität einer Zelle $a(t)$, von den festen globalen Parametern $a_{\min}$ und $a_{\max}$, sowie von den Transitionscharakteristiken f_α und f_ω ab. Die Berechnung letzterer erfolgt mit der Zellzahl im jeweiligen Zielkompartiment:

$$\alpha = \frac{a(t)}{a_{\max}} f_\alpha\big(N_A(t)\big)$$

$$\omega = \frac{a_{\min}}{a(t)} f_\omega\big(N_\Omega(t)\big).$$

Die Transitionscharakteristiken $f_{\alpha/\omega}$ werden durch eine sigmoidale Funktionsklasse modelliert:

$$f_{\alpha/\omega}\big(N_{A/\Omega}\big) = \frac{1}{\nu_1 + \nu_2 \cdot exp\left(\nu_3 \cdot \frac{N_{A/\Omega}}{\widetilde{N}_{A/\Omega}}\right)} + \nu_4.$$

Die Parameter ν_1, ν_2, ν_3 und ν_4 beschreiben die Form der Funktion, $\widetilde{N}_{A/\Omega}$ ist ein Skalierungsfaktor für $N_{A/\Omega}$. Man kann ν_1, ν_2, ν_3 und ν_4 durch die anschaulicheren Werte $f_{\alpha/\omega}(0)$, $f_{\alpha/\omega}(\widetilde{N}_{A/\Omega}/2)$, $f_{\alpha/\omega}\big(\widetilde{N}_{A/\Omega}\big)$ sowie $f_{\alpha/\omega}(\infty) := \lim_{N_{A/\Omega}\to\infty} f_{\alpha/\omega}\left(N_{A/\Omega}\right)$ eindeutig bestimmen:

$$\begin{aligned}
\nu_1 &= (h_1 h_3 - h_2^2)/(h_1 + h_3 - 2h_2)\\
\nu_2 &= h_1 - \nu_1\\
\nu_3 &= ln\big((h_3 - \nu_1)/\nu_2\big)\\
\nu_4 &= f_{\alpha/\omega}(\infty).
\end{aligned}$$

Die oben eingeführten Hilfsvariablen h_1, h_2 und h_3 lassen sich dabei wie folgt berechnen:

$$\begin{aligned}
h_1 &= 1/\big(f_{\alpha/\omega}(0) - f_{\alpha/\omega}(\infty)\big)\\
h_2 &= 1/\big(f_{\alpha/\omega}(\widetilde{N}_{A/\Omega}/2) - f_{\alpha/\omega}(\infty)\big)\\
h_3 &= 1/\big(f_{\alpha/\omega}(\widetilde{N}_{A/\Omega}) - f_{\alpha/\omega}(\infty)\big).
\end{aligned}$$

Beispiele für die Transitionscharakteristiken $f_{\alpha/\omega}$ finden sich in Abbildung 9.

Für die Durchführung von Simulationsrechnungen liegt das Modell in zwei Implementationen vor, welche sich nur in der Programmiersprache unterscheiden. Die erste Variante, welche sämtlichen in diese Arbeit eingeschlossenen Publikationen zu Grunde liegt, wurde in C++ programmiert. Darüber hinaus wurde von mir eine Programmversion in R geschrieben, um die Anwendung des Modells auch ohne tiefere IT-Kenntnisse zu ermöglichen.

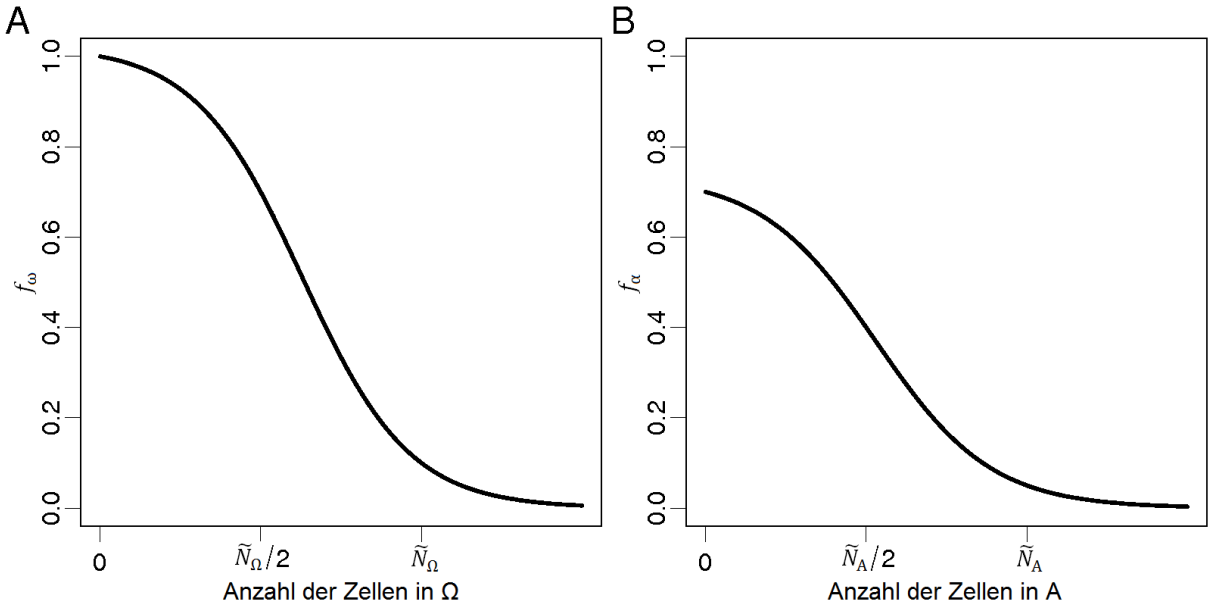

Abbildung 9: Beispiele für Transitionscharakteristiken f_α und f_ω. Der Funktionswert der Transitionscharakteristiken hängt von der Anzahl der Zellen in Kompartiment A bzw. Ω ab.

1.3.2 Allgemeine Modellannahmen

Es wird angenommen, dass normale und maligne Zellen gemeinsam im System vorhanden sind und um gemeinsame Ressourcen kompetieren. Eine solche Ressource können beispielsweise freie Bindungsplätze an stromalen Knochenmarkzellen sein, die für die Selbsterhaltung der Zellpopulationen von Bedeutung sind. Beide Zelltypen werden als in sich homogen betrachtet, das heißt, Zellen des gleichen Typs sind durch identische Parameterwerte charakterisiert. Zwischen den Zelltypen werden jedoch unterschiedliche Parameterwerte angenommen, so dass leukämische gegenüber normalen Zellen einen kompetitiven Vorteil besitzen.

Die Parameterwerte der normalen Zellen sind so gewählt, dass ein dynamisch stabilisiertes Gleichgewicht („Steady State“) zwischen proliferativen (Ω) und ruhenden (A) Stammzellen entsteht und aufrechterhalten wird. Dabei wird eng an Vorarbeiten angeknüpft, in denen die Parameter für verschiedene experimentelle und klinische Settings in Mäusen und Menschen verifiziert wurden (51; 17); siehe auch 1.4. Der Ausstrom aus dem Stammzellkompartiment Ω trägt zur Population der proliferativen Progenitorzellen bei, aus denen sich ein weiteres Kompartiment, bestehend aus nichtproliferativen Progenitoren und reifen Blutzellen, speist.

Da dieses Kompartiment zum „peripheren Blut“ korrespondiert, erfolgt auf Basis der darin befindlichen Zellen die Berechnung der Tumorlast in Form der *BCR-ABL*/*ABL*-Werte. Aufgrund einer starken Korrelation zwischen Tumorlastmessungen mittels Zytogenetik und qRT-

PCR (52) werden *BCR-ABL*-Transkriptlevel durch Zellzahlen approximiert. Es wird angenommen, dass das Kontrollgen (hier: *ABL*) in jeder Zelle zweimal vorhanden ist, das Onkogen *BCR-ABL* hingegen nur einmal. Sei n_1 die Anzahl der leukämischen Zellen und n_2 die Anzahl der normalen Zellen im „peripheren Blut“, dann gilt die folgende Beziehung:

$$BCR\text{-}ABL/ABL \approx \frac{n_1}{n_1 + 2n_2} \cdot 100\%.$$

Da eine Mutation in einer einzelnen HSC für die CML-Entstehung ursächlich ist, wird angenommen, dass sich während einer Steady-State-Hämatopoese eine normale Zelle zu einer malignen Zelle verändert. Technisch wird dies durch Änderung der Parameterwerte einer normalen Zelle realisiert. Die Parameterwerte dieser Zelle werden dabei so gewählt, dass sie konsistent mit einer Vielzahl klinisch beobachteter Charakteristika der CML-Entstehung sind, darunter die lange Latenzzeit von fünf bis sieben Jahren. Um die Kriterien erfüllen zu können, muss der neoplastische Klon gegenüber dem Wildtyp einen Wachstumsvorteil besitzen. Ein solcher Vorteil kann z.B. in veränderten Interaktionen zwischen den LSCs und ihrer Mikroumgebung, modelliert durch veränderte Transitionscharakteristiken f_α und f_ω, bestehen.

Es wird angenommen, dass die CML-Behandlung erfolgt, wenn der Anteil der leukämischen Zellen in der Population der nichtproliferativen Zellen 99% beträgt. Diese Zahl ist dadurch motiviert, dass in fast allen Patienten zu Therapiebeginn mittels Zytogenetik 100% Ph-positive Metaphasen gemessen werden. Therapiespezifische Annahmen sind durch biologische Beobachtungen hinsichtlich des jeweiligen Wirkmechanismus motiviert. So wird für IM angenommen, dass das Medikament selektiv die proliferative Aktivität der Tumorzellen hemmt und in diesen Zellen Apoptose auslöst. Dies lässt sich modelltechnisch durch eine reduzierte Wahrscheinlichkeit zur Aktivierung in den Zellzyklus ω sowie eine feste Killrate beschreiben.

Das Modell liegt in seiner oben beschriebenen allgemeinen Form sämtlichen in diese Arbeit eingeschlossenen Publikationen zu Grunde. Spezielle Modellannahmen sowie Modifikationen des Modells werden in den jeweiligen Publikationen (bzw. deren Supplement) beschrieben.

1.4 Vorarbeiten

Das Thema der CML-Modellierung mit Hilfe des im vorigen Abschnitt beschriebenen ABM, insbesondere mit Fokus auf verschiedenen medikamentösen Therapien, zählte bereits vor meiner Doktorandenzeit zu meinen wissenschaftlichen Interessen. Dabei entstanden einige Arbeiten, die als inhaltliche Vorarbeiten für diese Dissertation betrachtet werden müssen. Hierzu zählt neben meiner Diplomarbeit (16) und einer *Nature-Medicine*-Publikation mit deren wichtigsten Resultaten (17) auch eine 2008 in der Zeitschrift Cells Tissues Organs erschienene Arbeit, welche die Ergebnisse der Diplomarbeit ausführlich darstellt.[1] Da das dynamische Stammzellmodell ursprünglich für die Hämatopoese der Maus entwickelt wurde (15), wird darin die Anwendbarkeit des ABM auf die menschliche Hämatopoese im Allgemeinen sowie die CML im Besonderen gezeigt, sowie Modellannahmen für verschiedene medikamentöse CML-Therapien (inklusive IM) getroffen. Da es eine wichtige Grundlage für die vorliegende Arbeit darstellt, wird dieses von mir in Erstautorenschaft verfasste Paper der Dissertation im Folgenden komplett hinzugefügt.

Unter Anwendung des ABM war das Ziel des Papers die Identifizierung eines Modellmechanismus, der einen kompetitiven Vorteil des malignen Klons gegenüber den normalen Zellen induzieren kann, so dass sowohl CML-Entstehung als auch Daten zu mehreren CML-Therapien (HU, IFN-α, IM) konsistent erklärt werden können. Bezüglich CML-Entstehung waren die folgenden Kriterien zu erfüllen: (i) eine mehrjährige Koexistenz von normalen und malignen Zellen bis zur klinischen Manifestation der Krankheit; (ii) eine sukzessive Verdrängung der normalen Hämatopoese durch den malignen Klon; (iii) eine verglichen mit der normalen Situation erhöhte absolute Zellproduktion; und (iv) eine verzögerte Ph-Positivität in der Population der dormanten HSCs verglichen mit der proliferativen Fraktion.

Drei verschiedene Szenarios sind in der Lage, die vier vorgenannten Kriterien zu erfüllen. Dabei unterscheiden sich die malignen Zellen jeweils in zwei Parametern von den normalen Zellen. Allen drei Szenarios gemeinsam ist der Unterschied in der Transitionscharakteristik f_ω, der die Wahrscheinlichkeit der Aktivierung ruhender LSCs in den Zyklus verglichen mit normalen Zellen erhöht. Zusätzlich unterscheiden sich normale und maligne Zellen entweder in ihrer Zellzykluszeit τ_c, ihrer Differenzierungsrate d, oder ihrer Transitionscharakteristik f_α.

[1] Horn M, Loeffler M, Roeder I; *Cells Tissues Organs*. 2008;188(1-2):236-247

Um die Szenarios zu diskriminieren, wurde geprüft, inwiefern sie klinische Daten zur CML-Therapie reproduzieren können. Es zeigte sich, dass basierend auf entsprechenden Modellannahmen zu HU- und IFN-α-Therapie kein qualitativer Unterschied zwischen den Szenarios besteht. Hinsichtlich IM-Therapie ist jedoch nur ein Szenario in der Lage, den biphasischen Abfall der *BCR-ABL*-Transkriptlevel zu erklären. Dabei handelt es sich um das Szenario, das Unterschiede zwischen normalen und malignen Zellen in den Transitionscharakteristiken f_α und f_ω annimmt. Eine Interpretation ist, dass als Pathomechanismus der neoplastischen Zellen sowohl erhöhte Zyklusaktivierung als auch gestörte Stromabindung eine Rolle spielen.

Aufgrund der momentanen „Renaissance" von IFN-α im Rahmen einer potenziell synergistischen Kombinationsstrategie mit TKIs, sind in der Rückschau die in diesem Paper in Bezug auf IFN-α-Monotherapie getroffenen Annahmen von Interesse. Die postulierte Angleichung der Modellparameter zwischen normalen und malignen Zellen unter Einfluss von IFN-α lässt sich als immunologischer Effekt interpretieren, trägt aber nicht dem vermuteten stammzellaktivierenden Potenzial des Zytokins Rechnung. Diese Möglichkeit wird modellseitig in Publikation 2 (siehe „Eingeschlossene Publikationen") ausführlich betrachtet.

Cells Tissues Organs

Cells Tissues Organs 2008;188:236–247
DOI: 10.1159/000118786

Published online: February 27, 2008

Mathematical Modeling of Genesis and Treatment of Chronic Myeloid Leukemia

Matthias Horn Markus Loeffler Ingo Roeder

Institute for Medical Informatics, Statistics and Epidemiology, University of Leipzig, Leipzig, Germany

Key Words
Chronic myeloid leukemia · Imatinib · Hydroxyurea · Interferon-α · Stem cells · Mathematical modeling · Simulation study

Abstract
Chronic myeloid leukemia (CML) is a clonal hematopoietic disorder induced by translocation of chromosomes 9 and 22, resulting in an overproduction of myeloid blood cells. CML-specific characteristics include a latency time of several years, a period of coexistence of malignant and normal cells and an eventual dominance of the malignant clone. Different drug therapies are available, most notably imatinib, which inhibits the oncogenic *BCR-ABL1* tyrosine kinase. Although the chromosomal aberration causing CML is well known, the resulting dynamic effects on the system behavior are not sufficiently understood yet. Here, we apply an already established mathematical model of hematopoietic stem cell organization. Based on parameter estimates for normal hematopoiesis, we systematically explore the changes in these parameters necessary to reproduce CML-specific characteristics regarding emergence and course of disease as well as a variety of qualitative and quantitative clinical data on CML treatment. Our results indicate that 1 or more of the following mechanisms are compatible with the induction of a dominant clone in the proposed model: a retarded differentiation process, a reduced turnover time or a defective cell-microenvironment interaction of the neoplastic cells. However, in order to explain the massive overproduction of malignant cells, an unregulated and abnormal activation of leukemia stem cells into cycle has to be assumed additionally. Based on our simulation results we conclude that CML dynamics can most appropriately be explained by a modulation of the cell-microenvironment interactions of leukemia stem cells, including both the process of stem cell silencing and activation into cycle.

Abbreviations used in this paper

CML	chronic myeloid leukemia
HSC	hematopoietic stem cell
HU	hydroxyurea
IFN-α	interferon-α
IM	imatinib
PCR	polymerase chain reaction
Ph	Philadelphia chromosome

KARGER

Fax +41 61 306 12 34
E-Mail karger@karger.ch
www.karger.com

1422–6405/08/1882–0236$24.50/0

Accessible online at:
www.karger.com/cto

Mr. Matthias Horn
Institute for Medical Informatics, Statistics and Epidemiology
University of Leipzig, Haertelstrasse 16–18, DE–04107 Leipzig (Germany)
Tel. +49 341 97 161 92, Fax +49 341 97 161 09
E-Mail matthias.horn@imise.uni-leipzig.de

Introduction

Chronic myeloid leukemia (CML) is a clonal disorder of the hematopoietic system. It is induced by mutation on the hematopoietic stem cell (HSC) level and results in a malignant expansion and overproduction of (immature) myeloid blood cells [Mauro and Druker, 2001]. Cytogenetically, malignant cells are characterized by a reciprocal translocation of chromosomes 9 and 22 [Goldman and Melo, 2003]. It has been demonstrated that radiation is capable of inducing such a genetic aberration [Ichimaru et al., 1981]. However, the precise mechanisms as well as the frequency of the occurrence are only incompletely known. The shortened chromosome 22 is referred to as Philadelphia chromosome (Ph) which carries the *BCR-ABL1* fusion gene. Its gene product, the oncogenic BCR-ABL1 protein, is a constitutively activated tyrosine kinase, the expression of which has been shown to be responsible for the pathogenesis of CML [Deininger et al., 2000]. But even though these mechanisms within individual malignant cells are well understood, the resulting response of the system to the neoplasm on the cell population level is yet to be elucidated.

If left untreated, CML is a fatal disease. The only known curative treatment option of CML is stem cell or bone marrow transplantation [Goldman and Gordon, 2006]. This procedure, however, is associated with a high early mortality rate. Furthermore, several drug therapies are available. Hydroxyurea (HU) is a cytotoxic drug which specifically acts on proliferating cells, regardless of genotype, by inhibition of ribonucleotide reductase and, therefore, by inhibition of DNA synthesis. This effect prevents cell division and eventually leads to apoptosis [de Lima et al., 2003]. Currently, HU is primarily used as initial therapy to reduce the leukocyte count to normal levels before other treatment is applied. Interferon-α (IFN-α) has been used for many years in the management of patients in the chronic phase of CML, but the mechanisms by which it induces growth inhibitory effects in leukemia cells are not exactly known. Several different mechanisms have been suggested. It is widely accepted that IFN-α has an immunostimulating effect, that is, it renders leukemia cells visible to the immune system [Parmar and Platanias, 2003]. One indirect consequence of this immune effect may involve normalization of the adhesion to bone marrow stroma [Bhatia et al., 1994]. Downregulation of the expression of the *BCR-ABL1* oncogene might be another potential mechanism [Verma and Platanias, 2002].

Within the last decade, imatinib (IM) has rapidly become the front-line therapy for de novo CML. This drug inhibits the oncogenic *BCR-ABL1* tyrosine kinase by occupying the ATP-binding site of the BCR-ABL1 protein, thereby preventing phosphorylation of its substrates [Buchdunger et al., 1996]. This process ultimately results in the switching off of downstream signaling pathways that promote leukemogenesis [Savage and Antman, 2002]. Although these molecular mechanisms are well known, it is not sufficiently understood how they translate into the dynamic regulation of normal and leukemic cell growth. It is known that IM selectively acts on leukemia cells where it induces a proliferation inhibitory effect [Druker et al., 1996] as well as an increase in the apoptotic rate of actively proliferating cells [Oetzel et al., 2000; Vigneri and Wang, 2001; Holtz et al., 2007]. Molecular monitoring of tumor load revealed that IM induces a biphasic decline of *BCR-ABL1* transcript levels during the first year of treatment. It is characterized by an initially rapid followed by a moderate decline. Furthermore, a rapid relapse upon treatment cessation can be observed [Michor et al., 2005].

An important obstacle in the design of curative drug therapies is the fact that relevant details of the system behavior, such as resistance to IM treatment [Tauchi and Ohyashiki, 2004], are only insufficiently understood, irrespective of the above-mentioned molecular insights into pathogenesis of CML and IM activity.

It is the objective of this paper to apply an already established mathematical model of HSC organization [Roeder and Loeffler, 2002] to the situation of CML. Based on parameter estimates for normal hematopoiesis, we systematically investigate the changes in the cell-intrinsic parameters necessary to reproduce CML-specific characteristics. The model has to be consistent with a variety of qualitative and quantitative clinical data on CML treatment. Thereby, a comprehensive, predictive and interpretable picture of CML emergence, course of disease and treatment can be obtained. To be able to generate model predictions for new treatment options, an in silico disease model consistent with established treatment options is required. Therefore, also data on former first-line CML therapies, such as HU and IFN-α, are considered in order to guarantee the validity of the model.

Materials and Methods

In this work, we apply a single-cell-based, stochastic mathematical model [Roeder and Loeffler, 2002]. The model has been developed for the HSC system and has already been validated for

animal data, for example to describe clonal competition processes in mouse chimeras [Roeder et al., 2005]. Furthermore, it has also been applied to 1 very specific treatment scenario in chronic myeloid leukemia [Roeder et al., 2006]. A schematic representation of the model can be found in figure 1. It is assumed that cells can reside in 2 signaling contexts (**A**, Ω), which can be interpreted as different growth environments, with **A** representing a stem cell-supporting niche within the bone marrow. A short explanation of the model can be found in the next paragraph. For a more detailed mathematical description, we refer to the Appendix and Roeder et al. [2006].

Each cell has a property a, which represents the affinity to reside in **A**. If a is greater than a given threshold a_{min}, the respective cell is denoted as a stem cell. Affinity a can be interpreted as the state of differentiation of a stem cell: the smaller a, the less stem cell potential is attributed to a cell. Differentiation (that is, decrease in a) is considered to be a reversible process until a has reached a_{min}. Whereas cells gradually lose affinity a under the influence of environment Ω [$a(t + 1) = a(t)/d$], they regain it in **A** [$a(t + 1) = a(t)\cdot r$]. The latter can be interpreted as a regeneration process on the individual cell level. Parameters d and r represent differentiation and regeneration coefficients, respectively. If a falls below a_{min}, it is set to zero. Such a cell loses its potential to change to **A** and, therefore, to regain a. It is no longer denoted as a stem, but as a differentiated cell, which initiates a clone that amplifies and finally dies after a fixed lifetime. Whereas cells in **A** are assumed to be quiescent, that is, in G_0-phase of the cell cycle, cells in Ω are actively proliferating with an average generation time τ_c. The transition of cells between the 2 signaling contexts is modeled as a stochastic process, that is, at every time step each cell has a certain probability to change from one compartment to the other. The transition probabilities depend on the individual cellular affinity a and the transition characteristics f_α and f_ω. These characteristics depend on the current numbers of cells in **A** and Ω, respectively (for a schematic, see fig. 2).

The described model is implemented as a C++ computer program. The source code can be obtained from the authors. Each individual cell in the system is simulated according to the above-outlined set of rules. These rules are applied at discrete time steps (Δt = 1 h) to simultaneously update the status of all model cells. The algorithm includes stochastic decisions, for example, with respect to transitions from one signaling context to the other. Due to this system-intrinsic stochasticity, even different simulation runs using identical model parameters generate quantitatively different outcomes. A population of patients can be represented by averaging the results of many single simulation runs.

The model assumes CML to be a clonal competition process between the malignant clone (Ph+), comprising all cells originating from 1 mutated cell, and normal (Ph–) hematopoietic cells, with potential quantitative differences in model parameters.

As mentioned above, the model has already been applied to the murine system [Roeder and Loeffler, 2002; Roeder et al., 2005]. In these publications, parameter values were fitted to quantitative data on specific mouse strains. In order to obtain a parameter set, which we assume to adequately represent a normal human hema-

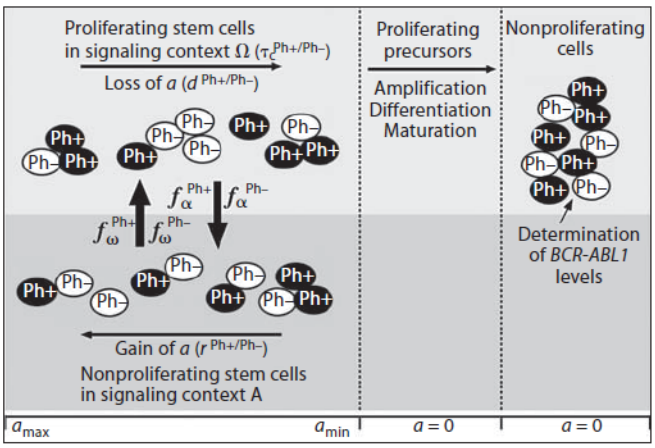

Fig. 1. Model scheme. Normal (Ph–) and malignant (Ph+) stem cells are assumed to coexist within 2 common signaling contexts (**A**, Ω). For a detailed model description, see text.

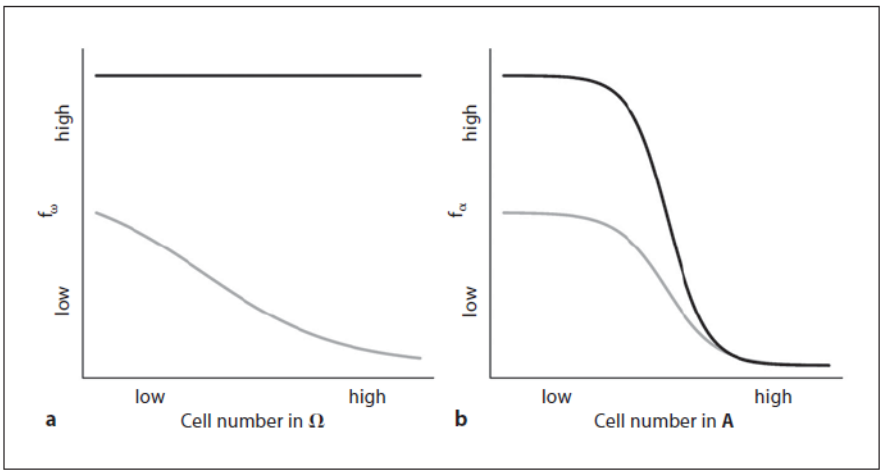

Fig. 2. Schematic of transition characteristics, showing examples of transition characteristics f_ω (**a**) and f_α (**b**) of normal (gray) and malignant (black) stem cells for the situation of untreated CML. For exact parameter values used in the computer simulations, see table 2.

topoiesis, the mouse parameter values served as a starting point. Although specific model parameters can be expected to differ considerably between mice and men, we assume the existence of fundamental interspecies similarities with regard to the general regulatory principles of hematopoiesis. Hence, it was an important goal to change only as few system parameters as necessary when applying the model to a new (here: the human) situation.

Using a parameter set capable of maintaining a steady state of normal hematopoiesis, the introduction of 1 Ph+ stem cell is assumed to represent the disease-initiating event. This stem cell is assumed to have a growth advantage compared to normal cells and is equipped with an inheritable marker, which allows tracking of its progeny, that is, the malignant clone, over time.

It is the aim of this study to investigate which model parameters are capable of inducing a growth advantage of leukemia cells that leads to the formation of a manifest CML clone. A set of model parameters which consistently describes the situation of untreated chronic myeloid leukemia is determined by applying the following qualitative criteria, all of which have been motivated by clinical and experimental observations.

(1) The emergence of the disease has to be accompanied by a long latency time of about 5–7 years [Ichimaru et al., 1981], characterized by a coexistence of normal and leukemia cells, until the proportion of neoplastic cells has reached more than 90%.

(2) If the disease remains untreated, the malignant clone eventually takes over the hematopoietic system, while the Ph– cells gradually disappear [Goldman and Melo, 2003].

(3) Compared to normal hematopoiesis, there is an increased absolute blood cell production primarily caused by an expansion of the malignant clone [Mauro and Druker, 2001].

(4) Quiescent leukemia stem cells show a delayed Ph positivity compared to actively proliferating cells, that is, the frequency of Ph+ stem cells in the quiescent pool lags behind that among proliferating cells [Dube et al., 1984].

All model parameters are systematically tested for the ability to reproduce these criteria. The agreement of simulation results and clinical/biological observations is judged by a consistency of average simulations with all above-stated criteria.

To further test the consistency of the derived parameter configurations beyond the emergence of CML, they are applied to different treatment strategies in silico. The simulation results are compared with qualitative and quantitative clinical data on CML patients. In particular, the following assumptions are applied for the simulation of treatment options.

HU treatment is assumed to induce an unselective kill of cells in S-phase, that is, a fixed percentage of S-phase cells per time step undergo apoptosis, regardless of their genotype. In contrast, IFN-α is assumed to affect leukemia cells only. At the moment of treatment initiation, the model parameters of malignant cells, which are capable of explaining the clonal dominance, are reset to the values assumed for normal cells. IM treatment is assumed to induce apoptosis and inhibition of the proliferative activity of proliferating Ph+ stem cells. Technically, the apoptotic effect is modeled by a selective kill of a fixed percentage of leukemia cells per time step (degradation rate r_{deg}), while the proliferation inhibition is modeled by a reduction of the activation of leukemia cells into cycle, that is, altering transition characteristic f_ω (transition from **A** to Ω), at the fixed inhibition rate r_{inh}.

Qualitatively, the model needs to reproduce that the majority of HU and IFN-α patients show a hematologic response, with HU inducing more rapid responses than IFN-α. In almost none of the HU patients, cytogenetic responses can be observed [Hehlmann et al., 1993]. In contrast, IFN-α is capable of inducing cytogenetic remissions in the majority of patients [Hehlmann et al., 1994]. Simulation of IM treatment needs to reproduce rapid hematologic and rapid cytogenetic remissions [Savage and Antman, 2002].

Furthermore, simulation results of IM treatment are compared with quantitative criteria, as highly sensitive measurements of tumor load, utilizing real-time quantitative polymerase chain reaction (PCR), are available [Michor et al., 2005; Roeder et al., 2006]. In these studies, *BCR-ABL1* transcript levels were measured at different time points during IM treatment. A typical biphasic decline of *BCR-ABL1* transcript levels during the first year of therapy as well as a rapid relapse upon treatment cessation can be observed [Michor et al., 2005]. An overview of the applied model assumptions and criteria can be found in table 1.

In order to compare clinically determined *BCR-ABL1* transcript levels to the mathematical model, *BCR-ABL1/ABL1* percentages are approximated using cell numbers in the population of nonproliferating differentiated cells according to the following relation: [number of Ph+ cells/(number of Ph+ cells + [2 × number of Ph– cells])] × 100%, motivated by the existence of 2 copies of each gene within individual cells and by a reported strong correlation between cytogenetics, assessing the proportion of Ph+ cells, and real-time quantitative PCR measurements of *BCR-ABL1* transcript levels in peripheral blood [Branford et al., 1999].

Results

CML Genesis

Based on a system of normal steady-state hematopoiesis (for model parameters, see table 2), 3 model parameters were found to be independently capable of inducing a competitive growth advantage, namely differentiation rate d, transition characteristic f_α and cell cycle duration τ_c. The possible parameter alterations can be found in table 3. Each of these 3 parameter changes, applied to exactly 1 proliferating stem cell (located in Ω), is capable of giving rise to a dominant clone. However, in each of these scenarios, this capability is realized in only about 20% of the cases, that is, in about 80% of the computer simulations there is only a transient low-level contribution of neoplastic cells. These cases, which are neglected in the following, are characterized by the extinction of the malignant clone owing to the stochasticity of the model.

Upon applying any of the parameter changes given in table 3, one obtains the results shown in figure 3. The percentage of the dominant clone relative to all cells within the computer simulation (average ± SD of 100 individual simulation runs) was determined using the population of nonproliferating differentiated cells. The disease-initiating single-cell mutation event occurred at time point

Table 1. Applied model assumptions and qualitative criteria for the simulation of CML treatment options HU, IFN-α and IM

Treatment	Assumptions	Criteria
HU	unselective kill of S-phase cells at a fixed rate per time step	rapid hematologic but no cytogenetic response
IFN-α	equalization of model parameters of normal and leukemia cells, which are capable of explaining the dominance of the malignant clone	hematologic and cytogenetic responses
IM	fixed degradation and proliferation inhibition rate selectively for leukemia cells	biphasic decline of *BCR-ABL1* transcript levels and rapid relapse after treatment stop

zero. Criteria 1 and 2 are met: after about 3 years, the proportion of malignant cells starts to rise. After about 5–7 years, clinically relevant levels of malignant cells can be detected. Finally, by outcompeting normal cells, the malignant clone takes over the hematopoietic system (fig. 3a). Criteria 3 and 4, however, cannot be met: compared to normal hematopoiesis, there is no increased production rate of malignant cells (fig. 3b). The overall count of normal (gray) and malignant (black) nonproliferating differentiated blood cells remains relatively constant over time. Furthermore, as indicated by figure 3c, quiescent HSCs (gray) do not show a delayed Ph positivity compared to actively proliferating cells (black). At each time point, the proportion of malignant quiescent stem cells is almost identical to the proportion of malignant proliferating precursors.

In the results shown so far, only 2 of 4 qualitative criteria could be met. Hence, a second parameter alteration had to be considered. Because there is evidence that leukemia cells show an unregulated cellular proliferation [Eaves et al., 1986], the transition characteristic f_ω of malignant stem cells, which normally depends on the absolute number of proliferating stem cells, was set to constant at a high level. The described alteration results in a cell number-independent and, therefore, in an unregulated activation of malignant cells into cycle.

Using this additional parameter modification, the system dynamics change in such a way that all 4 criteria can be met. The alteration of f_ω has to complement the change in either differentiation rate d, transition characteristic f_α

Table 2. Model parameter set for normal hematopoiesis

Parameter	Value
a_{min}	0.002
a_{max}	1.0
d	1.05
r	1.1
τ_c	48 h
τ_S	8 h
$\tau_{G_2/M}$	8 h
$\tilde{\tau}_c$	24 h
λ_p	20 days
λ_m	8 days
$f_\alpha(0)$	0.5
$f_\alpha(\tilde{N}_A/2)$	0.45
$f_\alpha(\tilde{N}_A)$	0.01
$f_\alpha(\infty)$	0.0
$\tilde{N}_A$	10^3
$f_\omega(0)$	0.5
$f_\omega(\tilde{N}_\Omega/2)$	0.3
$f_\omega(\tilde{N}_\Omega)$	0.1
$f_\omega(\infty)$	0.0
$\tilde{N}_\Omega$	10^3

The given parameters are capable of maintaining a normal steady-state hematopoiesis in silico. The parameters are as follows: (a_{min}, a_{max}) = range of affinity a that characterizes the propensity of a cell to reside in **A**; d = differentiation coefficient; r = regeneration coefficient; τ_c = cell cycle duration of stem cells; τ_S, $\tau_{G_2/M}$ = durations of S- and G_2/M-phase; $\tilde{\tau}_c$ = generation time of proliferating differentiated cells; λ_p = transition time for proliferating precursor cell stages; λ_m = life time of nonproliferating precursor cell stages and mature, terminally differentiated cells; f_α, f_ω = transition characteristics for change from Ω to **A** and **A** to Ω; $f_\alpha(\cdot)$, $f_\omega(\cdot)$ = function values of transition characteristic at given argument; $\tilde{N}_A$, $\tilde{N}_\Omega$ = scaling factors of transition characteristics.

Table 3. Parameter changes giving rise to a dominant clone

Parameter	Ph–	Ph+
$f_\alpha(\tilde{N}_A)$	0.01	0.015
d	1.05	1.045
τ_c	48 h	45 h

Each of these 3 parameter alterations, applied to a single normal (Ph–) stem cell, is capable of giving rise to a dominant clone (Ph+). Parameters are as follows: $f_\alpha(\tilde{N}_A)$ = function value of transition characteristic f_α (describing the transition from the proliferating to the quiescent compartment) at cell number $\tilde{N}_A = 10^3$; d = differentiation coefficient; τ_c = cell cycle duration.

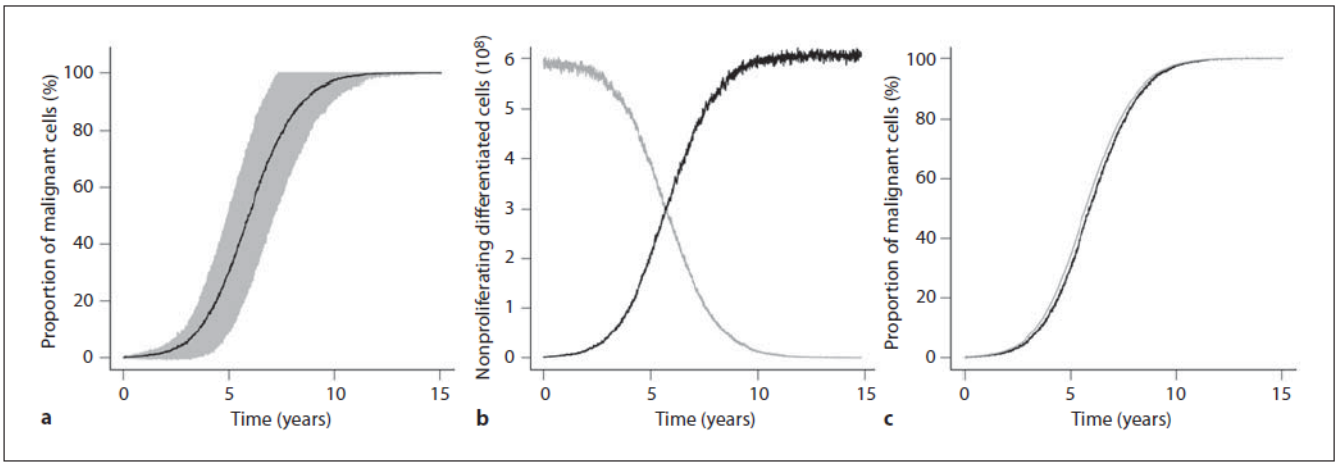

Fig. 3. CML genesis (1 altered model parameter), showing the scenario in which differences between normal and malignant cells are assumed for transition characteristic f_α. The other 2 scenarios are omitted because they are qualitatively identical. Each panel represents an average of 100 individual simulation runs. **a** Proportion of malignant nonproliferating differentiated cells (solid line) over 15 years postmutation. The gray shade indicates ± 1 SD. **b** Absolute cell counts in the nonproliferating differentiated cell compartment of normal (gray) and malignant (black) cells. **c** Proportion of cycling (black) and noncycling (gray) leukemia stem cells.

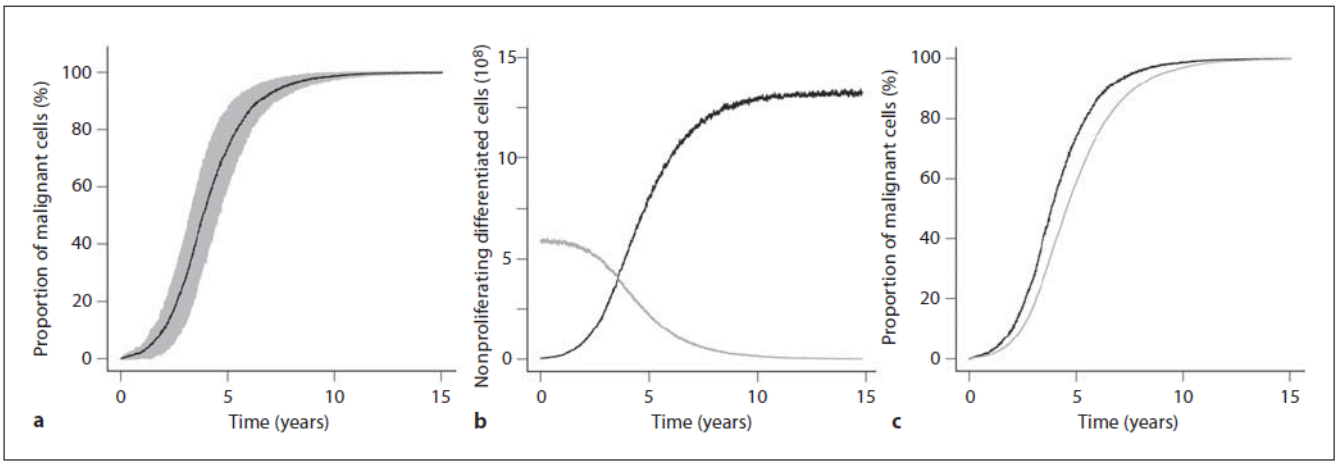

Fig. 4. CML genesis (2 altered model parameters), showing the scenario in which normal and malignant stem cells are assumed to differ in their transition characteristics f_α and f_ω (scenario 1). The other 2 scenarios are omitted because they are qualitatively identical. All graphs have been obtained averaging 100 individual simulation runs. **a** Proportion of malignant nonproliferating differentiated cells ± SD. **b** Absolute cell counts of normal (gray) and malignant (black) nonproliferating differentiated cells. **c** Proportion of actively proliferating (black) and quiescent (gray) malignant stem cells.

or cell cycle duration τ_c at the moment of the single-cell mutation. It should explicitly be noted that altering transition characteristic f_ω alone is not sufficient to induce a growth advantage necessary for the emergence of a dominant clone, because this parameter does neither influence criteria 1 nor 2. This means that changes in model parameters d, f_α or τ_c are required for clonal dominance, while the increased production of malignant cells, as well as the delayed Ph positivity of quiescent Ph+ stem cells are induced by the alteration of model parameter f_ω.

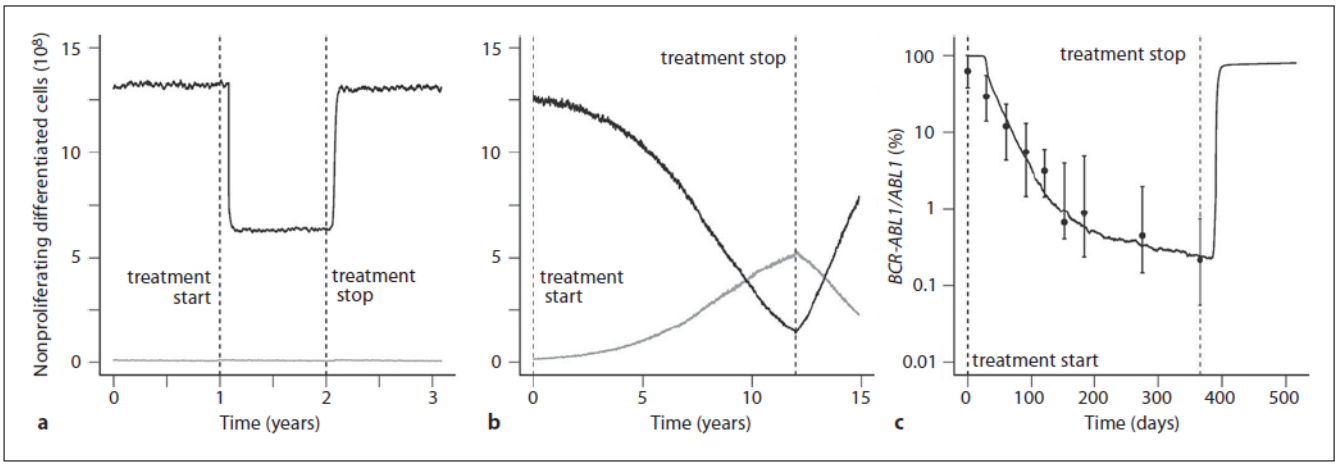

Fig. 5. CML treatment. All plots represent averages of 100 individual computer simulations. Shown is the scenario in which normal and malignant stem cells are assumed to differ in their transition characteristics f_α and f_ω (scenario 1). **a** HU treatment. Treatment is applied from year 1 to year 2 (as indicated by the dashed lines). Absolute numbers of normal (gray) and malignant (black) nonproliferating differentiated cells are shown. **b** IFN-α treatment. Treatment starts at time point zero and ends at the indicated time point. Normal (gray) and malignant (black) nonproliferating differentiated cells are shown. **c** IM treatment. Data points represent clinical measurements of *BCR-ABL1/ABL1* ratios, which are taken from Roeder et al. [2006]. The solid line shows the corresponding computer simulation.

Upon altering either of the parameter combinations f_α and f_ω (in the following referred to as scenario 1), d and f_ω (scenario 2) or τ_c and f_ω (scenario 3) for 1 proliferating stem cell, the results shown in figure 4 can be obtained (compare to fig. 3 for the situation of only 1 altered parameter value). Please note that in order to avoid redundancy, only 1 of the 3 scenarios is illustrated.

Scenarios 1, 2 and 3 are qualitatively identical, yet they represent different functional mechanisms potentially associated with the emergence of CML. Thus, an important goal was to discriminate between the scenarios by testing whether either of these is capable of reproducing clinically observed data on CML treatment strategies.

CML Treatment

First, HU treatment was analyzed. An unspecific kill of both normal and leukemia cells in S-phase at a constant rate of 2% per time step was applied to all 3 aforementioned CML scenarios. Because no estimates of this rate were available in the literature data, it was chosen arbitrarily. Therefore, it allows only for a qualitative analysis of the system behavior.

Due to the constant kill rate, cell numbers reach a much lower steady-state level, that is, a significant hematologic response can be observed. After cessation of therapy, the cell count rapidly returns to its pretreatment level. As HU was assumed to affect hematopoietic cells regardless of genotype, the cell count of both leukemia and normal cells is reduced. Please note that this reduction is only detectable with respect to malignant cells owing to the small number of normal cells. However, there is no change in the proportion of malignant cells during HU treatment, which also points to an equal relative cell number reduction of both cell types. Hence, a cytogenetic remission cannot be induced. In all scenarios, the procedure yields the results shown in figure 5a, that is, based on HU treatment, discrimination between the 3 scenarios is not possible.

IFN-α treatment was simulated by altering the model parameters, which are capable of explaining the dominance of the malignant clone. That is, at the moment of treatment initiation, transition characteristic f_α (scenario 1), differentiation rate d (scenario 2) or cell cycle duration τ_c (scenario 3) of malignant cells are reset to the values assumed for normal cells. Transition characteristic f_ω, however, remains unchanged. For the sake of simplicity, all cells were assumed to be simultaneously affected. Due to the applied parameter alterations, the growth advantage of the malignant clone is undone, resulting in a slow reduction of leukemia cells. At the same time, the popu-

lation of normal cells recovers slowly. Hence, significant hematologic as well as cytogenetic remissions can be observed in silico. After cessation of therapy, even after continuous IFN-α administration for several years, a clinically relevant relapse can be expected. In any of the 3 CML scenarios the results shown in figure 5b can be obtained, that is, a discrimination of the 3 scenarios by IFN-α treatment is not possible.

Finally, the simulation results were compared to clinical data on *BCR-ABL1* transcript levels of IM-treated CML patients. It was found that only scenario 1 was capable of reproducing the typical biphasic decline of *BCR-ABL1* transcript levels during the first year of IM treatment as well as the rapid relapse upon treatment cessation (fig. 5c). In scenario 1, differences between normal and leukemic cells in the transition characteristics f_α and f_ω are assumed, which can be interpreted as differences in the stem cell-microenvironment interaction (for example, stroma attachment/detachment kinetics). Fitting the mathematical model to the quantitative clinical data [Roeder et al., 2006], degradation rate r_{deg} and inhibition rate r_{inh} were estimated to be 2.8 and 5.0% per time step, respectively. The first (steep) decline is caused by a massive initial reduction of proliferating leukemia cells due to the selective degradation effect. The second (moderate) decline is induced by the dynamic regulation of the system in response to the initial cell reduction. The model predicts leukemic stem cells to accumulate in compartment **A** (that is, quiescent stem cells) during IM therapy. These cells are responsible for the rapid relapse of *BCR-ABL1* transcript levels after treatment stop.

Discussion

It could be shown that CML development can be explained as a clonal competition process of normal and malignant cells, induced by quantitative differences in cellular properties. It can be stated that the situation of human hematopoiesis, in particular the situation of chronic myeloid leukemia, can be explained within the context of a general concept of tissue stem cell organization, which is accounting for cell-cell and cell-microenvironment interactions, and which allows for a flexible and reversible development of cellular phenotypes [Loeffler and Roeder, 2002; Roeder and Loeffler, 2002].

Quantitative differences in at least 1 of 3 model parameters (differentiation coefficient d, transition characteristic f_α, cell cycle time τ_c) were found to be capable of inducing a dominant clone, which at first coexists with normal cells for a couple of years, but ultimately takes over the hematopoietic system. It is sufficient to apply the parameter alteration to exactly 1 actively proliferating stem cell, representing a single-cell mutation, to induce a macroscopic CML.

Note that owing to clonal fluctuations, this potential is only realized in about 20% of the cases. Hence, our model predicts that the formation of Ph does not necessarily lead to the formation of CML. This result seems to be confirmed by reports that very low levels of Ph+ cells can be detected in healthy individuals, who, in the long run, do not develop CML [Biernaux et al., 1995]. It can be speculated that in about 80% of the cases the initially very small neoplastic clone might not be able to maintain its own population, but differentiates and finally undergoes apoptosis. Interestingly, another group, which used a fundamentally quite different mathematical model to analyze general issues of clonal domination in myeloproliferative disorders, found a similar percentage of about 80% [Catlin et al., 2005]. It must be mentioned, however, that the authors fitted their model to adequately reproduce mouse and cat data; they did not apply it to the human situation. Catlin et al. [2005] explain the dominance of the malignant clone without any modification of cellular properties but by extra stem cell-supporting resources (for example, alternative niches in the spleen or liver) that only neoplastic HSCs can make use of.

Within our proposed model, differentiation rate d can be interpreted as the velocity of stem cell differentiation. Parameter d of neoplastic cells needs to be decreased to induce the necessary growth advantage, which might correspond to a retarded differentiation process of malignant stem cells. In the clinical situation, highly immature myeloid cells can be found in peripheral blood [Goldman and Melo, 2003]. This observation might relate to an impaired differentiation process of leukemia stem cells. However, the impaired regulation might as well be induced at more mature cell stages.

Because 1 prominent mechanism involved in HSC quiescence is the adhesion to bone marrow stroma, transitions of cells from signaling context **Ω** (actively dividing cells) to **A** (quiescent cells) can be interpreted as stroma attachment processes. Based on this interpretation, an altered transition characteristic f_α in leukemia cells represents a defective adhesion to bone marrow stroma, which has also been reported experimentally [Gordon et al., 1987; Bhatia et al., 1995].

The third critical parameter alteration (cell cycle time τ_c) that was proposed by the model analysis has so far not been reported in the literature, as data on human in vivo

cell kinetics (for example, cycle time distributions) are lacking almost completely.

Additionally to each of these parameter changes, transition characteristic f_ω of neoplastic cells was set to constant at a high level in order to induce an increased production of leukemia cells. This parameter alteration can be interpreted as an unregulated and increased activation of quiescent stem cells into cycle. Such observations can also be found in the literature [Eaves et al., 1986].

We would like to emphasize that within the proposed model, only the given parameter values are capable of inducing the desired model behavior, represented by the criteria stated above. Different parameter values necessarily result in a different competitive behavior of the clones (normal, malignant) and, for example, thus fail to reproduce criterion 1, that is, the delay from the initial malignant transformation to the formation of a manifest CML which is estimated to be about 5–7 years.

In the present work, we could demonstrate that the proposed model consistently explains a variety of clinical data on CML monotherapies such as HU, IFN-α and IM. Qualitative data on HU treatment can be reproduced based on the assumption of a constant kill rate of S-phase cells, independent of genotype. This conforms to biological insights regarding modes of action of HU [de Lima et al., 2003]. Qualitative data on IFN-α therapy can be explained under the assumption that the model parameters of malignant cells, which are capable of explaining the clonal dominance (for example, transition characteristic f_α), are reset to the values assumed for normal cells. Such a normalization of cellular properties could also be observed in biological experiments with respect to adhesion to bone marrow stroma [Bhatia et al., 1994]. This model assumption, however, which predicts a complete eradication of the malignant clone after about 15 years of treatment (fig. 5b), is likely to represent only the theoretically best possible scenario for IFN-α therapy. As there are no reports on the cure of CML with continuous IFN-α administration, it can be speculated that in the clinical situation the growth advantage of malignant cells is only reduced but not entirely eliminated. Please note that the assumption made for IFN-α treatment is sufficient to induce significant cytogenetic remissions, that is, no explicit cell kill has to be assumed.

Beyond the qualitative description of the HU/IFN-α effects, the model is capable of explaining quantitative clinical data on IM treatment [Roeder et al., 2006] by assuming 2 different functional mechanisms. First, a constant degradation rate was applied selectively for proliferative leukemia cells. This conforms to reports on an increased apoptotic rate of malignant cells [Oetzel et al., 2000; Vigneri and Wang, 2001; Holtz et al., 2007]. Second, selectively for leukemia cells, transition characteristic f_ω was decreased to a lower constant level. This can be interpreted as follows: IM reduces the rate at which leukemia cells are activated into cycle. Therefore, the excessive proliferation of malignant cells can be stopped. However, stroma detachment kinetics are still unregulated, that is, independent of cell numbers. The decrease in f_ω has no impact on the biphasic decline kinetics of *BCR-ABL1* transcript levels, but as a result a considerable number of malignant cells is kept in a quiescent state during therapy. Upon cessation of treatment, the therapy-induced reduction of cell cycle activity is replaced by a rapid activation of a large amount of malignant G_0 stem cells into cycle, resulting in the clinically observed rapid relapse of *BCR-ABL1* transcript levels. The potential accumulation of quiescent leukemia stem cells in the course of IM treatment leads to the model prediction of a benefit of the application of proliferation stimulating drugs additional to IM [Roeder et al., 2006]. This strategy has also been suggested experimentally. Jorgensen et al. [2006] and Holtz et al. [2007] performed in vitro studies and found that quiescent stem cells are resistant to IM therapy but can be activated into cycle by cytokines such as G-CSF, rendering them more accessible to IM therapy.

Only 1 of 3 model scenarios, which are capable of inducing CML, is additionally capable of explaining the quantitative clinical data on IM therapy. It is the scenario which assumes parameter differences between normal and malignant cells in transition characteristics f_α and f_ω. The other 2 scenarios, involving differentiation rate d and cell cycle duration τ_c, neither reproduce the typical biphasic decline kinetics of *BCR-ABL1* transcript levels nor the observed rapid relapse after termination of therapy.

Concluding from our theoretical results, we suggest that neither a retarded differentiation process of primitive stem cells nor different cell cycle time distributions in leukemia cells underlie the observed phenomena. Instead, we suggest differences in the dynamic regulation of cell-to-stroma attachment/detachment kinetics as possible key pathologic mechanisms. However, additional influences of, for instance, an impaired differentiation process, particularly of leukemia precursor cells, cannot be ruled out.

The quantitative model presented in this study represents human hematopoiesis in a simplified fashion. Therefore, transition characteristics f_α and f_ω subsume a

variety of cell-intrinsic and cell-extrinsic factors, for example, complex interactions of growth factors. In reality, this is most likely a high-dimensional system. Furthermore, the presented mathematical model does not discriminate between different functional end cells, that is, lineage commitment has been ignored completely at this stage. In hematopoietic disorders such as CML, however, the overproduction of particular lineages, for example myeloid blood cells, is an important endpoint, which was not investigated in this work owing to the limitations of the model. These processes, which can also be explained within the general concept of this model [Glauche et al., 2007a], have to be incorporated in a future version. Another simplification affects mature cell stages, which are called differentiated cells in the model. Feedback mechanisms from more mature cell stages into stem cell regulation processes are not yet included. The same is true for regulatory mechanisms of differentiated cell stages. As a technical consequence, kill rates have exclusively been applied to stem cells. There is no dynamic regulation in the model which compensates for an increased death rate of differentiated cells, for example by an increased amplification of previous cell stages. Consequently, treatment interventions may result in a short-term underestimation of absolute numbers of differentiated cell stages.

Despite these limitations, the stochastic model used in this paper is still the most comprehensive mathematical model which has so far been applied to the situation of CML. Previous model approaches could explain only a subset of the experimentally and clinically observed phenomena. Michor et al. [2005] used a 4-compartment model approach based on a hierarchical view of hematopoietic differentiation. They show that their model can reproduce clinical data on IM treatment on a short time scale of 1 year. The authors conclude from their model analysis that leukemia stem cells are not at all depleted by IM therapy. This statement has since been controversially discussed [Glauche et al., 2007b; Michor, 2007]. Furthermore, it is assumed that normal and malignant cells grow totally independent of each other. As this presumption seems to be unlikely, the authors recently presented a more sophisticated model, which assumes a competition process between normal and malignant cells [Dingli and Michor, 2006]. This model is in principle also able to consistently explain short- and long-term *BCR-ABL1* transcript dynamics.

It could be shown in the present study that the applied stochastic model represents a powerful tool to study emergence and development of CML. Furthermore, this work provides the first systematic model analysis of the functional mechanisms potentially associated with CML emergence. It will be a future challenge to further contribute to a better understanding of the disease. For example, IM resistance, which currently represents a major obstacle to successful treatment, will be analyzed from a modeling point of view. So-called secondary mutations, which are thought to play an important role in IM resistance, are currently neglected in our modeling analyses. They will be considered in future studies. Furthermore, mathematical modeling might contribute to an optimization of treatment planning.

Appendix

The presented model is mathematically represented as a single-cell-based, stochastic process. This means that the development of each individual cell in the system is simulated according to a set of defined rules including stochastic decisions. These rules are applied at discrete time steps ($\Delta t = 1$ h) to simultaneously update the status of all model cells. Each cell is characterized by a triple $[a(t), m(t), c(t)]$, defined by its affinity $a(t) \in \{0\} \cup [a_{min}, a_{max}]$, its signaling context $m(t) \in \{\mathbf{A}, \Omega\}$ and its position in the cell cycle $c(t) \in \{0,1, \ldots, \tau_c\}$, with τ_c representing the cell cycle time. To realize an update step, the actual total number of stem cells in $\mathbf{A}$ and Ω $[N_A(t), N_\Omega(t)]$ is determined. Based on these numbers, the new status of each model cell $[a(t+1), m(t+1), c(t+1)]$ is calculated as follows.

(1) If the cell resides in signaling context $\mathbf{A}$, it changes to Ω or stays in $\mathbf{A}$ with probabilities $\omega = a_{min}/a(t) \cdot f_\omega[N_\Omega(t)]$ and $1 - \omega$, respectively, where f_ω denotes the transition characteristic describing the change from $\mathbf{A}$ to Ω (see below). If the cell stays in $\mathbf{A}$, its affinity a is increased by multiplication with regeneration coefficient $r \geq 1$ $[a(t+1) = a(t) \cdot r]$, until a has reached its maximum value a_{max}. If the cell changes to signaling context Ω $[m(t+1) = \Omega]$, its position in the cell cycle is set to the beginning of S-phase $[c(t+1) = c_1]$, which is calculated by $c_1 = \tau_c + (\tau_S + \tau_{G_2/M})$. Here, τ_S denotes the length of S-phase and $\tau_{G_2/M}$ defines the combined duration of G_2- and M-phase.

(2) If the cell resides in signaling context Ω, it changes to $\mathbf{A}$ or stays in Ω with probabilities $\alpha = a(t)/a_{max} \cdot f_\alpha[N_A(t)]$ and $1 - \alpha$, respectively, where f_α denotes the transition characteristic describing the change from Ω to $\mathbf{A}$ (see below). Herein, a change to signaling context $\mathbf{A}$ is only possible in G_1-phase of the cell cycle, that is, $c(t) < c_1$. If the cell changes to $\mathbf{A}$, only its signaling context is modified $[m(t+1) = \mathbf{A}]$. If it stays in Ω, it is tested whether a has already reached its minimum value a_{min}. If not, a is decreased by division by differentiation coefficient $d \geq 1$ $[a(t+1) = a(t)/d]$ and the cell cycle position is incremented $[c(t+1) = c(t) + 1]$. In case of cell cycle completion [that is, $c(t) > \tau_c$], $c(t+1)$ is set to zero and a new identical cell is generated (cell division). If, in contrast, a has reached the minimum value a_{min}, it is set to zero and the cell is considered to start a terminal differentiation program. This means that the cell initiates a clone with a fixed life time $\lambda = \lambda_p + \lambda_m$. Herein, the first period λ_p represents the status of proliferating precursors where the clone still amplifies with a duplica-

tion time $\tilde{\tau}_c$. The second period λ_m represents the status of non-proliferating precursors and mature cells (for a schematic of the model, see fig. 1).

The transition probabilities α and ω depend on the actual affinity of the cell $a(t)$, on the fixed parameters a_{min} and a_{max}, and on the transition characteristics $f_\alpha[N_A(t)]$ and $f_\omega[N_\Omega(t)]$, respectively. The latter 2 functions depend on the total number of stem cells (N_A, N_Ω) in the respective target signaling contexts. They are modeled by a general class of sigmoid functions:

$$f_{\alpha/\omega}(N_{A/\Omega}) = \frac{1}{\nu_1 + \nu_2 \cdot \exp\left(\nu_3 \frac{N_{A/\Omega}}{\tilde{N}_{A/\Omega}}\right)} + \nu_4$$

The parameters ν_1, ν_2, ν_3 and ν_4 determine the shape of $f_{\alpha/\omega}$. $\tilde{N}_{A/\Omega}$ is a scaling factor for $N_{A/\Omega}$. It is possible to uniquely determine ν_1, ν_2, ν_3 and ν_4 by the more intuitive values $f_{\alpha/\omega}(0)$, $f_{\alpha/\omega}(\tilde{N}_{A/\Omega}/2)$, $f_{\alpha/\omega}(\tilde{N}_{A/\Omega})$ and $f_{\alpha/\omega}(\infty) := \lim_{N_{A/\Omega}\to\infty} f_{\alpha/\omega}(N_{A/\Omega})$:

$$\nu_1 = (h_1 h_3 - h_2^2)/(h_1 + h_3 - 2h_2)$$
$$\nu_2 = h_1 - \nu_1$$
$$\nu_3 = \ln[(h_3 - \nu_1)/\nu_2]$$
$$\nu_4 = f_{\alpha/\omega}(\infty)$$

with

$$h_1 = 1/[f_{\alpha/\omega}(0) - f_{\alpha/\omega}(\infty)]$$
$$h_2 = 1/[f_{\alpha/\omega}(\tilde{N}_{A/\Omega}/2) - f_{\alpha/\omega}(\infty)]$$
$$h_3 = 1/[f_{\alpha/\omega}(\tilde{N}_{A/\Omega}) - f_{\alpha/\omega}(\infty)].$$

Examples of transition characteristics f_α and f_ω can be found in figure 2. For exact parameter values used in the computer simulations, see table 2.

References

Bhatia, R., E.A. Wayner, P.B. McGlave, C.M. Verfaillie (1994) Interferon-α restores normal adhesion of chronic myelogenous leukemia hematopoietic progenitors to bone marrow stroma by correcting impaired β1 integrin receptor function. J Clin Invest *94:* 384–391.

Bhatia, R., P.B. McGlave, G.W. Dewald, B.R. Blazar, C.M. Verfaillie (1995) Abnormal function of the bone marrow microenvironment in chronic myelogenous leukemia: role of malignant stromal macrophages. Blood *85:* 3636–3645.

Biernaux, C., M. Loos, A. Sels, G. Huez, P. Stryckmans (1995) Detection of major BCR-ABL gene expression at a very low level in blood cells of some healthy individuals. Blood *86:* 3118–3122.

Branford, S., T.P. Hughes, Z. Rudzki (1999) Monitoring chronic myeloid leukaemia therapy by real-time quantitative PCR in blood is a reliable alternative to bone marrow cytogenetics. Br J Haematol *107:* 587–599.

Buchdunger, E., J. Zimmermann, H. Mett, T. Meyer, M. Muller, B.J. Druker, N.B. Lydon (1996) Inhibition of the Abl protein-tyrosine kinase in vitro and in vivo by a 2-phenylaminopyrimidine derivative. Cancer Res *56:* 100–104.

Catlin, S.N., P. Guttorp, J.L. Abkowitz (2005) The kinetics of clonal dominance in myeloproliferative disorders. Blood *106:* 2688–2692.

Deininger, M.W., J.M. Goldman, J.V. Melo (2000) The molecular biology of chronic myeloid leukemia. Blood *96:* 3343–3356.

de Lima, P.D., P.C. Cardoso, A.S. Khayat, M. de Oliveira Bahia, R.R. Burbano (2003) Evaluation of the mutagenic activity of hydroxyurea on the G1-S-G2 phases of the cell cycle: an in vitro study. Genet Mol Res *2:* 328–333.

Dingli, D., F. Michor (2006) Successful therapy must eradicate cancer stem cells. Stem Cells *24:* 2603–2610.

Druker, B.J., S. Tamura, E. Buchdunger, S. Ohno, G.M. Segal, S. Fanning, J. Zimmermann, N. B. Lydon (1996) Effects of a selective inhibitor of the Abl tyrosine kinase on the growth of Bcr-Abl positive cells. Nat Med *2:* 561–566.

Dube, I.D., C.M. Gupta, D.K. Kalousek, C.J. Eaves, A.C. Eaves (1984) Cytogenetic studies of early myeloid progenitor compartments in Ph1-positive chronic myeloid leukaemia (CML). I. Persistence of Ph1-negative committed progenitors that are suppressed from differentiating in vivo. Br J Haematol *56:* 633–644.

Eaves, A.C., J.D. Cashman, L.A. Gaboury, D.K. Kalousek, C.J. Eaves (1986) Unregulated proliferation of primitive chronic myeloid leukemia progenitors in the presence of normal marrow adherent cells. Proc Natl Acad Sci USA *83:* 5306–5310.

Glauche, I., M. Cross, M. Loeffler, I. Roeder (2007a) Lineage specification of hematopoietic stem cells: mathematical modeling and biological implications. Stem Cells *25:* 1791–1799.

Glauche, I., M. Horn, I. Roeder (2007b) Leukaemia stem cells: hit or miss? Br J Cancer *96:* 677–678.

Goldman, J.M., J.V. Melo (2003) Chronic myeloid leukemia – advances in biology and new approaches to treatment. N Engl J Med *349:* 1451–1464.

Goldman, J., M. Gordon (2006) Why do chronic myelogenous leukemia stem cells survive allogeneic stem cell transplantation or imatinib: does it really matter? Leuk Lymphoma *47:* 1–7.

Gordon, M.Y., C.R. Dowding, G.P. Riley, J.M. Goldman, M.F. Greaves (1987) Altered adhesive interactions with marrow stroma of haematopoietic progenitor cells in chronic myeloid leukaemia. Nature *328:* 342–344.

Hehlmann, R., H. Heimpel, J. Hasford, H.J. Kolb, H. Pralle, D.K. Hossfeld, W. Queisser, H. Loffler, B. Heinze, A. Georgii et al. (1993) Randomized comparison of busulfan and hydroxyurea in chronic myelogenous leukemia: prolongation of survival by hydroxyurea. The German CML Study Group. Blood *82:* 398–407.

Hehlmann, R., H. Heimpel, J. Hasford, H.J. Kolb, H. Pralle, D.K. Hossfeld, W. Queisser, H. Loffler, A. Hochhaus, B. Heinze, et al. (1994) Randomized comparison of interferon-α with busulfan and hydroxyurea in chronic myelogenous leukemia. The German CML Study Group. Blood *84:* 4064–4077.

Holtz, M., S.J. Forman, R. Bhatia (2007) Growth factor stimulation reduces residual quiescent chronic myelogenous leukemia progenitors remaining after imatinib treatment. Cancer Res *67:* 1113–1120

Ichimaru, M., T. Ishimaru, M. Mikami, Y. Yamada, T. Ohkita (1981) Incidence of leukemia in a fixed cohort of atomic bomb survivors and controls, Hiroshima and Nagasaki, October 1950–December 1978. Technical Report No. 13-81. Hiroshima, Radiation Effects Research Foundation.

Jorgensen, H.G., M. Copland, E.K. Allan, X. Jiang, A. Eaves, C. Eaves, T. Holyoake (2006) Intermittent exposure of primitive quiescent chronic myeloid leukemia cells to granulocyte-colony stimulating factor in vitro promotes their elimination by imatinib mesylate. Clin Cancer Res *12:* 626–633.

- Loeffler, M., I. Roeder (2002) Tissue stem cells: definition, plasticity, heterogeneity, self-organization and models – a conceptual approach. Cells Tissues Organs *171:* 8–26.
- Mauro, M.J., B.J. Druker (2001) Chronic myelogenous leukemia. Curr Opin Oncol *13:* 3–7.
- Michor, F., T.P. Hughes, Y. Iwasa, S. Branford, N.P. Shah, C.L. Sawyers, M.A. Nowak (2005) Dynamics of chronic myeloid leukemia. Nature *435:* 1267–1270.
- Michor, F. (2007) The long-term response to imatinib treatment of CML. Br J Cancer *96:* 679–680.
- Oetzel, C., T. Jonuleit, A. Gotz, H. van der Kuip, H. Michels, J. Duyster, M. Hallek, W.E. Aulitzky (2000) The tyrosine kinase inhibitor CGP 57148 (STI 571) induces apoptosis in BCR-ABL-positive cells by down-regulating BCL-X. Clin Cancer Res *6:* 1958–1968.
- Parmar, S., L.C. Platanias (2003) Interferons: mechanisms of action and clinical applications. Curr Opin Oncol *15:* 431–439.
- Roeder, I., M. Loeffler (2002) A novel dynamic model of hematopoietic stem cell organization based on the concept of within-tissue plasticity. Exp Hematol *30:* 853–861.
- Roeder, I., L.M. Kamminga, K. Braesel, B. Dontje, G. de Haan, M. Loeffler (2005) Competitive clonal hematopoiesis in mouse chimeras explained by a stochastic model of stem cell organization. Blood *105:* 609–616.
- Roeder, I., M. Horn, I. Glauche, A. Hochhaus, M.C. Mueller, M. Loeffler (2006) Dynamic modeling of imatinib-treated chronic myeloid leukemia: functional insights and clinical implications. Nat Med *12:* 1181–1184.
- Savage, D.G., K.H. Antman (2002) Imatinib mesylate – a new oral targeted therapy. N Engl J Med *346:* 683–693.
- Tauchi, T., K. Ohyashiki (2004) Molecular mechanisms of resistance of leukemia to imatinib mesylate. Leuk Res *28(suppl 1):* S39–S45.
- Verma, A., L.C. Platanias (2002) Signaling via the interferon-α receptor in chronic myelogenous leukemia cells. Leuk Lymphoma *43:* 703–709.
- Vigneri, P., J.Y. Wang (2001) Induction of apoptosis in chronic myelogenous leukaemia cells through nuclear entrapment of BCR-ABL tyrosine kinase. Nat Med *7:*156–157.

2. Eingeschlossene Publikationen

2.1 „Leukaemia stem cells: hit or miss?“ (Publikation 1)

Glauche I, Horn M, Roeder I; *Br J Cancer*. 2007;96(4):677-678

Im Zusammenhang mit der Publikation der Ergebnisse meiner Diplomarbeit (16) in *Nature Medicine* (17) und *Cells Tissues Organs* (siehe Vorarbeiten) zeigte sich, dass hinsichtlich der Modellannahme einer IM-suszeptiblen LSC-Population in der wissenschaftlichen Community kein Konsens besteht. Eine andere Gruppe (F. Michor und Kollegen) hatte ein dynamisches CML-Modell publiziert, in dem insgesamt vier verschiedene Zellpopulationen betrachtet werden: Stammzellen, Progenitorzellen, differenzierte Zellen sowie terminal differenzierte Zellen (43). Die vier Kompartimente, welche unidirektional in Reihe geschaltet sind, repräsentieren Zellstufen der Hämatopoese. Das mit gewöhnlichen Differentialgleichungen (ODE) beschriebene Modell wurde an IM-Therapie-Daten nach einjährigem Follow-up angepasst. Motiviert durch die Beobachtung schneller molekularer Rückfälle nach Therapieabbruch (insgesamt lagen drei entsprechende Fälle vor) basiert das Modell auf der Annahme, dass Stammzellen von IM in keiner Weise angegriffen werden, sondern auch unter Therapie weiter (exponentiell) expandieren. Diese Zellpopulation ist gemäß der Hypothese der Autoren für den raschen Wiederanstieg der Tumorlast nach Ende der Behandlung verantwortlich.

Die Tatsache, dass die Autoren ihre Annahme, gegeben die vorliegenden Daten, als alternativlos darstellen[2], war Motivation für das Verfassen eines „Letter to the Editor“. Wir stellen darin fest, dass die Anpassung unseres ABM an Einjahresdaten auch gelingt, wenn wir eine IM-Wirkung auf (proliferative) LSCs postulieren. Weiterhin liefert längeres Follow-up (ca. fünf Jahre) Evidenz für eine kontinuierliche Reduktion der Tumorlast unter IM-Therapie. Diese Dynamik kann unser Modell mit längerer Simulationszeit ohne Parameteränderungen reproduzieren. Wir zeigen darüber hinaus, dass das publizierte ODE-Modell selbst unter fortgesetzter IM-Therapie bereits im zweiten Behandlungsjahr einen Wiederanstieg der *BCR-ABL*-Transkriptlevel vorhersagt, was im Widerspruch zu den beobachteten klinischen Daten steht.

Natürlich ist auch unser Modell nicht die einzig mögliche Hypothese. In Anbetracht der gegenwärtig verfügbaren Daten zur IM-Langzeittherapie scheint jedoch eine Unterscheidung der LSCs hinsichtlich ihrer Zellzyklusaktivität (proliferierend, ruhend) essentiell zu sein.

[2] Originalwortlaut aus Abbott und Michor (61): “(...) the conclusion that leukemic stem cells cannot be depleted by imatinib can safely be drawn based on the available information.”

British Journal of Cancer (2007) 96, 677 – 678

www.bjcancer.com

Letter to the Editor

Leukaemia stem cells: hit or miss?

I Glauche*,[1], M Horn[1] and I Roeder[1]

[1]*Institute for Medical Informatics, Statistics and Epidemiology, Medical Faculty, University of Leipzig, Haertelstr. 16/18 04107, Leipzig, Germany*

British Journal of Cancer (2007) **96,** 677 – 678. doi:10.1038/sj.bjc.6603603 www.bjcancer.com
Published online 6 February 2007

Sir,

In their publication 'Mathematical models of targeted cancer therapy' Abbott and Michor (2006) emphasise the role of theoretical modelling for the understanding of cancer initiation, progression and treatment. Herein, they draw a number of general conclusions from a model of BCR-ABL1-positive chronic myeloid leukaemia (CML) under imatinib treatment that has recently been published by Michor *et al* (2005). This model relies on the existence of four subsequent compartments, through which haematopoietic cell differentiation proceeds. Chronic myeloid leukaemia development is initiated by the mutation of a single stem cell, and the expansion of the malignant (i.e. BCR-ABL1-positive) clone is assumed to be completely independent of the normal cells. Imatinib treatment, which is known to specifically affect BCR-ABL1-positive cells, is assumed to act on progenitor and differentiated cells only. In contrast, malignant stem cells are not affected and continue to expand exponentially. Abbott and Michor (2006) show that these assumptions are consistent with clinical data on BCR-ABL1 transcript levels during the first year of imatinib treatment as well as after treatment cessation.

Recent data on the long-term development of CML under imatinib monotherapy show a continuing decrease of BCR-ABL1 transcript levels even after the first year of treatment (Roeder *et al*, 2006) (Figure 1A). This long-term behaviour cannot be explained within the model of CML dynamics discussed by Abbott and Michor (2006). Owing to the contribution of CML cells from the

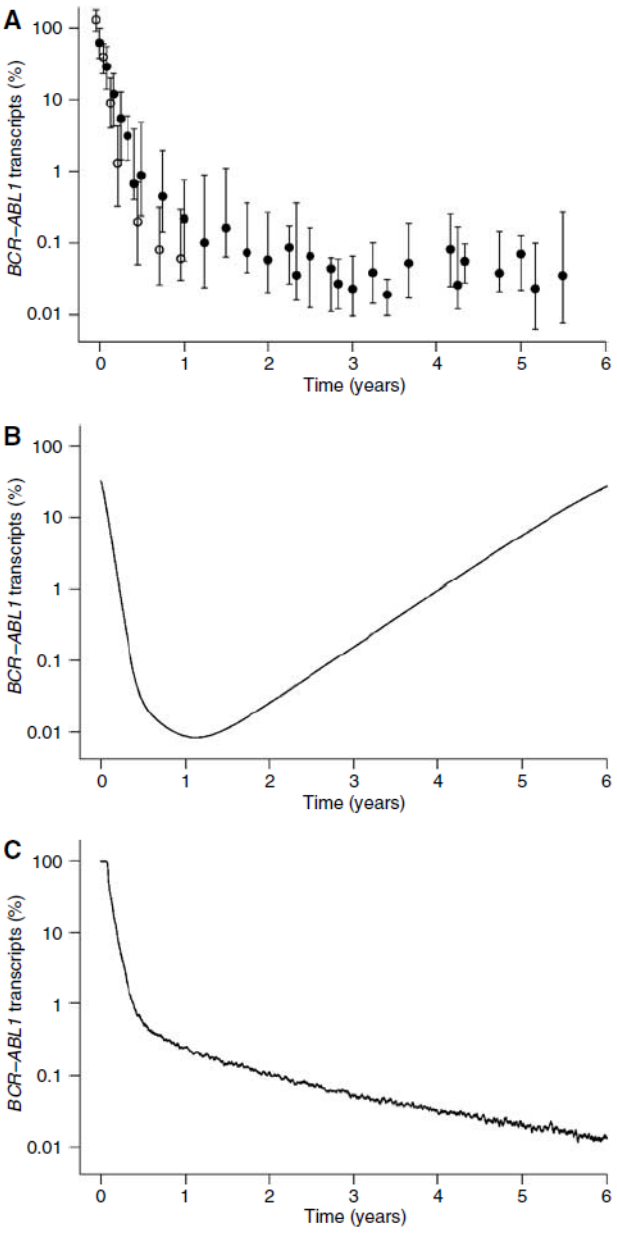

Figure 1 BCR-ABL1 transcript dynamics for CML under imatinib treatment: (**A**) Datapoints represent median and interquartile range of BCR-ABL1 transcript levels in peripheral blood, determined in two independent study populations: BCR-ABL1/BCR percentages of 68 individuals with imatinib-treated CML over 1 year, previously published by Michor *et al* (2005) (open circles) and BCR-ABL1/ABL1 percentages of 69 individuals with imatinib-treated CML from the German cohort of the IRIS trial over 5.5 years, previously published by Roeder *et al* (2006) (filled circles). (**B**) Long-term simulation results of BCR-ABL1 levels according to the model discussed by Abbott and Michor (2006). Parameters are taken from the original publication of this model (Michor *et al*, 2005). (**C**) Long-term simulation results of BCR-ABL1 levels according to the model introduced by Roeder *et al* (2006). Parameters are taken from the given reference.

*Correspondence: I Glauche;
E-mail: ingmar.glauche@imise.uni-leipzig.de
Published online 6 February 2007

exponentially growing malignant stem cell compartment, this model inevitably predicts a relapse of BCR-ABL1 transcript levels after about 1.5 years, even under continuing imatinib treatment and without the occurrence of resistance mutations (Figure 1B).

Within the aforementioned publication (Roeder *et al*, 2006), our group proposed an alternative explanation of the imatinib effect, which is consistent with the observed short- and long-term BCR-ABL1 levels (Figure 1C) as well as with the relapse dynamics after treatment cessation. In contrast to the model described by Abbott and Michor, we predict a selective imatinib effect on proliferating BCR-ABL1-positive cells, including stem cells, whenever they are activated into cell cycle.

In the light of the clinical long-term data, complemented by our alternative explanation of the imatinib effect, the statement by Abbott and Michor – 'the conclusion that leukaemic stem cells cannot be depleted by imatinib can safely be drawn' – cannot be uphold. In order to correctly describe the long-term dynamics of BCR-ABL1 transcript levels, certain modifications of the model are unavoidable. Such modifications could include a (possibly reduced) imatinib effect on malignant stem cells or a saturating growth kinetics of the malignant stem cell population.

It should be noted that although our explanation of the imatinib effect is consistent with the clinically observed long-term behaviour, it still remains a hypothesis and might not be without alternative. Particularly in comparison to the hypothesis discussed by Abbott and Michor (2006), the proposed role of the cell-cycle status of leukaemic stem cells might point to an important aspect of the imatinib effect and possibly other tyrosine kinase inhibitors. It is a particular strength of mathematical models to provide testable predictions and, therefore, to guide experimental and clinical research. However, a definite answer whether any proposed mode of imatinib action is true or not can only be given by data-based validation.

REFERENCES

Abbott LH, Michor F (2006) Mathematical models of targeted cancer therapy. *Br J Cancer* **95:** 1136 – 1141

Michor F, Hughes TP, Iwasa Y, Branford S, Shah NP, Sawyers CL, Nowak MA (2005) Dynamics of chronic myeloid leukaemia. *Nature* **435:** 1267 – 1270

Roeder I, Horn M, Glauche I, Hochhaus A, Mueller MC, Loeffler M (2006) Dynamic modeling of imatinib-treated chronic myeloid leukemia: functional insights and clinical implications. *Nat Med* **12:** 1181 – 1184

2.2 „Therapy of chronic myeloid leukaemia can benefit from the activation of stem cells: simulation studies of different treatment combinations“ (Publikation 2)

Glauche I, Horn K, Horn M, Thielecke L, Essers MAG, Trumpp A, Roeder I;
Br J Cancer. 2012;106(11):1742-1752

Ziel des Papers war es, mit Hilfe von Modellsimulationen die Frage zu beantworten, ob eine Kombinationstherapie aus TKI und IFN-α hinsichtlich MRD-Eradikation nützlich sein kann. Nachdem TKIs wie IM vor einigen Jahren IFN-α als Standardtherapie bei *de-novo*-CML abgelöst haben, ist zwar hinsichtlich Überlebens- und Remissionsraten unter IM eine enorme Verbesserung der Prognose zu beobachten (8), dennoch sind auch nach vielen Behandlungsjahren in den meisten Patienten residuale Leukämiezellen vorhanden, die nach Therapieende potenziell einen Rückfall auslösen (11). Es gibt Evidenz, dass hierfür ruhende LSCs verantwortlich sind (19). Wenn diese sich durch einen nichtproliferativen Zustand der TKI-Wirkung entziehen, könnte das Ziel einer Kombinationstherapie darin bestehen, LSCs in den Zellzyklus zu aktivieren und sie so der selektiven Zytotoxizität des TKIs auszusetzen. Eine Substanz, für die man im Mausexperiment stammzellaktivierendes Potenzial zeigen konnte, ist IFN-α (14).

Da die genaue Wirkweise von IFN-α bis heute unbekannt ist, wurden im Paper systematisch verschiedene Annahmen zu Grunde gelegt. Dabei werden drei verschiedene Dimensionen betrachtet: Die erste Dimension stellt die Frage, wie stark der aktivierende Effekt von IFN-α auf LSCs wirkt: (i) ebenso stark wie auf normale Stammzellen; (ii) deutlich schwächer als auf normale Zellen; (iii) überhaupt keine aktivierende Wirkung. Die zweite Dimension untersucht, welche Auswirkungen eine von IFN-α möglicherweise zusätzlich induzierte aberrante Selbsterneuerung hat. Die dritte Dimension betrachtet verschiedene Arten der Applikation: (i) kontinuierliche IFN-α- und TKI-Gabe; (ii) gepulstes IFN-α plus kontinuierliche TKI-Gabe; (iii) kontinuierliches IFN-α plus gepulste Verabreichung des TKI.

Unter den betrachteten idealen Voraussetzungen und Vereinfachungen führt eine kontinuierliche Gabe von TKI und IFN-α zu einer deutlich schnelleren Eradikation der residualen LSCs. Wird IFN-α aufgrund starker Nebenwirkungen nur gepulst verabreicht, verlangsamt sich die MRD-Eradikation, ist aber immer noch deutlich schneller als unter TKI-Monotherapie. Die Kombination mit IFN-α kann allerdings sogar nachteilig sein, falls IFN-α nur normale HSCs aktiviert und die Fähigkeit dieser Zellen zur Selbsterneuerung beeinträchtigt. Eventuelle immunologische Wirkmechanismen von IFN-α könnten den Vorteil der Kombinationstherapie zusätzlich beeinflussen, werden in der Publikation aber bewusst vernachlässigt.

British Journal of Cancer (2012) 106, 1742–1752

www.bjcancer.com

Therapy of chronic myeloid leukaemia can benefit from the activation of stem cells: simulation studies of different treatment combinations

I Glauche*[,1], K Horn[1,2,3], M Horn[2], L Thielecke[1], MAG Essers[4,5], A Trumpp[4,5] and I Roeder[1]

[1]Institute for Medical Informatics and Biometry (IMB), Faculty of Medicine Carl Gustav Carus, Dresden University of Technology, Fetscherstr. 74, D-01307 Dresden, Germany; [2]Institute for Medical Informatics, Statistics and Epidemiology, Medical Faculty, University of Leipzig, D-04107 Leipzig, Germany; [3]LIFE Center (Leipzig Interdisciplinary Research Cluster of Genetic Factors, Phenotypes and Environment), University of Leipzig, D-04103 Leipzig, Germany; [4]Division of Stem Cells and Cancer, German Cancer Research Center (DKFZ), D-69120 Heidelberg, Germany; [5]Heidelberg Institute for Stem Cell Technology and Experimental Medicine (HI-STEM), D-69120 Heidelberg, Germany

BACKGROUND: Newly diagnosed patients with chronic myeloid leukaemia (CML) are currently treated with tyrosine kinase inhibitors (TKIs) such as imatinib, nilotinib or dasatinib. However, incomplete eradication of residual disease is a general problem of long-term TKI therapy. Activation of mouse haematopoietic stem cells by interferon-α (IFNα) stimulated the discussion of whether a combination treatment leads to accelerated eradication of the CML clone.

METHODS: We base our simulation approach on a mathematical model describing human CML as a competition phenomenon between normal and malignant cells. We amend this model to incorporate the description of IFNα activity and simulate different scenarios for potential treatment combinations.

RESULTS: We demonstrate that the overall sensitivity of CML stem cells to IFNα activation is a crucial determinant for the benefit of a potential combination therapy. We furthermore show that pulsed IFNα together with continuous TKI administration is the most promising strategy for a combination treatment in which the therapeutic benefit prevails adverse side effects.

CONCLUSION: Our modelling approach is a highly beneficial tool to quantitatively address the competition between normal and leukaemic haematopoiesis in treated CML patients. We derive testable predictions for different experimental settings that are suggested before the clinical implementation of the combination treatment.

British Journal of Cancer (2012) **106,** 1742–1752. doi:10.1038/bjc.2012.142 www.bjcancer.com
Published online 26 April 2012

Keywords: CML; interferon-α; combination therapy; mathematical modelling

The clinical application of tyrosine kinase inhibitors (TKIs) such as imatinib, nilotinib or dasatinib for the treatment of chronic myeloid leukaemia (CML) had important implications not only for treatment success but also for the understanding of the pathomechanisms of the disease (Savage and Antman, 2002). Although treatment with imatinib could still not be demonstrated to be curative, it is suited to achieve a sustained control of the disease in the majority of patients. The 6-year overall survival rate achieved 88% and exceeds all other CML therapies (Hochhaus *et al*, 2009).

The TKI imatinib was one of the first cancer-specific drugs that proved efficient to specifically inhibit the action of the BCR–ABL oncoprotein. BCR–ABL is commonly expressed in cells with the so-called 'Philadelphia chromosome', a translocation between chromosomes 9 and 22 that is characteristic for CML cells. However, it appears that even after a massive reduction of the tumour load over many years of treatment (referred to as cytogenetic/molecular remission) a residual disease is retained in many patients (Goldman, 2009). Regularly, these patients show a rapid increase in cancer load if imatinib treatment is stopped (Michor *et al*, 2005). These observations lead to the hypothesis that at least some leukaemic stem cells are able to hide from the imatinib effect, for example, by entering an inactive, quiescent state (Komarova and Wodarz, 2007). Contrasting the above mentioned relapse kinetics, a sustained molecular remission after imatinib cessation is observed in a small number of patients (Rousselot *et al*, 2007; Mahon *et al*, 2010). These cases suggest that an eradication of the leukaemia is in principle possible and propose the view that CML stem cells are not always found in a treatment-protected (potentially quiescent) state but can be targeted over time.

These findings add to a long-standing discussion on whether TKIs affect CML stem cells or whether these particular cells are protected from the therapeutic effect (Michor *et al*, 2005; Glauche *et al*, 2007). Although it is regularly suggested that leukaemic cells treated with imatinib survive in a state of extended quiescence, the long-term treatment success in a number of patients is a strong argument in favour of an occasional activation of these cells, which makes them susceptible to the (cytotoxic) drug effect. Six-year follow-up data for patients under long-term imatinib treatment indicates that the majority of patients, which do not show resistance mutations against imatinib, remain in sustained molecular remission and show further declining BCR–ABL/ABL

*Correspondence: Dr I Glauche; Email: ingmar.glauche@tu-dresden.de
Received 28 November 2011; revised 6 March 2012; accepted 21 March 2012; published online 26 April 2012

ratios (Hochhaus *et al*, 2009). These findings can only be explained under the assumption that the expansion of the leukaemic stem cell clone is stopped or even inverted, indicating that imatinib also acts on the level of stem cells. We advocate the view that imatinib preferentially targets activated, cycling stem and non-stem cells whereas only quiescent stem cells remain sheltered (Roeder *et al*, 2006). Assuming that normal haematopoiesis as well as the growth of the malignant CML clone is based on the reversible activation of preferentially quiescent stem cells, the cytotoxic effect of TKI imatinib on activated CML stem cells leads to a slow but sustained reduction of the CML clone. But, as documented in *in vitro* experiments (Druker *et al*, 1996; Graham *et al*, 2002), imatinib itself appears to induce prolonged quiescence among the CML stem cells and, therefore, make them less sensitive to cell-cycle-dependent drug effects. The persistence of residual CML cells in many patients is in good agreement with this assumption.

Others and we have previously raised the idea that a combination of TKIs with a cell-cycle-stimulating drug could potentially increase the efficacy of treatment (Jorgensen *et al*, 2006; Roeder *et al*, 2006; Drummond *et al*, 2009; Foo *et al*, 2009; Essers and Trumpp, 2010). This idea is based upon the assumption that the activating effect on CML stem cells makes them more susceptible to the cytotoxic effect of TKIs and leads to a faster reduction of the residual clone. Granulocyte colony-stimulating factor (G-CSF) has already been used in the clinic for the activation and mobilisation of human haematopoietic stem cells (HSCs) into peripheral blood before stem cell extraction and appeared as a first candidate drug for a combination treatment alongside with imatinib (Jorgensen *et al*, 2006). However, a small clinical trial with cyclic administration of TKI imatinib and G-CSF did not show the expected results; in fact no clinical benefit of the combination treatment was observed (Drummond *et al*, 2009). However, both the choice of the stem cell-activating drug as well as the conducted cyclic treatment regimen might be critical determinants of the specific, nonbeneficial outcome. We will come back to these objections in the context of the analysis provided below.

Recently, we reported about the activating effect of interferon-α (IFNα) that directly acts on murine HSCs and induces increased cell-cycle activity (Essers *et al*, 2009). Although the findings were obtained in mice, these results again fostered the discussion on enhancing the TKI treatment in CML patients by cell-cycle-stimulating drugs (Essers and Trumpp, 2010). Before the introduction of TKI treatment, IFNα monotherapy was the standard therapy for patients with CML. Both the role of IFNα in innate and acquired immune responses as well as its anti-proliferative properties in many cell types *in vitro* made the drug a highly attractive therapy for the treatment of cancer (Borden *et al*, 2007). The novel findings on the stem cell-activating effects of IFNα add another aspect to this interpretation, suggesting an additional mechanism on the stem cell level that seems to differ from the immunological effect. Without necessarily focussing on the stem cell-activating effect of IFNα, a number of recently published studies hint towards an advantage of the combination therapy (Guilhot *et al*, 2009; Simonsson *et al*, 2011) but also demonstrate that severe side effects put a natural limit on treatment combinations (Cortes *et al*, 2010).

Owing to such heterogeneous results, our objective is to apply a comprehensive and validated, although simplifying, mathematical model of CML progression and therapy, which is suitable to address different treatment regimens in a systematic manner. The suggested model has been successfully used to describe the pathogenesis of CML and the sustained treatment response of patients under imatinib monotherapy. Within the amended model framework, we are able to study different possible pharmacological scenarios for the IFNα-mediated stem cell activation and predict long-term outcomes for different treatment regimens. The model represents a useful tool to identify promising and safe treatment combinations that could decrease potential side effects. Within the scope of this study, we address three different aspects of a possible combination treatment of TKIs and IFNα:

- We investigate different possibilities of how a potentially quiescence-inducing effect of TKIs combines with the stem cell-activating effect of IFNα. Specifically, we consider three scenarios: (i) strong activation of leukaemic stem cells similar to normal HSCs, (ii) weak activation of leukaemic stem cells and (iii) no activation of leukaemic stem cells.
- Furthermore, we study the possibility that the application of a cell-cycle-activating drug leads to an additional temporary reduction of the self-renewal ability of the affected cells. As we demonstrate below, the results in Essers *et al* (2009) suggest that the application of IFNα induces an impaired self-renewal ability of HSCs, potentially due to the stimulated proliferation and an alteration of the stem cell–niche interaction.
- Finally, we address the question how these effects need to be combined in a temporal manner as we predict that the timing of administration is crucial for the clinical benefit. Therefore, we analyse three distinct temporal treatment regimens: (i) continuous TKI plus continuous application of IFNα as a cell-cycle-activating drug, (ii) continuous TKI plus pulsed application of IFNα and (iii) pulsed TKI plus pulsed application of IFNα.

The outlined, three-step analysis results in a matrix of possible outcome scenarios. Within this matrix, we identify the scenarios in which the combination of imatinib with a stem cell-activating drug such as IFNα appears beneficial for the clinical outcome and the reduction of the minimal residual disease. We will further discuss these results and suggest critical experiments that need to be carried out before a clinical implementation of the combination treatment.

METHODS

Modelling normal haematopoiesis and CML

CML is perceived as a clonal competition phenomenon between normal haematopoietic and leukaemic stem cells. This concept has been translated into a single-cell-based model framework that was originally developed to describe murine and human haematopoiesis (Roeder and Loeffler, 2002; Roeder *et al*, 2005), and has been successfully applied to CML (Roeder *et al*, 2006; Horn *et al*, 2008). Owing to small differences in their cell-specific parameters, the leukaemic cells are able to outcompete the normal cells in a dynamic process, thus mimicking the clinically observed chronic phase in human CML.

Technically, the mathematical model assumes that (both normal and leukaemic) stem cells reside in either of the two signalling contexts, named A and Ω, and that they can reversibly change between them (Figure 1). Importantly, the signalling contexts impose different effects on the cellular development: whereas context A is inspired by the concept of a stem cell-supporting niche and promotes cellular quiescence and regeneration, context Ω represents an escape of HSCs from the niche signals and promotes proliferation and differentiation. A cell's tendency to switch from one context to the other is determined by the cell number in the target context (i.e., the 'packing density' given a certain niche-specific carrying capacity that is implemented by a specific sigmoid activation/deactivation function $f_{\alpha/\omega}$) and by a cell-specific affinity a to reside in context A. The affinity a is gradually lost in context Ω, but regained in A up to the maximum value $a_{\max}$. Therefore, the system is able to establish a dynamically stabilised equilibrium, balancing quiescent cells in A and proliferating cells in Ω.

If the cell-specific affinity a decreases below a certain threshold $a_{\min}$, the cell loses the ability to change back to context A, and is

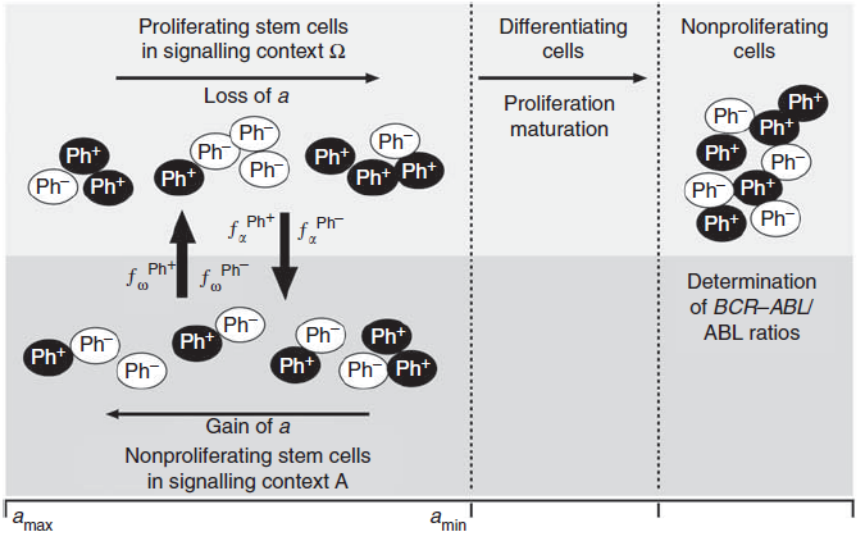

Figure 1 Stem cell model. The model setup is characterised by two different signal contexts, A and Ω between which the cells can reversibly change depending on the cell number within the target context and the cell-specific affinity a (encoded in the transition functions $f_{\alpha/\omega}$). Whereas activated cells in Ω undergo divisions and exponentially degrade their cell-specific affinity a, cells in A are quiescent and regain their affinity value. Cells with $a > a_{min}$ are referred to as stem cells, whereas cells with $a < a_{min}$ are referred to as differentiating cells. The differentiating cells undergo a proliferative phase before they mature without further division. Leukaemic cells (Ph+) have slightly altered transition kinetics between A and Ω. Model parameters are further adapted depending on the particular treatment scenario. BCR–ABL/ABL ratios are calculated based on the fraction of leukaemic cells in the pool of maturing cells.

committed to undergo further proliferation and differentiation. Hence, the affinity a can be interpreted as a measure of the long-term repopulation potential of an individual cell. Accordingly, the residence in context A is necessary to prevent differentiation and, therefore, to maintain the HSC population. In this interpretation, self-renewal appears as a mechanistic consequence of the stem cells' ability to attach to the niche-like environment and is functionally independent from their proliferative abilities.

In order to explain the competitive advantage of leukaemic cells compared with normal HSCs, we assume that the leukaemic cells have an increased and unregulated proliferative activity (Figure 2A). Technically, the transition characteristics f_α and f_ω, which describe the transit of cells between A and Ω, differ such that leukaemic cells have (I) an increased and cell number-independent probability per time step to be activated into cycle and (II) a slightly increased propensity to find an empty niche site, which is modelled by an altered probability to change to the niche-like signalling context A. Both assumptions are necessary to consistently explain characteristics of CML pathogenesis (Roeder *et al*, 2006; Horn *et al*, 2008). Further details of the implementation are provided in the Supplementary Material.

Tumour load in the peripheral blood is clinically measured in terms of BCR–ABL transcript levels. Within the mathematical model, BCR–ABL/ABL percentages are approximated using cell numbers in the population of fully differentiated cells according to the following equation:

$$BCR-ABL/ABL \approx \frac{n_1}{n_1+2n_2}\cdot 100\ \% \qquad (1)$$

in which n_1 denotes the number of leukaemic cells and n_2 the number of normal cells (Branford *et al*, 1999).

Modelling the TKI effect

Treatment of CML patients with TKI imatinib is assumed to induce (I) a cytotoxic effect and (II) inhibition of the proliferative activity of leukaemic stem cells (Figure 2B). Technically, the apoptotic effect (I) is modelled by a selective kill of a fixed percentage of leukaemic cells per time step (degradation rate r_{deg}), while the proliferation inhibition (II) is modelled by a reduction of the activation of leukaemic cells into cycle, that is, altering transition characteristic f_ω to a basal level (Supplementary Figure 1). The transition characteristic f_ω is assumed to remain unregulated, that is, independent of cell numbers in Ω. Thus, in our mathematical model imatinib therapy effects are described within a two-dimensional parameter space (r_{deg}, f_ω). It has been shown previously that these assumptions are sufficient to consistently explain CML emergence, genesis and treatment with TKI imatinib for a population of patients (Roeder *et al*, 2006; Horn *et al*, 2008). For a detailed parameter overview see Supplementary Tables 1 and 2.

In earlier applications of our model (Roeder *et al*, 2006), we assumed a gradual onset of the effect of TKI activity within the leukaemic stem cell population resulting in an optimal fitting of the short-term BCR–ABL/ABL response within the first 6 months after start of imatinib therapy. However, for the analysis of different treatment scenarios within the scope of this manuscript we use a simplified model version and suppose that all drugs act instantly and only as long as they are administered. Building on this simplification, we do not model the effect of single administrations of either TKI or IFNα but rather describe their cumulative effect within the bone marrow as a binary/on–off variable. It can be shown that model results on long-term kinetics of CML patients under TKI administration are not affected by these simplifications (Supplementary Figure 3).

Stem cell activation by IFNα

Although activation of HSCs with IFNα could so far only be shown in mice, we here explore whether and under which conditions a potentially similar effect in the human situation could improve TKI therapy of CML patients. In Essers *et al* (2009), it has been demonstrated that IFNα treatment (at time point 0) increases the fraction of dividing HSCs in a B6 mouse model within a 24 h interval from 20 up to 70%. In terms of the model, a similar effect is achieved under the assumption that about 3 to 4% of the stem cells are additionally activated from A into Ω during each simulation time step measuring 1 h (IFNα-mediated activation,

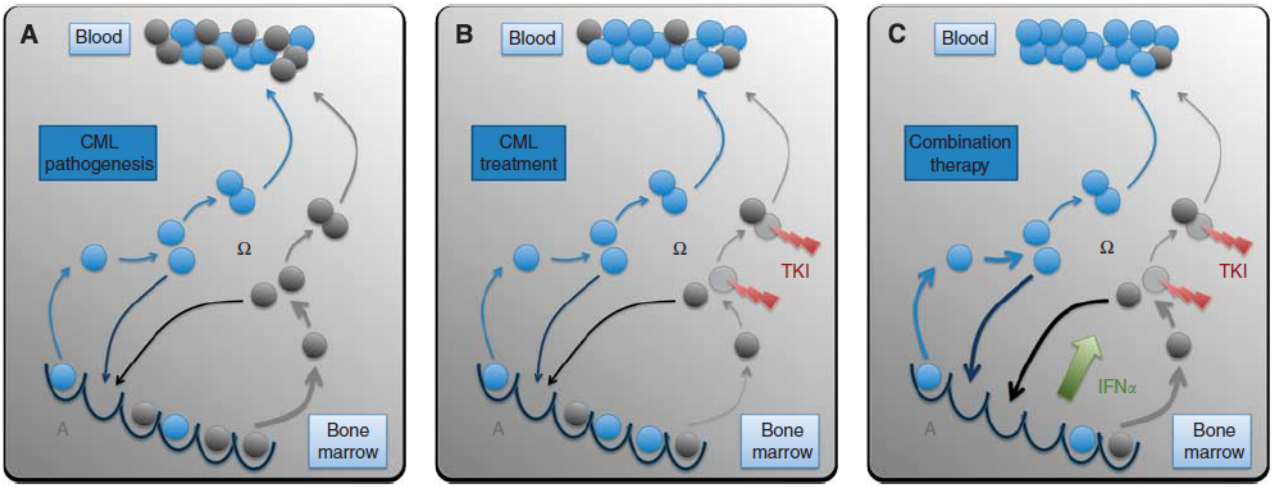

Figure 2 CML pathogenesis and treatment. (**A**) Normal (blue) and leukaemic (grey) stem cells are regularly activated from their bone marrow niches (bottom, signalling context A) and subsequently divide (signalling context Ω). For the maintenance of a balance between quiescent and activated cells, some cells return to the niches and self-renew while others undergo further proliferation and differentiation, and contribute to peripheral blood. Owing to an increased activation of the leukaemic cells compared with normal cells the leukaemic pool slowly outcompetes normal haematopoiesis. (**B**) TKIs preferentially target activated leukaemic cells, thus leading to a significant reduction of tumour load. However, we also assume that leukaemic stem cells are even less likely to be activated under TKI treatment (indicated by the thinner arrows). Therefore, a residual pool of leukaemic cells persists over long time scales. (**C**) IFNα-mediated activation of both normal and leukaemic stem cells leads to a fast and sustained reduction of the residual leukaemic cells as these activated leukaemic (stem) cells are target for the primary TKI-mediated cell kill.

for technical details see Supplementary Materials and Supplementary Figure 2).

Essers *et al* (2009) additionally showed that in a chimeric situation between wild-type and IFNα-receptor knockout cells the continuous administration of IFNα over the course of 3 weeks leads to a complete eradication of the wild-type clone. However, application of IFNα to wild-type mouse did not significantly influence peripheral blood cell counts and showed no long-term effect on the stem cell level after 3 weeks application. In terms of the model, this fast out-competition in the chimeric situation can only be explained under the assumption that IFNα (besides the stem cell activation) induces an additional defect in the cells ability to reattach to the niche-like signalling context A and, thus, to retain their self-renewal ability (IFNα-mediated self-renewal deficit (SRD)). However, for small stem cell numbers this effect is alleviated as the system aims to compensate a total loss of HSCs, which in turn can explain the stabilised haematopoiesis in the nonchimeric situation. As this secondary effect of the IFNα-mediated SRD has important consequences for therapy outcome, it is studied separately in the Results section.

Modelling the combination of effects

Although the IFNα effects on stem cells are only demonstrated in mice, we here make the assumption that IFNα acts similarly in humans (Figure 2C). Building on this working hypothesis, we provide a model description of the TKI effect on leukaemic cells and of a set of different potential IFNα effects on normal as well as on leukaemic cells. However, it is still speculative how these effects superimpose in the case of a combination therapy. To disentangle the superposition of effects in a systematic manner we study the system response in three dimensions:

(1) We analyse the stem cell-activating effect of IFNα under the assumptions that IFNα activates normal HSCs and has no/weak/strong activating effect on CML stem cells. Technically, for the strong activation, 3% of the normal and leukaemic stem cells in context A are additionally activated into context Ω per simulation time step (1 h). For the weak activation, only 0.2% of the leukaemic stem cells are additionally activated while activation of the normal HSCs remains at 3%. In the case of no activation, the leukaemic stem cells are completely insensitive to IFNα-mediated activation. Additional, potentially immunological effects of IFNα are neglected for this study.
(2) We analyse whether the additional IFNα-mediated SRD of normal and leukaemic cells changes the therapeutic prediction for the first dimension.
(3) For the range of combinations in (1) and (2), we address whether the continuous or pulsed administration of the drugs appears both safe and clinically beneficial.

Table 1 Overview of the simulation scenarios

	Strong activation	Weak activation	No activation
Cont. TKI and cont. IFNα			
w/o SRD	Figure 3 (+)	Figure 3 (+)	Figure 3 (+)
with SRD	Figure 4 (+)	Figure 4 (!)	Figure 4 (−)
Cont. TKI and pulsed IFNα			
w/o SRD	Figure 5 (+)	Figure 5 (+)	Figure 5 (+)
with SRD	Supp. Figure 4 (+)	Supp. Figure 4 (+)	Supp. Figure 4 (+)
Pulsed TKI and pulsed IFNα			
w/o SRD	Figure 6A–C (−)	Figure 6D–F (!)	Figure 6G–I (!)
with SRD	Supp. Fig. 5A–C (−)	Supp. Fig. 5D–F (!)	Supp. Fig. 5G–I (!)
Pulsed TKI and cont. IFNα			
w/o SRD	Supp. Figure 7 (−)	Supp. Figure 7 (−)	Supp. Figure 7 (−)
with SRD	Supp. Figure 6 (!)	Supp. Figure 6 (−)	Supp. Figure 6 (−)

Abbreviations: cont. = continuous; IFNα = interferon-α, SRD = self-renewal deficit; Supp. = Supplementary; TKI = tyrosine kinase inhibitor. *w/o (or with) SRD* refers to the simulation scenarios in which the additional IFNα-mediated SRD of normal and leukaemic cells was taken into account (or not, respectively). Symbols in parentheses indicate whether the simulation scenarios predict beneficial or neutral treatment effects (+), therapy failure (−), or scenarios in which temporary, high values of BCR–ABL/ABL ratios have to be expected (!).

An overview about the different simulated scenarios is provided in Table 1.

Technical implementation

The simulation model is implemented in C++. All simulation results shown are averages over 100 simulation runs with identical

parameters. Averaging is required to represent a generalised behaviour as the model-inherent stochasticity induces small quantitative differences between different simulation runs, even if using identical parameter values. Further details as well as parameter specifications are provided in the Supplementary Material.

RESULTS

Administration of TKI with a stem cell-activating drug

For the systematic investigation of a combination therapy for CML patients, we use an idealised 'average patient' under monotherapy with TKI imatinib as the standard reference. First-line response under imatinib leads to a rapid molecular response within the first year of treatment, but model simulations suggest that tumour eradication is only expected to occur after about 25 years of continuous treatment. However, the initial treatment effect of the TKI can hardly be enhanced. Therefore, we argue that a combination therapy with IFNα, aiming at the accelerated eradication of the residual pool of leukaemic stem cells, appears most advisable after 9 to 12 months of initial, successful imatinib therapy. This corresponds to the time frame in which the decline of BCR–ABL/ABL ratios changes from the rapid initial reduction towards the slower long-term decline.

Under the assumption that continuous administration of IFNα induces an activation of both normal and leukaemic stem cells, the selective cytotoxic effect of TKI imatinib on leukaemic cells leads to a fast eradication of the malignant clone (Figure 3A). In fact, the continuous administration of both TKI imatinib and IFNα leads to a new constellation among the stem cell population (Figure 3B and C) with an increased number of activated stem cells as compared with the quiescent ones (owing to the stem cell-activating effect of IFNα). Under these novel conditions, the leukaemic clone has a competitive disadvantage as it is primarily targeted by the cytotoxic TKI effect. The intensity of the activation of leukaemic cells (i.e., whether it is comparable to the activation of normal cells or gradually weaker) only influences the speed of eradication but does not change the outcome qualitatively (compare the red and green curves in Figure 3A–E). However, if the activation only affects normal HSCs but not the leukaemic cells, the therapeutic benefit is lost (blue line in Figure 3A). In fact, the model predicts reduced BCR–ABL/ABL ratios in the peripheral blood, while the dynamics on the stem cell level only show an increased number of activated normal stem cells. Although normal cells undergo repeated activation (Figure 3G; and thus have an increased contribution to peripheral blood) these cells do also regularly re-enter the niche-like environment A (Figure 3F), thus keeping the overall ratio between normal and leukaemic stem cells at levels similar to TKI monotherapy (indicated by the slow decline in Figure 3A, parallel to the grey curve).

Stem cell activation with SRD

For the case that IFNα also induces a SRD in the affected stem cells, it makes a difference whether normal and leukaemic stem cells are activated equally. For the simplest scenario that both cell types are activated equally into the cell cycle due to IFNα administration (and have an equal SRD induced by the drug), the cytotoxic TKI effect on leukaemic cells influences the clonal composition in favour of the normal cells. The dynamics of this process are similar to the above scenario without the SRD (Figure 4A).

The dynamics of tumour reduction are delayed for the scenario in which leukaemic cells are only weakly activated by IFNα compared with normal HSCs. Figure 4A indicates that only after a massive initial increase of leukaemic cells in the peripheral blood the combination treatment results in a beneficial therapeutic effect.

The picture changes drastically for the case that the stem cell-activating effect acts only on normal cells but spares the leukaemic cells. In this scenario, the leukaemic stem cell pool is preserved but the normal cells are repeatedly activated. Owing to their SRD, the normal cells are rapidly diluted (Figure 4F and G), which is indicated by the fast increase in BCR–ABL/ABL ratios, corresponding to immediate therapy failure (Figure 4A). In this scenario, the beneficial effect of the TKI treatment specifically acting on leukaemic stem cells is neutralised by the selective activation of normal HSCs by IFNα that spares the leukaemic cells and induces an additional binding deficit of the normal cells.

Influence of the treatment regimen

Severe side effects of a continuous combination therapy with imatinib and IFNα raise the question whether a treatment benefit can still be achieved by a scheduled and discontinuous administration of the drugs. From a clinical point of view, two general strategies for a pulsed treatment regimen need to be distinguished: (1) continuous TKI plus pulsed application of IFNα, and (2) pulsed TKI plus pulsed IFNα. Both regimens are studied in more detail below. The hypothetical, third option (continuous IFNα plus pulsed TKI) is clinically not relevant as it places IFNα as primary therapy instead of the TKI. However, our model predicts no therapeutic benefit in the majority of cases (Supplementary Figure 6 and 7).

Continuous TKI plus pulsed IFNα As a general case, we study the scenario that IFNα is administered once every second week while TKI treatment continues without interruption. The overall outcome is closely similar to the above scenario of the continuous administration of both drugs with slower therapeutic benefit: For the case that both leukaemic and normal stem cells are equally activated by IFNα, the malignant clone declines but can only be eradicated after about 3 years past initial therapy start (Figure 5A). This overall trend is superimposed by an oscillation resulting from the pulsed administration of IFNα, which is also distinctly visible on the level of stem cells (Figure 5B–G). This oscillation is most likely less pronounced in a clinical setting as oscillations on the stem cell level would be compensated and/or washed-out at later cell stages of blood differentiation. It should also be kept in mind that if blood samples of patients are drawn at a rhythm that coincides with the pulsed therapeutic regimen, the results can be severely biased as potential treatment-induced oscillations might not be detected owing to a confounding of the treatment effect and the measurement frequency.

For weaker activation of the leukaemic cells, the overall decline of tumour load is even further slowed down (Figure 5A). Again, for the case that IFNα does not activate leukaemic stem cells there is no therapeutical benefit, as the ratio between normal and leukaemic stem cells remains largely untouched, also resulting in similar dynamics on the stem cell level (Figure 5F and G).

Surprisingly, under the assumption that IFNα induces an additional SRD among both the normal and leukaemic cells, therapy failure is not observed as for the scenario described above in which only normal HSCs are activated while leukaemic ones are not. In the pulsed scenario, the time interval between successive IFNα administrations is sufficient for the system to stabilise the pool of normal cells instead of its rapid dilution. The same, close correspondence between the scenarios with and without SRD applies in the cases of strong and weak activation of the leukaemic clone (Figure 5A and Supplementary Figure 4).

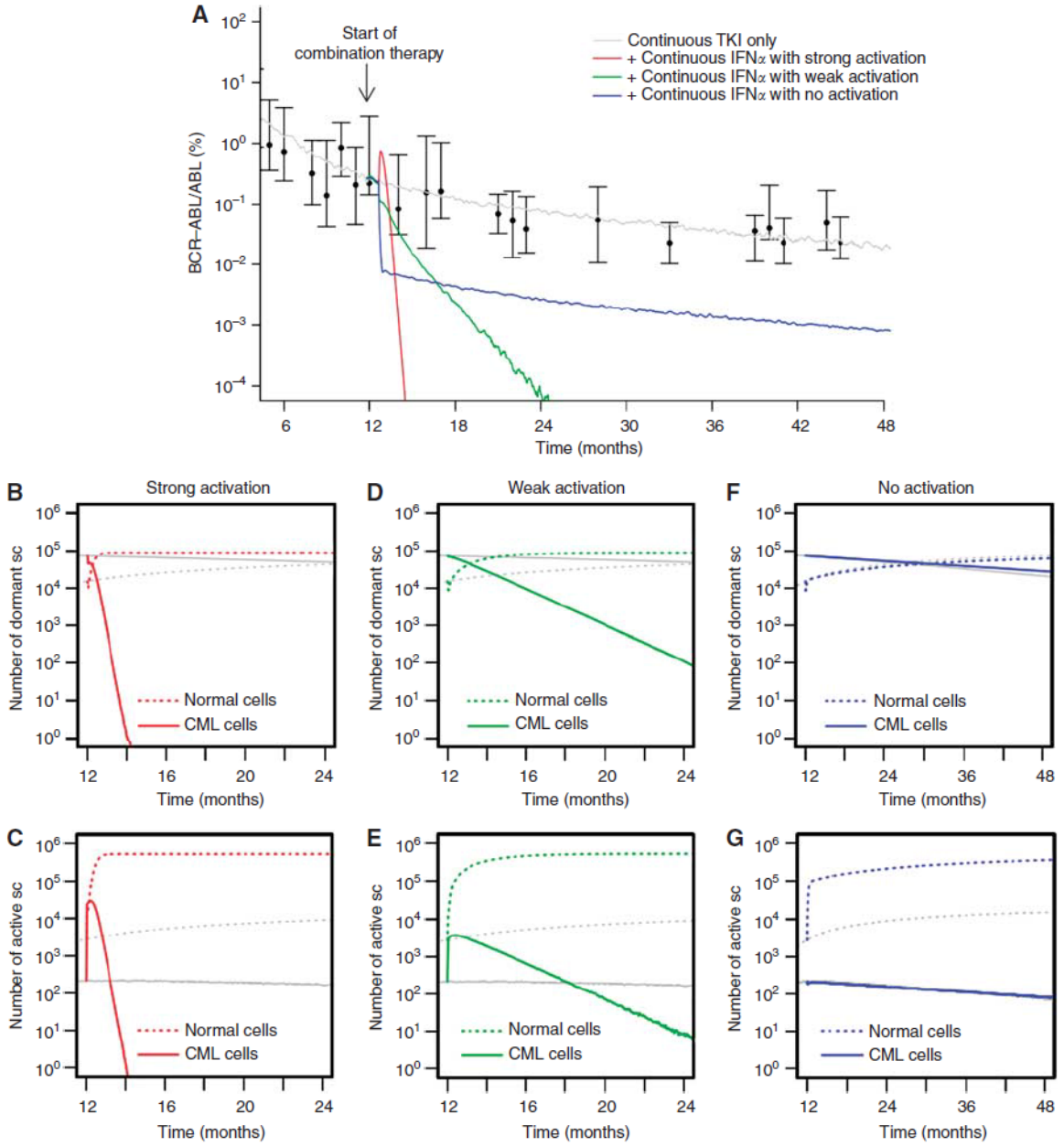

Figure 3 Continuous TKI plus continuous IFNα. (**A**) Shown are different response scenarios on the level of BCR–ABL/ABL ratios in peripheral blood: strong activation of leukaemic stem cells similar to normal HSCs (red), weak activation (green) and no activation of leukaemic cells (blue, only normal cells are activated by IFNα). Patient data (black) from the German cohort of the IRIS study (Hochhaus *et al*, 2009; Roeder *et al*, 2006) and simulation results for monotherapy with TKI imatinib (grey) are provided for reference. Subfigures (**B**–**G**) show corresponding stem cell number in A (quiescent) and Ω (activated), compared with TKI monotherapy (grey) for strong (**B**, **C**), weak (**D**, **E**), and no activation scenarios (**F**, **G**).

Pulsed TKI plus pulsed IFNα For the case that both TKI and IFNα are applied in a pulsed fashion, the overall therapeutic outcome changes significantly. As a representative example, we study the case in which the TKI is administered continuously for 2 weeks and then suspended. After 1 day of IFNα administration (without parallel TKI application), the TKI therapy starts again after a time shift of 6 days (Figure 6A).

Apparently, the pulsed treatment regimens induce a cyclic behaviour in the BCR–ABL/ABL ratios. However, as our model does not include any regulation of cellular output on the level of later cell stages, such as precursors, this effect might be overestimated. Nevertheless, our simulation results indicate that a treatment interruption of TKI after the administration of IFNα is not beneficial for the therapeutic outcome and might in fact counteract the strategy of the combination treatment. Even though our model does not appropriately reflect the pharmacokinetics of the drugs (i.e., the model does not account for the sustained presence of the drugs post administration), the simulations show in principle that no clinical benefit is obtained if the action of the two drugs does not superimpose at any given point of time.

For the scenarios in which we assume that IFNα activates both leukaemic stem cells and normal HSCs similarly (strong activation, Figure 6A–C), we observe a regrowth of the leukaemic clone. In these cases, the increased potential of the leukaemic cells to reoccupy empty niches after the activation cycle turns into a competitive advantage that overcompensates the TKI-mediated

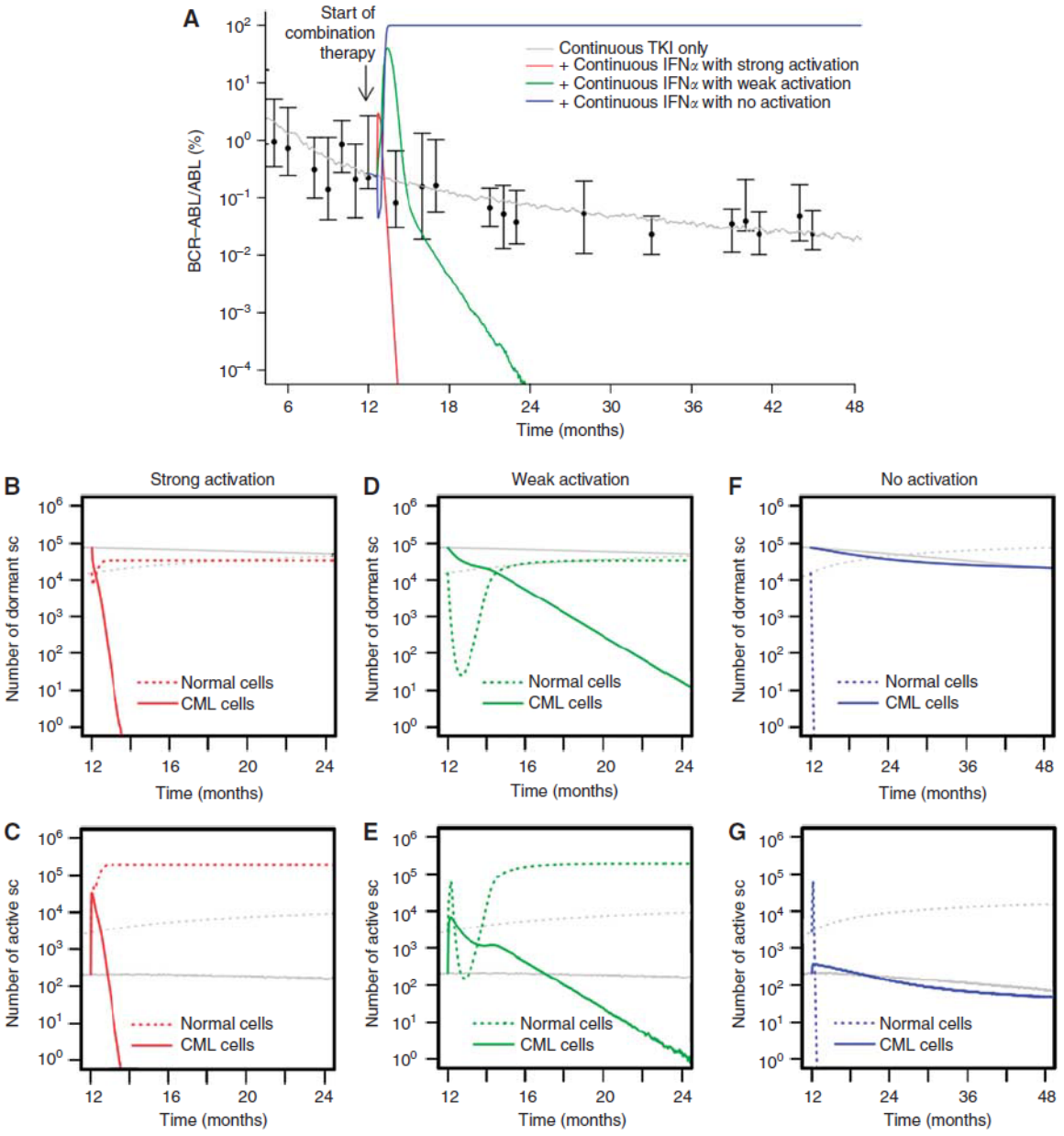

Figure 4 Continuous TKI plus continuous IFNα with SRD. (**A**) BCR–ABL/ABL ratios in peripheral blood are shown for strong activation of leukaemic stem cells similar to normal HSCs (red), weak activation (green) and no activation of leukaemic cells (blue). However, in contrast to Figure 3, we assume that IFNα induces an additional SRD among normal and leukaemic cells. Subfigures (**B**–**G**) show corresponding stem cell numbers in A (quiescent) and **Ω** (activated), compared with monotherapy with TKI imatinib (grey) for strong (**B**, **C**), weak (**D**, **E**), and no activation scenarios (**F**, **G**).

therapeutical benefit. Shortening the treatment interruption of the TKI increases the time to therapy failure as the cytotoxic effect on leukaemic cells is more pronounced in a phase where the cells are still activated.

For the other scenarios in which leukaemic stem cells are only weakly, or not at all, activated by IFNα there is no additional benefit of the combination therapy (Figure 6D–I). Although the pulsed application induces a typical fluctuation pattern, the balance between leukaemic stem cells and normal HSCs is not effectively changed. In the limit of shorter breaks between IFNα application and the next TKI treatment cycle, the BCR–ABL/ABL ratios converge towards the results of TKI monotherapy (Figure 6F and I).

Compared with the results in Figure 5, in which pulsed doses of IFNα are administered simultaneously with the continuous TKI application, none of the results for the pulsed/pulsed therapy in Figure 6 shows a superior behaviour. Therefore, we argue that a clinical benefit from potential IFNα-mediated stem cell activation can only be achieved for the case that TKI and IFNα are both pharmacologically active in an overlapping time interval.

Simulation results for the pulsed/pulsed application scenario in Figure 6 are obtained under the assumption that IFNα does not induce an additional SRD. However, taking this effect into account yields qualitatively similar results (Supplementary Figure 5).

CONCLUSION

We presented a novel mathematical model analysis to describe the combined effects of TKI such as imatinib and the

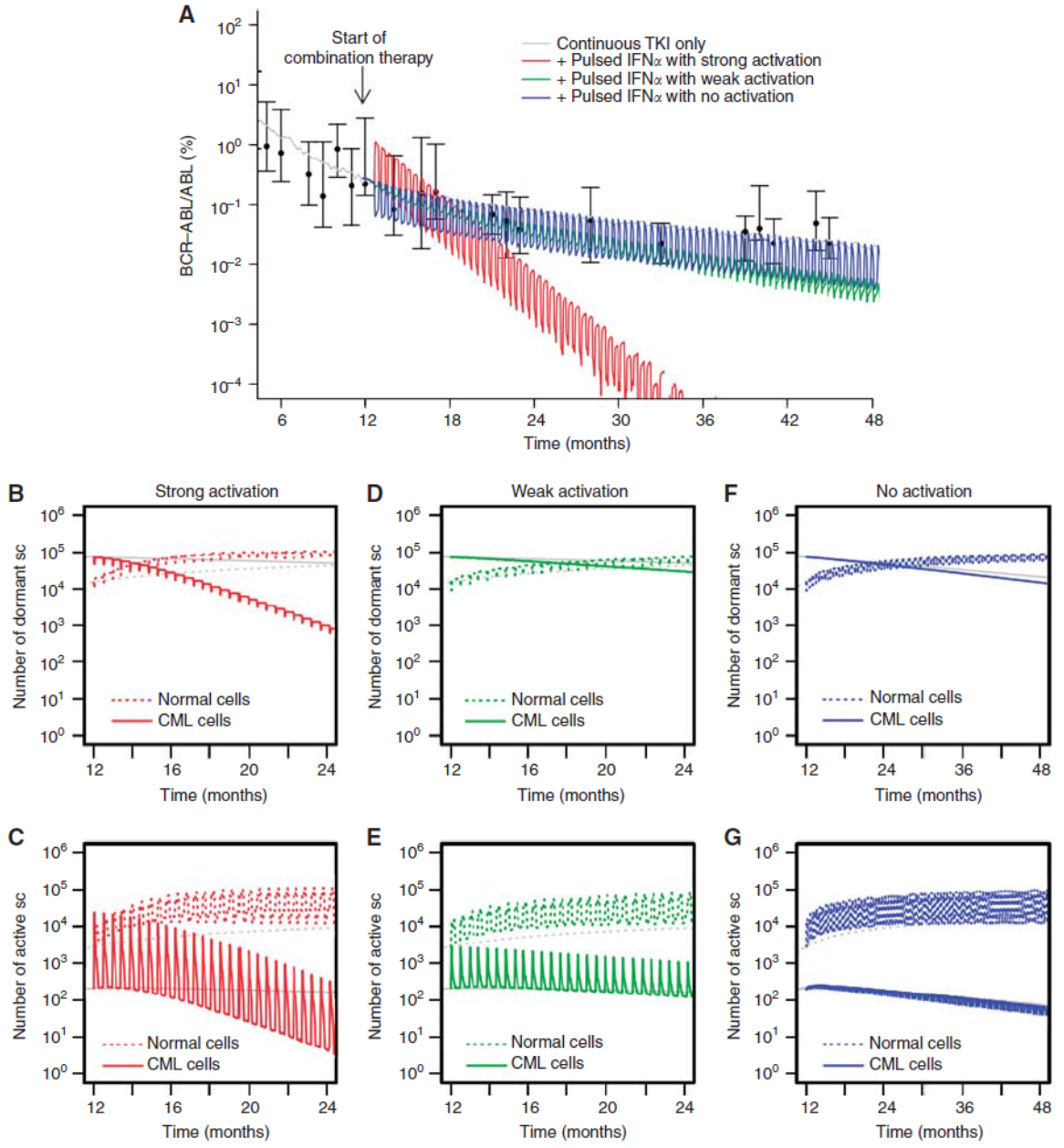

Figure 5 Continuous TKI plus pulsed IFNα. (**A**) BCR–ABL/ABL ratios in peripheral blood are shown for pulsed application of IFNα (1 day within 14 days) for different activation scenarios: strong activation of leukaemic stem cells similar to normal HSCs (red), weak activation (green) and no activation of leukaemic cells (blue, only normal cells are activated by IFNα). For the corresponding simulations we do not include the additional, IFNα-induced SRD. However, the simulation results only change marginally if the effect is taken into account (Supplementary Figure 4). Subfigures (**B**–**G**) show corresponding stem cell numbers in A (quiescent) and Ω (activated), compared with monotherapy with TKI imatinib (grey) for strong (**B**, **C**), weak (**D**, **E**), and no activation scenarios (**F**, **G**).

cell-cycle-activating drug IFNα for the treatment of human CML. The model approach allowed us to study a variety of different pharmacological combination effects between TKIs and IFNα as well as different treatment regimens and to gain a systematic understanding of the combination therapy with the ultimate goal to guide clinical applications.

Summarising our model suggests that a successful combination therapy of TKIs with IFNα in CML patients requires the simultaneous application of both drugs in overlapping time intervals. In addition, a less-frequent application of IFNα reduces the speed of eradication but might also prevent a possible exhaustion of normal haematopoiesis. We showed that such adverse behaviour is possible for the case that IFNα does not activate leukaemic stem cells but induces a SRD among normal cells (cf. Figure 4). Furthermore, it has been documented that combination of TKI imatinib with IFNα imposes severe side effects on the patients (Cortes *et al*, 2010). Our findings indicate that a less-frequent administration of IFNα, which could decrease potential side effects of the combination therapy, is still helpful even though the time to eradication is predicted to increase. We demonstrated that a weekly or biweekly administration of IFNα under optimal conditions still shows a significant advantage compared with imatinib monotherapy and can reduce time to tumour eradication from ~25 years to 3 years. Even in a

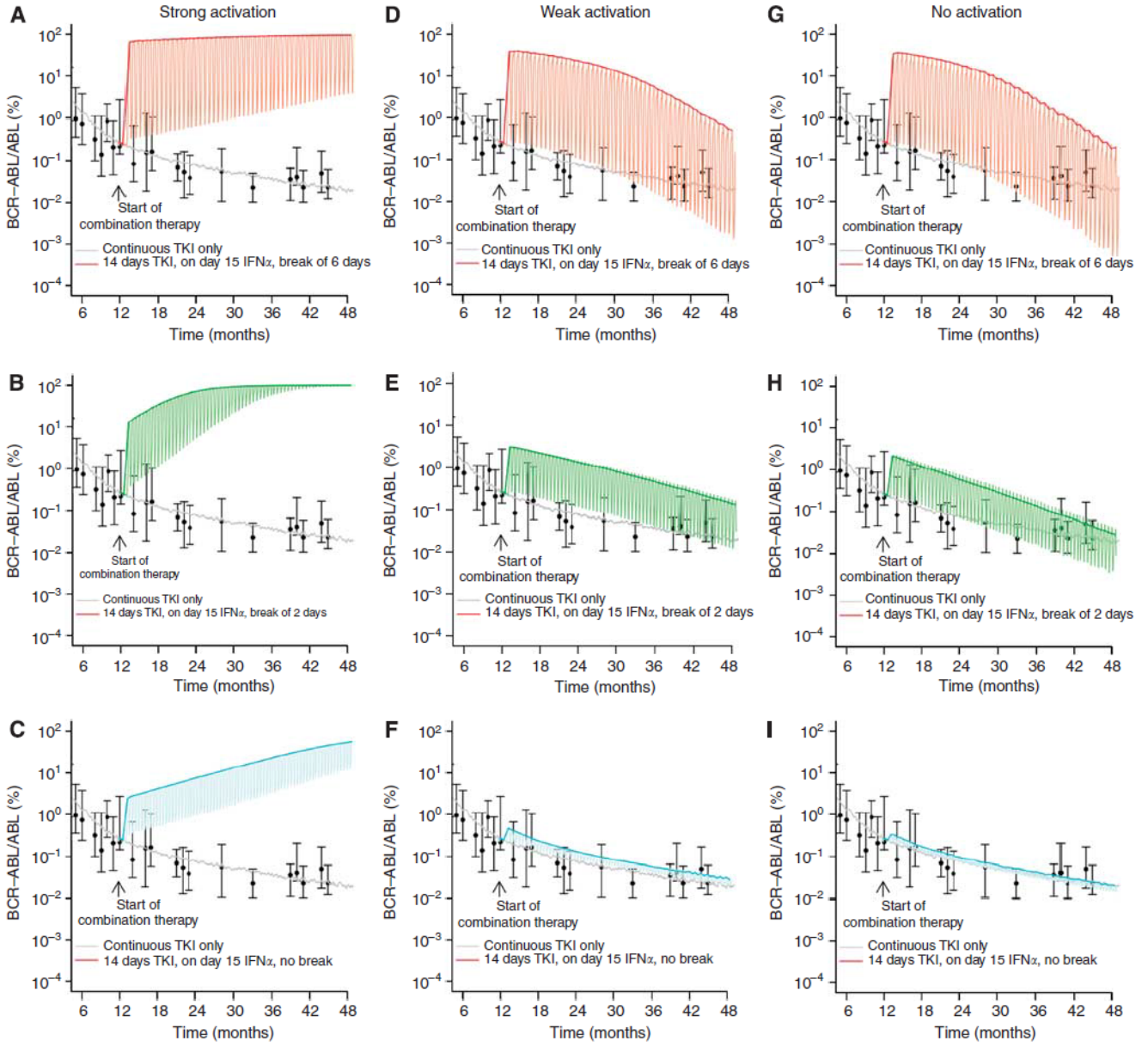

Figure 6 Pulsed TKI plus pulsed IFNα. We show predicted BCR–ABL/ABL ratios in peripheral blood for the following representative treatment cycles: pulsed application of the TKI (day 1 to 14, no IFNα), pulsed application of only IFNα (day 15, no TKI), treatment interruption of x subsequent days past day 15 for different durations of the treatment interruption x: $x = 6$ days (**A, D, G**, shown in red), $x = 2$ days (**B,E, H**, shown in green) and $x = 0$ days (**C, F, I**, shown in blue). Subfigures A–C correspond to the scenarios with strong activation of leukaemic stem cells by IFNα, subfigures **D–F** to the weak activation and subfigures **G–I** to the scenario in which leukaemic stem cells are not activated by IFNα. Thick curves correspond to smoothed values of the maximal BCR–ABL/ABL ratios, whereas the thin lines indicate the expected oscillations due to the cyclic treatment regimen.

less-favourable situation (i.e., IFNα does not induce activation of leukaemic stem cells), a pulsed IFNα therapy under continuing TKI administration shows no adverse effects compared with standard TKI monotherapy. These findings support recent clinical results that argue in favour of lower doses/longer cycles of IFNα administration in combination therapies to reduce severe side effects, but retaining the curative intent (Simonsson *et al*, 2011).

It remains speculative how the pharmacological effects of IFNα and TKIs act together on the level of HSCs in general and on leukaemic stem cells in particular. However, as shown by our simulation study, it is the combination of effects (whether they are, e.g., independent from each other or mutually compensating) as well as the translation into the human system that determine the possible clinical benefit. We demonstrated that especially the level of activation of the leukaemic stem cells is a major determinant of the speed of tumour eradication. For the continuous application of TKIs and IFNα, our model predicts therapy failure in cases in which leukaemic stem cells (but not normal HSCs) are completely insensitive to the activating effect of IFNα. A similarly critical situation is observed if both TKI and IFNα are administered in a pulsed, but sequential, fashion, which does not allow for a simultaneous pharmacological effect of both drugs. In these cases, a strong activation of leukaemic stem cells compared with normal HSCs induces a competitive advantage of the leukaemic clone and results in therapy failure. As we are not aware of any reports that suggest a correlation between IFNα administration and rapid leukaemic relapse, we consider this as an indirect evidence that CML stem cells are at least partially sensitive to IFNα.

It has been repeatedly discussed that the occurrence of secondary mutations in CML stem cells alters their responsiveness to TKIs and induces therapy failure (La Rosee and Deininger, 2010). Although it is not yet resolved whether such critical secondary mutations already pre-exist in the leukaemic clone before initial treatment or whether they are generated under TKI therapy (Sorel *et al*, 2004; Komarova and Wodarz, 2005; Jiang *et al*, 2007), it is sensible to assume that increased cell proliferation due to IFNα administration increases the risk for such unfavourable alterations. However, a quantification of this risk is nontrivial and beyond the scope of this publication. We argue that lower doses/longer cycles of IFNα administration in combination with TKI treatment appear as the favourable option, which should also minimise the risk for secondary mutations.

The presented model accounts for clonal behaviour of CML in the untreated and treated situation but it does not correctly represent the pharmacokinetic residence times of the administered drugs. Unlike in earlier applications of our model (e.g., in Roeder *et al*, 2006 in which we assumed a decelerated effect on the leukaemic stem cell population with a better fitting of the short-term BCR–ABL/ABL response after start of imatinib therapy), we made the simplifying assumption that all drugs act instantly and only as long as they are administered. Especially in the case of pegylated IFNα these assumptions do not hold. However, to account for the temporal extension of the drug activity, we model drug application as a temporal process extending over at least 24 h instead of modelling single-application events with sophisticated pharmacokinetics. Under these limitations, our general conclusion holds true that a therapeutic benefit is only achieved if IFNα is at any time supported by the immediate presence of the selective cytotoxic effect on the activated leukaemic cells.

Second-generation TKIs (like dasatinib or nilotinib) show increased efficiency against CML and currently replace imatinib as a first-line therapy (Kantarjian *et al*, 2010; Saglio *et al*, 2010). However, as the mechanism of action of these drugs, namely the inhibition of *BCR–ABL* tyrosine kinase and the resulting, targeted cytotoxic effect on leukaemic cells, are reportedly very similar to imatinib (Sawyers, 2010), our modelling results will in principle also apply for the situation that imatinib is replaced by a second-generation TKI.

The situation is different for alternative drugs that are regularly used to activate HSCs. Some of these drugs, like HU or 5-FU, induce a strong cytotoxic effect on proliferating cells while others, like G-CSF and AMD3100, lead to a mobilisation of HSCs from the bone marrow into the peripheral blood. Owing to these differences in their modes of action, the adaptation of the simulation results for IFNα to these alternative drugs would require a more detailed understanding of the drug effects on the stem cell level. Furthermore, we have restricted our model analysis of IFNα to the experimentally described activation of HSCs (Essers *et al*, 2009), thus intentionally neglecting additional immunological effects, which might also show a therapeutical benefit for the treatment of leukaemia patients.

Summarising our findings, we argue that before a clinical implementation of a combination therapy it is necessary to experimentally verify whether (1) IFNα leads to a similar activation of human HSCs as in mice, (2) CML stem cells are also activated by IFNα and (3) how this activation changes under the additional administration of a TKI. Appropriate experimental models in the mouse, such as xenografts with human HSCs and CML cells, are valuable systems for studying the drug combinations. However, especially the IFNα-dependent activation of both normal and leukaemic cells might require the correct environmental context, which is only given in the human situation. Simulation approaches, as the one presented here, are important tools to direct and justify the necessary experimental and clinical research that is currently pursued by our collaborators and us.

ACKNOWLEDGEMENTS

We thank Andreas Hochhaus for discussions and critical comments on our manuscript. This research was supported by the European Commission project EuroSyStem (200 270), by the German Research Council (DFG), grant RO3500/1-2, and by the German Ministry for Education and Research, BMBF-grant on Medical Systems Biology 'HaematoSys' (BMBF-FKZ 0315452). KH was partly funded by the Leipzig Interdisciplinary Research Cluster of Genetic Factors, Clinical Phenotypes, and Environment (LIFE Centre, Universität Leipzig). LIFE is funded by means of the European Union, by the European Regional Development Fund (ERDF), the European Social Fund (ESF) and by means of the Free State of Saxony within the framework of its excellence initiative. ME and AT are supported by the Dietmar Hopp Foundation.

Supplementary Information accompanies the paper on British Journal of Cancer website (http://www.nature.com/bjc)

REFERENCES

Borden EC, Sen GC, Uze G, Silverman RH, Ransohoff RM, Foster GR, Stark GR (2007) Interferons at age 50: past, current and future impact on biomedicine. *Nat Rev Drug Discov* 6(12): 975–990

Branford S, Hughes TP, Rudzki Z (1999) Monitoring chronic myeloid leukaemia therapy by real-time quantitative PCR in blood is a reliable alternative to bone marrow cytogenetics. *Br J Haematol* 107(3): 587–599

Cortes J, Quintas-Cardama A, Jones D, Ravandi F, Garcia-Manero G, Verstovsek S, Koller C, Hiteshew J, Shan J, O'Brien S, Kantarjian H (2010) Immune modulation of minimal residual disease in early chronic phase chronic myelogenous leukemia: a randomized trial of frontline high-dose imatinib mesylate with or without pegylated interferon alpha-2b and granulocyte-macrophage colony-stimulating factor. *Cancer* 117(3): 572–580

Druker BJ, Tamura S, Buchdunger E, Ohno S, Segal GM, Fanning S, Zimmermann J, Lydon NB (1996) Effects of a selective inhibitor of the Abl tyrosine kinase on the growth of Bcr-Abl positive cells. *Nat Med* 2(6): 561–566

Drummond MW, Heaney N, Kaeda J, Nicolini FE, Clark RE, Wilson G, Shepherd P, Tighe J, McLintock L, Hughes T, Holyoake TL (2009) A pilot study of continuous imatinib vs pulsed imatinib with or without G-CSF in CML patients who have achieved a complete cytogenetic response. *Leukemia* 23(6): 1199–1201

Essers MA, Offner S, Blanco-Bose WE, Waibler Z, Kalinke U, Duchosal MA, Trumpp A (2009) IFNalpha activates dormant haematopoietic stem cells *in vivo*. *Nature* 458(7240): 904–908

Essers MA, Trumpp A (2010) Targeting leukemic stem cells by breaking their dormancy. *Mol Oncol* 4(5): 443–450

Foo J, Drummond MW, Clarkson B, Holyoake T, Michor F (2009) Eradication of chronic myeloid leukemia stem cells: a novel mathematical model predicts no therapeutic benefit of adding G-CSF to imatinib. *PLoS Comput Biol* 5(9): e1000503

Glauche I, Horn M, Roeder I (2007) Leukaemia stem cells: hit or miss? *Br J Cancer* 96(4): 677–678; author reply 679–680

Goldman JM (2009) Treatment strategies for CML. *Best Pract Res Clin Haematol* 22(3): 303–313

Graham SM, Jorgensen HG, Allan E, Pearson C, Alcorn MJ, Richmond L, Holyoake TL (2002) Primitive, quiescent, Philadelphia-positive stem cells from patients with chronic myeloid leukemia are insensitive to STI571 *in vitro*. *Blood* 99(1): 319–325

Guilhot F, Preudhomme C, Guilhot J, Mahon F-X, Nicolini FE, Rigual-Huguet F, Legros L, Guerci A, Rea D, Coiteux V, Maloisel F, Gardembas M, Bulabois C-E, Berger MG (2009) Significant higher rates of undetectable molecular residual disease and molecular responses with pegylated form of interferon a2a in combination with imatinib (IM) for

the treatment of newly diagnosed chronic phase (CP) chronic myeloid leukaemia (CML) patients (pts): confirmatory results at 18 months of part 1 of the spirit phase III randomized trial of the french CML group (FI LMC). *ASH Annu Meeting Abstracts* **114**(22): 340

Hochhaus A, O'Brien SG, Guilhot F, Druker BJ, Branford S, Foroni L, Goldman JM, Muller MC, Radich JP, Rudoltz M, Mone M, Gathmann I, Hughes TP, Larson RA (2009) Six-year follow-up of patients receiving imatinib for the first-line treatment of chronic myeloid leukemia. *Leukemia* **23**(6): 1054–1061

Horn M, Loeffler M, Roeder I (2008) Mathematical modeling of genesis and treatment of chronic myeloid leukemia. *Cells Tissues Organs* **188**(1–2): 236–247

Jiang X, Saw KM, Eaves A, Eaves C (2007) Instability of BCR-ABL gene in primary and cultured chronic myeloid leukemia stem cells. *J Natl Cancer Inst* **99**(9): 680–693

Jorgensen HG, Copland M, Allan EK, Jiang X, Eaves A, Eaves C, Holyoake TL (2006) Intermittent exposure of primitive quiescent chronic myeloid leukemia cells to granulocyte-colony stimulating factor *in vitro* promotes their elimination by imatinib mesylate. *Clin Cancer Res* **12**(2): 626–633

Kantarjian H, Shah NP, Hochhaus A, Cortes J, Shah S, Ayala M, Moiraghi B, Shen Z, Mayer J, Pasquini R, Nakamae H, Huguet F, Boque C, Chuah C, Bleickardt E, Bradley-Garelik MB, Zhu C, Szatrowski T, Shapiro D, Baccarani M (2010) Dasatinib versus imatinib in newly diagnosed chronic-phase chronic myeloid leukemia. *N Engl J Med* **362**(24): 2260–2270

Komarova NL, Wodarz D (2005) Drug resistance in cancer: principles of emergence and prevention. *Proc Natl Acad Sci USA* **102**(27): 9714–9719

Komarova NL, Wodarz D (2007) Effect of cellular quiescence on the success of targeted CML therapy. *PLoS One* **2**(10): e990

La Rosee P, Deininger MW (2010) Resistance to imatinib: mutations and beyond. *Semin Hematol* **47**(4): 335–343

Mahon FX, Rea D, Guilhot J, Guilhot F, Huguet F, Nicolini F, Legros L, Charbonnier A, Guerci A, Varet B, Etienne G, Reiffers J, Rousselot P (2010) Discontinuation of imatinib in patients with chronic myeloid leukaemia who have maintained complete molecular remission for at least 2 years: the prospective, multicentre Stop Imatinib (STIM) trial. *Lancet Oncol* **11**(11): 1029–1035

Michor F, Hughes TP, Iwasa Y, Branford S, Shah NP, Sawyers CL, Nowak MA (2005) Dynamics of chronic myeloid leukaemia. *Nature* **435**(7046): 1267–1270

Roeder I, Horn M, Glauche I, Hochhaus A, Mueller MC, Loeffler M (2006) Dynamic modeling of imatinib-treated chronic myeloid leukemia: functional insights and clinical implications. *Nat Med* **12**(10): 1181–1184

Roeder I, Kamminga LM, Braesel K, Dontje B, Haan Gd, Loeffler M (2005) Competitive clonal hematopoiesis in mouse chimeras explained by a stochastic model of stem cell organization. *Blood* **105**(2): 609–616

Roeder I, Loeffler M (2002) A novel dynamic model of hematopoietic stem cell organization based on the concept of within-tissue plasticity. *Exp Hematol* **30**(8): 853–861

Rousselot P, Huguet F, Rea D, Legros L, Cayuela JM, Maarek O, Blanchet O, Marit G, Gluckman E, Reiffers J, Gardembas M, Mahon FX (2007) Imatinib mesylate discontinuation in patients with chronic myelogenous leukemia in complete molecular remission for more than 2 years. *Blood* **109**(1): 58–60

Saglio G, Kim DW, Issaragrisil S, le Coutre P, Etienne G, Lobo C, Pasquini R, Clark RE, Hochhaus A, Hughes TP, Gallagher N, Hoenekopp A, Dong M, Haque A, Larson RA, Kantarjian HM (2010) Nilotinib versus imatinib for newly diagnosed chronic myeloid leukemia. *N Engl J Med* **362**(24): 2251–2259

Savage DG, Antman KH (2002) Imatinib mesylate–a new oral targeted therapy. *N Engl J Med* **346**(9): 683–693

Sawyers CL (2010) Even better kinase inhibitors for chronic myeloid leukemia. *N Engl J Med* **362**(24): 2314–2315

Simonsson B, Gedde-Dahl T, Markevarn B, Remes K, Stentoft J, Almqvist A, Bjoreman M, Flogegard M, Koskenveesa P, Lindblom A, Malm C, Mustjoki S, Myhr-Eriksson K, Ohm L, Rasanen A, Sinisalo M, Sjalander A, Stromberg U, Weiss Bjerrum O, Ehrencrona H, Gruber F, Kairisto V, Olsson K, Sandin F, Nagler A, Lanng Nielsen J, Hjorth-Hansen H, Porkka K (2011) Combination of pegylated interferon-{alpha}2b with imatinib increases molecular response rates in patients with low or intermediate risk chronic myeloid leukemia. *Blood* **118**: 3228–3235

Sorel N, Bonnet ML, Guillier M, Guilhot F, Brizard A, Turhan AG (2004) Evidence of ABL-kinase domain mutations in highly purified primitive stem cell populations of patients with chronic myelogenous leukemia. *Biochem Biophys Res Commun* **323**(3): 728–730

CML therapy can benefit from the activation of HSCs: simulation studies of different treatment combinations
-
Supplemental data

Ingmar Glauche, Katrin Horn, Matthias Horn, Lars Thielecke,
Marieke Essers, Andreas Trumpp, Ingo Roeder

1 Simulation algorithm and model equations

The described model of HSC organization and leukaemia is mathematically represented as a single-cell based, stochastic process. I.e., the development of each individual cell in the system is simulated according to a set of defined rules including stochastic decisions. These rules are applied at discrete time steps ($\Delta t = 1$ hour) to simultaneously update the status of all model cells.
Normal and leukaemic cells are both present simultaneously within the model. The cell types differ only with respect to some of their defining parameters. The differences and their impact are outlined below. The status of each model cell, irrespective of its type, is given by its cell specific affinity a, its membership to a signaling context $m \in \{A, \Omega\}$, and its position in the cell cycle c.
The cell cycle for an activated cell in signaling context Ω is modeled as a sequence of $G1$ phase, S phase, and $G2/M$ phase, in which the duration of latter phases (τ_S and $\tau_{G2/M}$) is fixed. Cells changing into signaling context A exit from $G1$ and enter a cell cycle inactive phase ($G0$) until they are activated again and transit into signaling context Ω.
To realize an update step, the actual total number of cells with $a > a_{\min}$ in signaling context A ($N_A(t)$) and Ω ($N_\Omega(t)$) is determined. Based on these numbers, the status of each model stem cell is updated as follows:

(1) If the cell resides in signaling context A, it changes to signaling context Ω or stays in A with probabilities ω and $1-\omega$, respectively. If it stays in A, its cell specific affinity a is increased by the factor r (regeneration coefficient), until a has reached the maximal

regeneration limit $a_{\max} = 1$. If the cell changes to signaling context Ω, its position in the cell cycle will be set to the begin of S-phase.

(2) If the cell resides in signaling context Ω, it changes to context A or stays in Ω with probabilities α and $1 - \alpha$, respectively. Herein, a change to signaling context A is only possible in $G1$-phase of the cell cycle for cells with $a > a_{\min}$. If the cell stays in signaling context Ω, a is decreased by the factor $1/d$ (with differentiation coefficient d) and the cell cycle position is incremented. In case of cell cycle completion (i.e., $c(t) = \tau_{G1} + \tau_S + \tau_{G2/M}$), $c(t)$ is set to 0 and a new identical cell is generated (cell division). If a has reached the minimal value $a_{\min}$, the cells cannot reenter into signaling context A and proceed development in Ω. Within the model all cells with $a > a_{\min}$ are referred to a as stem cells, whereas cells with $a < a_{\min}$ are referred to as differentiating cells. The differentiating cells undergo an proliferative phase of 480 hours before they mature for another 192 hours. BCR-ABL/ABL ratios are calculated based in the fraction of leukaemic cells among this pool of maturing cells. A conceptual sketch of the model is provided in Figure 1 of the main document.

The transition probabilities α and ω depend on the actual affinity $a(t)$ of the cell, on the fixed parameters $a_{\min}$ and $a_{\max}$, and on the transition characteristics f_α and f_ω, respectively:

$$\alpha = \frac{a(t)}{a_{\max}} f_\alpha(N_A(t)) \tag{1}$$

$$\omega = \frac{a_{\min}}{a(t)} f_\omega(N_\Omega(t)) \tag{2}$$

The transition characteristics f_α and f_ω are crucial regulators to describe the dynamic differences between normal and leukaemic cells, and also to account for the action of different drugs (i.e. tyrosine kinase inhibitor (TKI) Imatinib or IFNα). Besides their cell type specificity, the transition characteristics depend on the total number of cells (N_A, N_Ω) in the respective target context. They are modelled by a general class of sigmoid functions:

$$f_{\alpha/\omega}(N_{A/\Omega}) = \frac{1}{\nu_1 + \nu_2 \cdot exp\left(\nu_3 \cdot \frac{N_{A/\Omega}}{\tilde{N}_{A/\Omega}}\right)} + \nu_4. \tag{3}$$

The parameters ν_1, ν_2, ν_3, and ν_4 determine the shape of $f_{\alpha/\omega}$. $\tilde{N}_{A/\Omega}$ is a scaling factor for $N_{A/\Omega}$.
It is possible to uniquely determine ν_1, ν_2, ν_3, and ν_4 by the more intuitive values $f_{\alpha/\omega}(0)$, $f_{\alpha/\omega}(\frac{\tilde{N}_{A/\Omega}}{2})$, $f_{\alpha/\omega}(\tilde{N}_{A/\Omega})$, and $f_{\alpha/\omega}(\infty) := lim_{N_{A/\Omega} \to \infty} f_{\alpha/\omega}(N_{A/\Omega})$:

$$\begin{aligned}\nu_1 &= (h_1 h_3 - h_2^2)/(h_1 + h_3 - 2h_2)\\ \nu_2 &= h_1 - \nu_1\\ \nu_3 &= \ln((h_3 - \nu_1)/\nu_2)\\ \nu_4 &= f_{\alpha/\omega}(\infty)\end{aligned}$$

with

$$\begin{aligned}h_1 &= 1\,/\,[f_{\alpha/\omega}(0) - f_{\alpha/\omega}(\infty)]\\ h_2 &= 1\,/\,\left[f_{\alpha/\omega}\left(\tilde{N}_{A/\Omega}/2\right) - f_{\alpha/\omega}(\infty)\right]\\ h_3 &= 1\,/\,[f_{\alpha/\omega}(\tilde{N}_{A/\Omega}) - f_{\alpha/\omega}(\infty)].\end{aligned}$$

Details of the parameter choice are discussed below.

The mathematical model is implemented in C++ and has been tested for UNIX-derived operating systems. The source code (including parameter files for the described scenarios) can be obtained from the authors.

2 Definition of cell types

Within the modelling approach, normal and leukaemic cells are represented by different choices of parameters for the treated and untreated situation. These are referred to as type I to VI and are motivated below.

Normal hematopoietic stem cells (type I). Parameters for normal hematopoietic stem cells are chosen such that a dynamically stabilized balance between quiescent cells in A and activated cells in Ω is established and maintained (verified for different experimental and clinical situations in mice and humans). A surplus of cells contributes to the pool of differentiating cells and later feeds into a compartment corresponding to "peripheral blood". Characteristic transition functions f_α and f_ω are shown in Supplementary Figure 1 row I.

Leukaemic stem cells (type II). Due to a single mutation event (corresponding to the translocation between chromosomes 9 and 22 forming the BCR-ABL oncogene) we assume that the characteristic parameters of one single model stem cell are initially changed compared to the normal HSCs. In particular, we assume that this leukaemic cell and all its clonal progeny have an uncontrolled activation, i.e. activation occurs independently of the cell number in Ω. Furthermore we assume a superior ability to change from Ω to A for leukaemic stem cells compared to normal hematopoietic stem cells. The corresponding transition functions f_α and f_ω are shown in Supplementary Figure 1 row II.

Leukaemic stem cells under TKI treatment (type III). For the situation that CML is treated with TKI Imatinib we assume that (i) activated leukaemic stem cells are killed with degradation rate $r_{\text{deg}} = 3.2\%$ per time step. (ii) We furthermore assume that the TKI leads to a reduced activation of the leukaemic cells which corresponds to a downregulation of the activation function f_ω. Corresponding transition functions are shown in Supplementary Figure 1 row III.
These assumptions proved extremely resilient to successfully predict the long-term behavior of Imatinib treated CML patients [1, 2].

Normal HSCs under IFNα (type IV). The behavior of normal human HSCs under IFNα is assumed to be similar to the murine situation. Here, it was shown in [3] that HSCs are activated by IFNα. Within the model we had to assume that about $p_a = 3\%$ of the quiescent HSCs are additionally activated at each time step (see Supplementary Figure 2). Although the overall activation of about 50% is still below the experimentally detected level of 70%, we argue that the use of BrdU as a means to estimate the fraction of cycling HSCs might itself lead to an additional activation of HSCs [4]. Corresponding transition functions are shown in Supplementary Figure 1 row IV. The case of the additional self-renewal deficit is discussed below.

Leukaemic stem cells under IFNα (type V). For the leukaemic stem cells it is currently speculative whether they are activated by IFNα or not. In order to address this uncertainty we study three different scenarios spanning a range of biologically plausible assumptions: (i) Leukaemic stem cells behave similar to normal cells and are similarly activated by IFNα ($p_a = 3\%$), (ii) leukaemic stem cells are only weakly activated by IFNα ($p_a = 0.2\%$), and (iii) leukaemic stem cells do not respond to IFNα activation at all ($p_a = 0$). Corresponding transition functions are shown in Supplementary Figure 1 row V.

Leukaemic stem cells under TKI and IFNα (VI). As for the above situation, the IFNα mediated activation of leukaemic stem cells under simultaneous TKI treatment remains speculative. The resulting effect for the combined treatment is even more uncertain since we assume the induction of prolonged quiescence of the leukaemic stem cells under TKI treatment (i.e. downregulation of f_ω) while at the same time we also assume IFNα to induce additional activation ($p_a > 0$). However, as these effects are modelled separately within the model, we are able to study the same scenarios as above: (i) leukaemic stem cells are strongly activated by IFNα ($p_a = 3\%$), (ii) leukaemic stem cells are weakly activated by IFNα ($p_a = 0.2\%$), and (iii) leukaemic stem cells do not respond to IFNα activation at all ($p_a = 0$). Corresponding transition functions are shown in Supplementary Figure 1 row VI.

Self-renewal deficit (SRD) mediated by IFNα It could also be demonstrated by Essers et al. [3] that in a chimeric situation between wild-type and IFNα-receptor knock-out cells the continuous administration of IFNalpha over the course of three weeks leads to

a complete eradication of the wild-type clone. In contrast, application of IFNalpha to wild-type mouse did not significantly influence peripheral blood cell counts and showed no long-term effect on the stem cell level after three weeks application. In terms of the model, this fast out-competition in the chimeric situation can only be explained under the assumption that IFNα (besides the stem cell activation) induces an additional defect in the cells ability to reattach to the niche-like signalling context A. However, for small stem cell numbers this effect is alleviated as the system aims to compensate a total loss of HSCs. Technically, this is modelled by an overall reduction of the f_α transition function for large cell numbers and for all cell types under administration of IFNα. Only for small cell numbers we have to assume increased transition rates in order to prevent bone marrow exhaustion. A precise quantification of this effect would require further measurements with low stem cell numbers, which are difficult to obtain. Altered transition curves are provided in the right column of Supplementary Figure 1.

Numerical values for all transition functions and further model parameters are provided in Supplementary Tables 1 and 2.

3 Pathogenesis and TKI treatment of human CML

For the pathogenesis of CML we assume that at a certain time point one hematopoietic stem cell (type I) alters its cell type to become a leukaemic cell (type II). For the case that the clone engrafts, normal hematopoiesis is replaced over the time course of about 5 to 7 years. We assume clinical manifestation and treatment start with TKI when BCR-ABL/ABL ratios in the pool of non-proliferating maturing cells exceeds 99 %. Treatment start is considered to be time point $t = 0$ and the leukaemic cells are switched from type (II) to type (III), mimicking the TKI treatment. 5.5 year clinical follow-up data from a cohort of 69 CML patients treated with TKI Imatinib [1, 5] is used to adapt the model parameters. Due to the immediate action of Imatinib on all leukaemic cells the initial decline of BCR-ABL/ABL ratios is slightly overestimated.
The long-term behavior of an "average patient" is depicted in Supplementary Figure 3 and is used as a reference to estimate the clinical benefit of a combination therapy.

4 Combination therapy

Initiation of combination therapy. Combining IFNα administration with TKI treatment is a potential strategy to eradicate residual disease. Given the rapid cytogenetic and molecular remission in most CML patients after administration of TKI Imatinib, we argue that a combination therapy should reasonably start around months 9 to 12. For the modelling approach we assume combination therapy to start at month 12 without loss of generality.
The different treatment regimes are at each time point defined by the presence or absence of TKI or IFNα. According to this stetting the normal and leukaemic cells are modelled as cells of type (I) to (VI). Technically, changes in the drug administration are

modelled by switching the type of the affected cells (see Supplementary Table 3).

In addition to the presented analysis in the main document further scenarios are outlined below:

Continuous TKI + pulsed IFNα with self-renewal deficit. Supplementary Figure 4 contains the same simulations as Figure 5 of the main document but with additional self-renewal deficit induced by the IFNα treatment. No significant deviations are observed.

Pulsed TKI + pulsed IFNα with self-renewal deficit. Supplementary Figure 5 contains the same simulations as Figure 6 of the main document but with additional self-renewal deficit induced by the IFNα treatment. No significant deviations are observed.

Pulsed TKI + continuous IFNα . For completeness we provide simulation results for this clinically less relevant scenario in which TKI is administered once every 14 days on top of a continuous IFNα treatment. Figure 6 and 7 show the corresponding simulation results with and without the additional assumption of an IFNα induced self-renewal deficit. Therapy failure is expected in almost all studied cases. Only if leukaemic stem cells are strongly activated by IFNα and under the assumption that the drug also induces a self-renewal deficit, we would predict a therapeutic benefit. However, in the initial phase of the combination therapy one would expect a temporary increase in leukaemic cells due to their strong activation.

References

[1] I. Roeder, M. Horn, I. Glauche, A. Hochhaus, M. C. Mueller, and M. Loeffler. Dynamic modeling of imatinib-treated chronic myeloid leukemia: functional insights and clinical implications. *Nat Med*, 12(10):1181–1184, 2006.

[2] Matthias Horn, Markus Loeffler, and Ingo Roeder. Mathematical modeling of genesis and treatment of chronic myeloid leukemia. *Cells Tissues Organs*, 188(1-2):236–247, 2008.

[3] Marieke A G Essers, Sandra Offner, William E Blanco-Bose, Zoe Waibler, Ulrich Kalinke, Michel A Duchosal, and Andreas Trumpp. Ifnalpha activates dormant haematopoietic stem cells in vivo. *Nature*, 458(7240):904–908, Apr 2009.

[4] Anne Wilson, Elisa Laurenti, Gabriela Oser, Richard C van der Wath, William Blanco-Bose, Maike Jaworski, Sandra Offner, Cyrille F Dunant, Leonid Eshkind, Ernesto Bockamp, Pietro Lio, H. Robson Macdonald, and Andreas Trumpp.

Hematopoietic stem cells reversibly switch from dormancy to self-renewal during homeostasis and repair. *Cell*, 135(6):1118–1129, Dec 2008.

[5] A. Hochhaus, S. G. O'Brien, F. Guilhot, B. J. Druker, S. Branford, L. Foroni, J. M. Goldman, M. C. Mueller, J. P. Radich, M. Rudoltz, M. Mone, I. Gathmann, T. P. Hughes, R. A. Larson, and I. R. I. S. Investigators. Six-year follow-up of patients receiving imatinib for the first-line treatment of chronic myeloid leukemia. *Leukemia*, 23(6):1054–1061, Jun 2009.

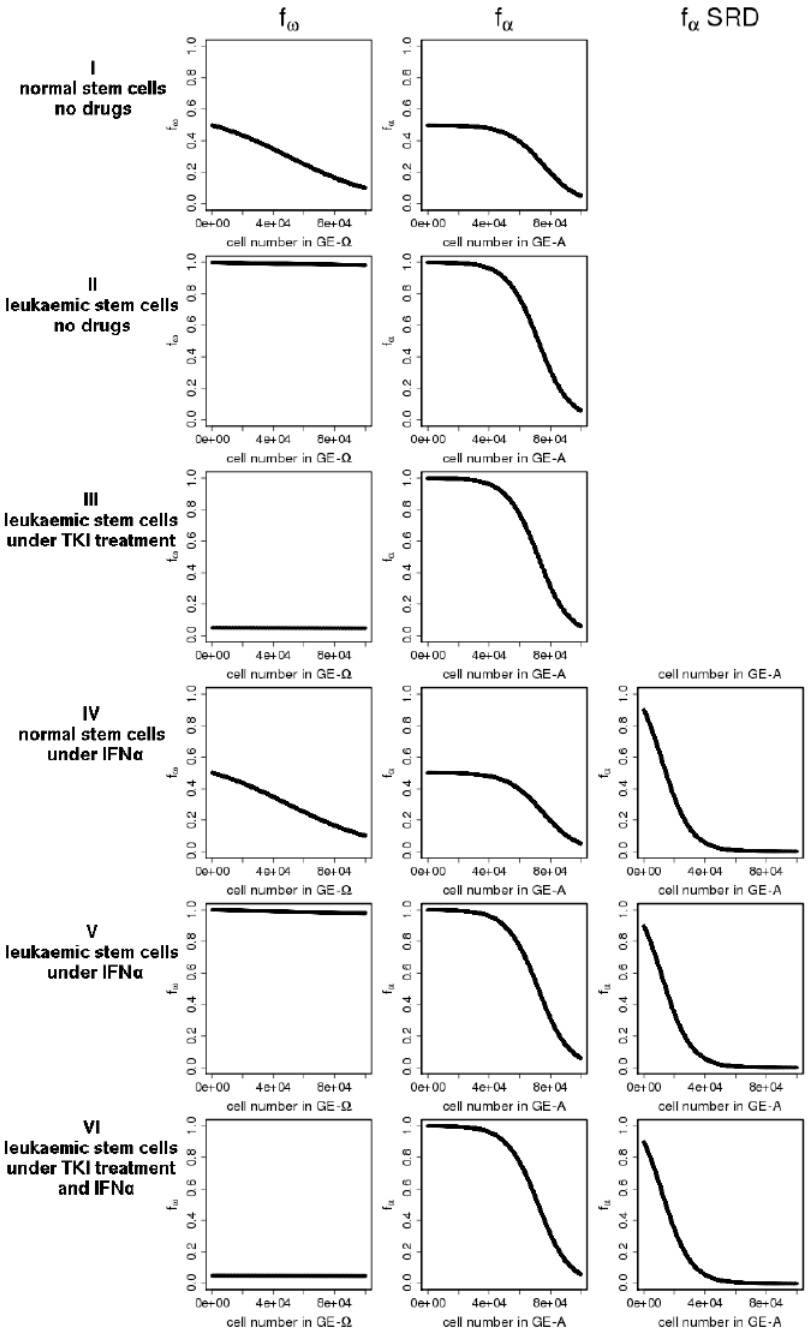

Supplementary Figure 1: Transition characteristics. Characteristic transition functions f_ω and f_α are provided for the different parameter choices represented as cell types I to VI. For the IFNα treated scenarios an additional function for f_α with self-renewal deficit is provided in the right column.

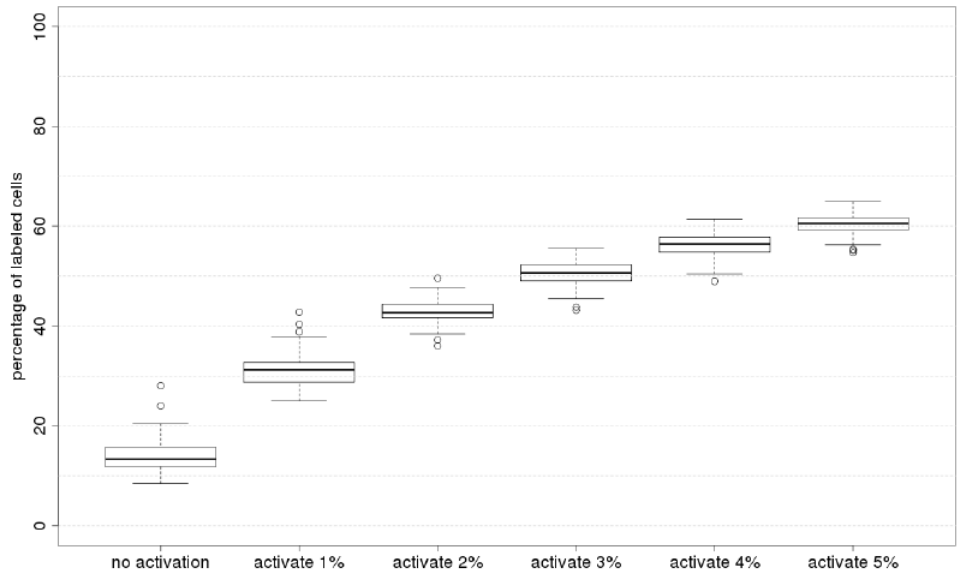

Supplementary Figure 2: Activation of quiescent HSCs by IFNα. The boxplot shows the percentage of modelled HSCs that entered into cell cycle within 72 hours past treatment with IFNα, thus mimicking a typical labelling experiment using BrdU to identify division events. For the IFNα treatment we assumed different levels of activation shown on the x-axis (percentage p_a of HSCs being activated from A into Ω during one time step). Beyond $p_a = 3\%$ there is only a marginal increase of the percentage of labeled cells, which is a result of the particular model setup.

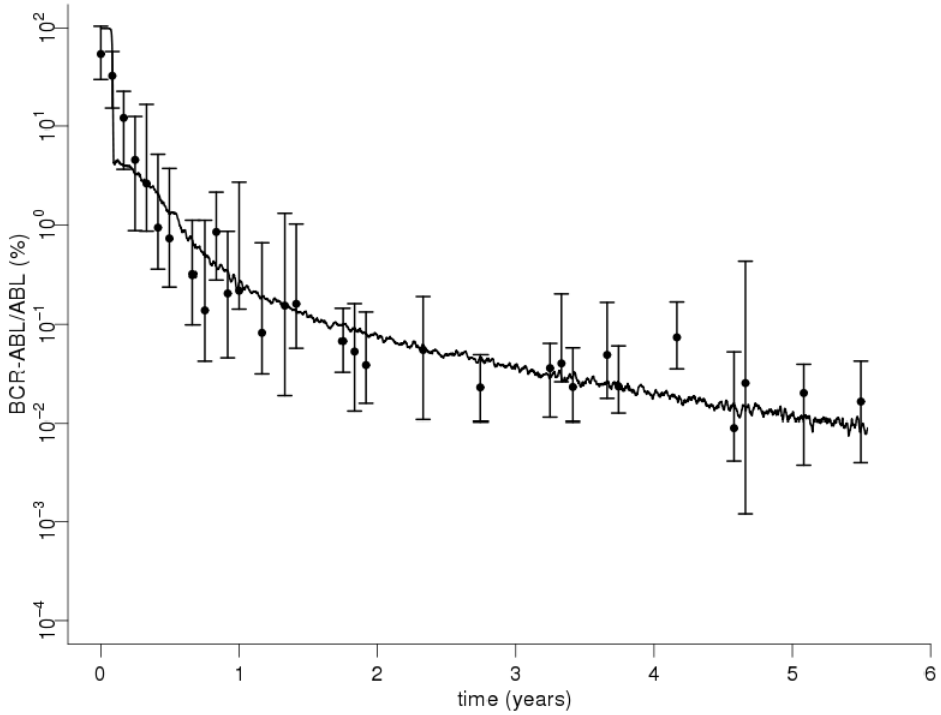

Supplementary Figure 3: Long-term treatment of CML patients with TKI Imatinib monotherapy. Model simulations (solid line) are compared with 5.5 year clinical follow-up data of 69 Imatinib treated CML patients from the german cohort of the IRIS study [1, 5].

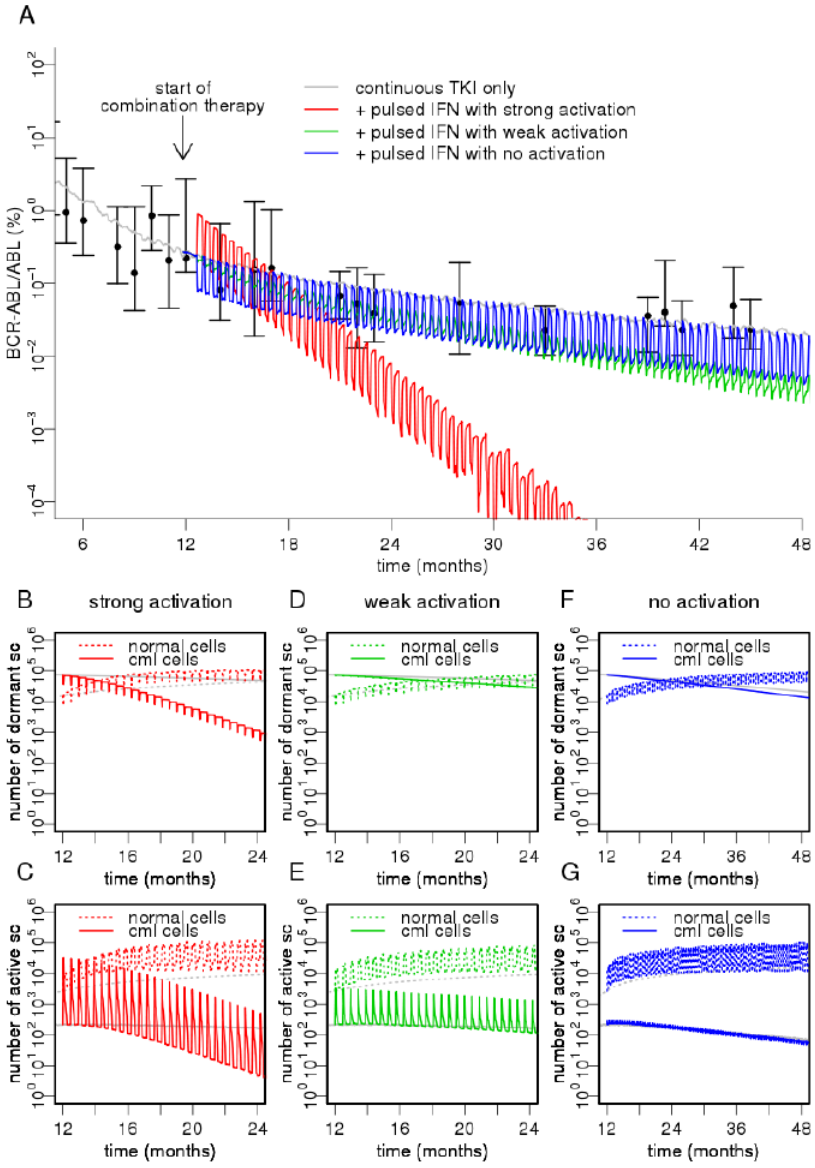

Supplementary Figure 4: Treatment of CML with continuous administration of TKI and pulsed IFNα with self-renewal deficit. The Figure corresponds to Figure 5 in the main document but includes the self-renewal deficit.

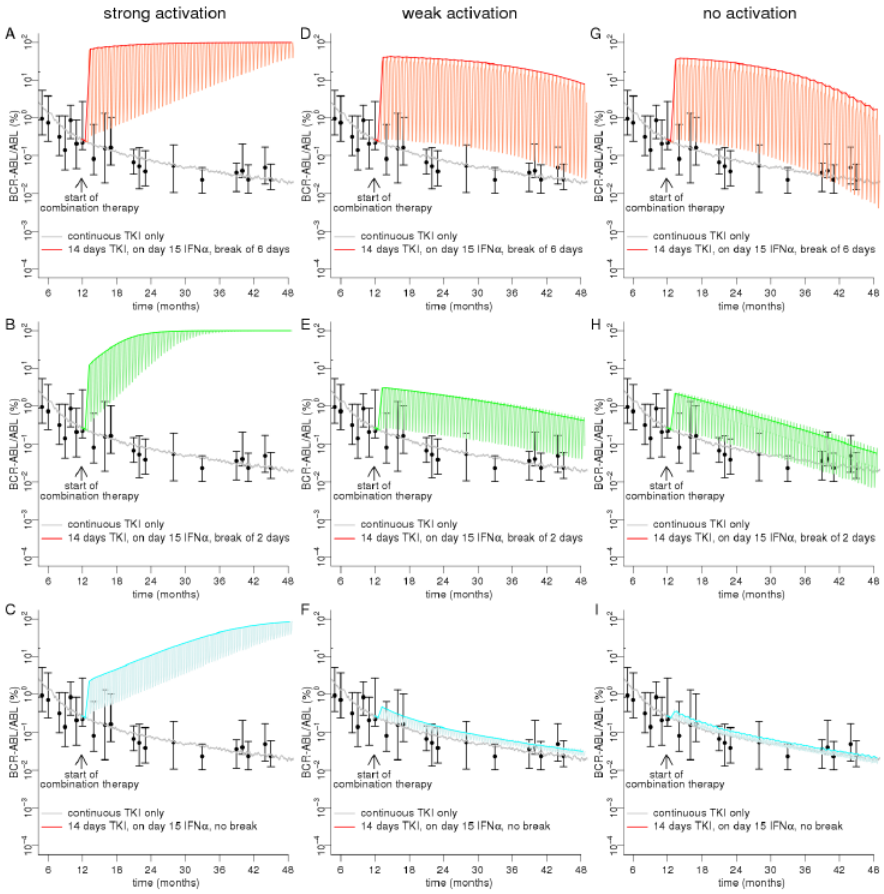

Supplementary Figure 5: Treatment of CML with pulsed administration of TKI and pulsed IFNα with self-renewal deficit. The Figure corresponds to Figure 6 in the main document but includes the self-renewal deficit.

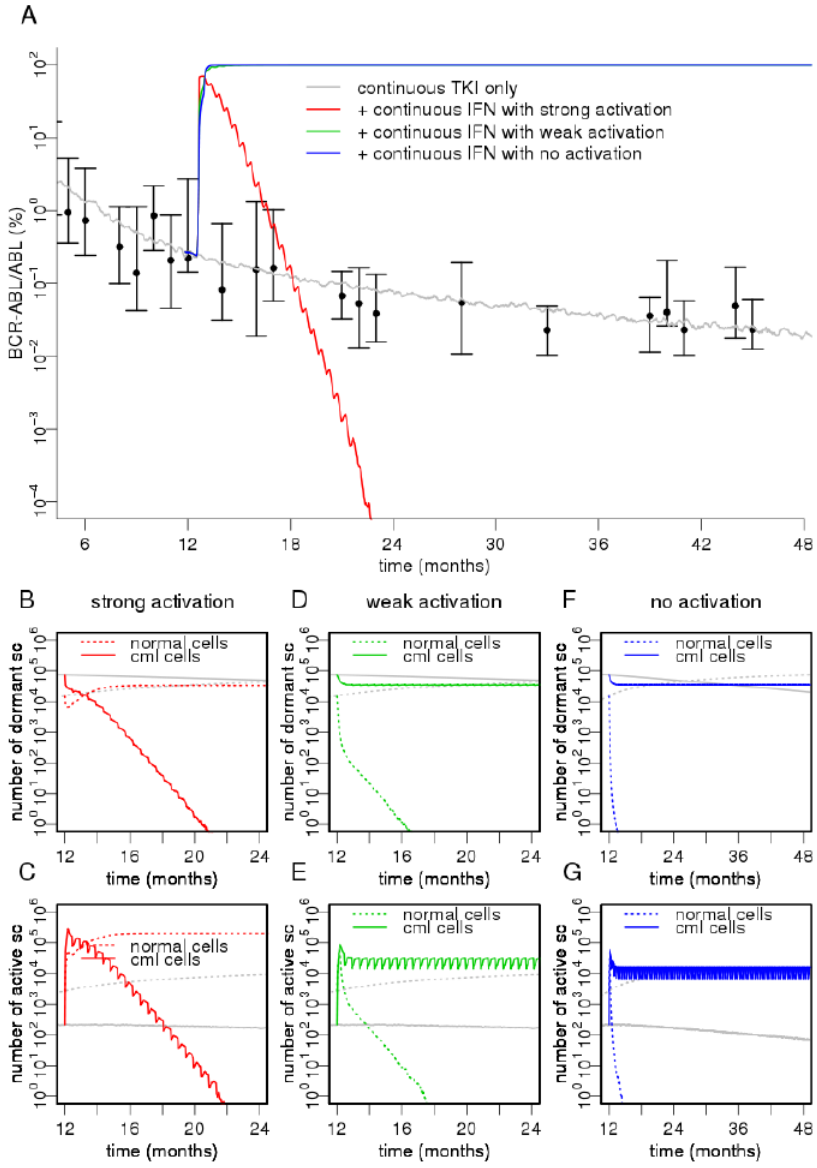

Supplementary Figure 6: Treatment of CML with pulsed administration of TKI and continuous IFNα with self-renewal deficit. BCR-ABL/ABL ratios in peripheral blood are shown for pulsed application of TKI (1 day within 14 days of continuous IFNα treatment) for different activation scenarios: strong activation of leukaemic stem cells similar to normal HSCs (red), weak activation (green), no activation of leukaemic cells (blue, only normal cells are activated by IFNα). Subfigures show corresponding stem cell numbers in A (quiescent) and Ω (activated), compared to monotherapy with TKI Imatinib (grey).

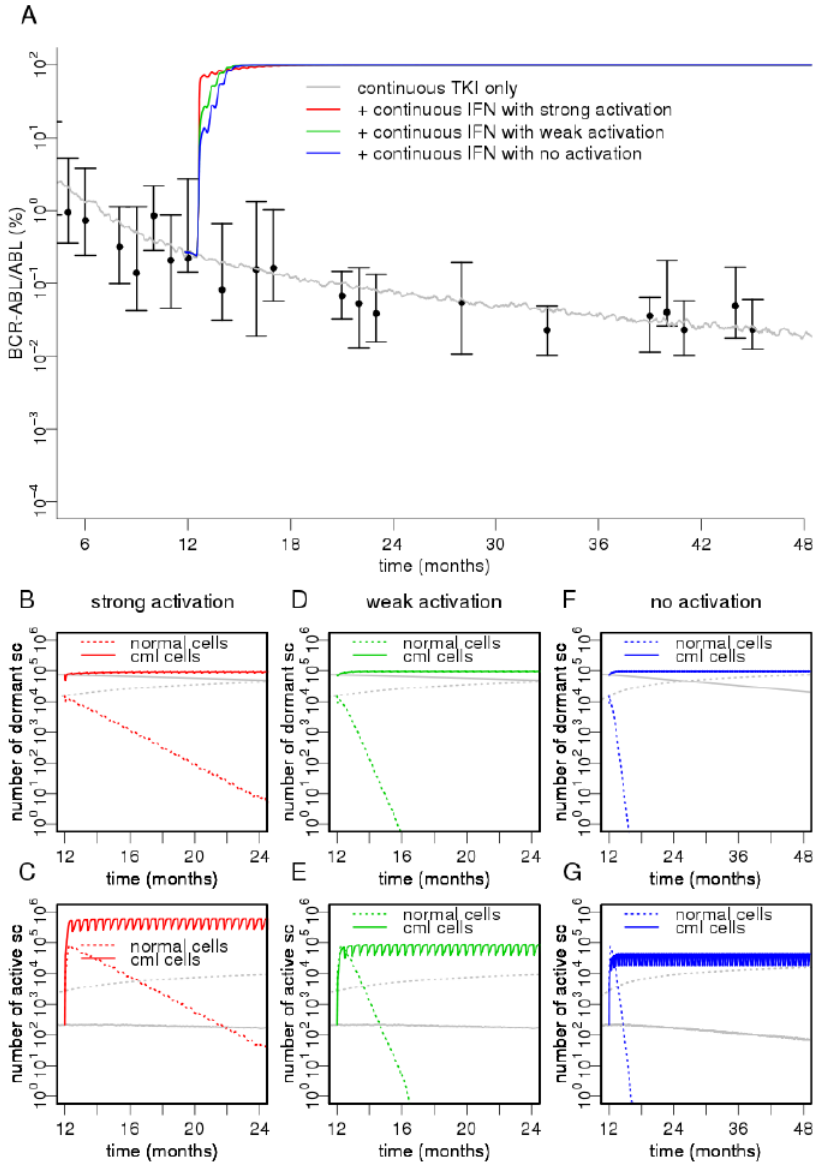

Supplementary Figure 7: Treatment of CML with pulsed administration of TKI and continuous IFNα without self-renewal deficit. BCR-ABL/ABL ratios in peripheral blood are shown for pulsed application of TKI (1 day within 14 days of continuous IFNα treatment) for different activation scenarios: strong activation of leukaemic stem cells similar to normal HSCs (red), weak activation (green), no activation of leukaemic cells (blue, only normal cells are activated by IFNα). Subfigures show corresponding stem cell numbers in A (quiescent) and Ω (activated), compared to monotherapy with TKI Imatinib (grey).

cell type	transition characteristic	$f(0)$	$f(\frac{\tilde{N}_{A/\Omega}}{2})$	$f(\tilde{N}_{A/\Omega})$	$f(\infty)$	$N_{A/\Omega}$
normal cells (I)	f_ω	0.5	0.3	0.1	0.0	100,000
	f_α	0.5	0.45	0.05	0.0	100,000
cml cells (II)	f_ω	1.0	0.99	0.98	0.96	100,000
	f_α	1.0	0.90	0.058	0.0	100,000
cml cells under TKI treatment (III)	f_ω	0.05	0.049	0.048	0.046	100,000
	f_α	1.0	0.90	0.058	0.0	100,000
normal cells under IFNα (IV)	f_ω	0.5	0.3	0.1	0.0	100,000
	f_α	0.5	0.45	0.05	0.0	100,000
	f_α with SRD	0.9	0.02	0.0001	0.0	100,000
cml cells under IFNα (V)	f_ω	1.0	0.99	0.98	0.96	100,000
	f_α	1.0	0.90	0.058	0.0	100,000
	f_α with SRD	0.9	0.02	0.0001	0.0	100,000
cml cells under TKI treatment and IFNα (VI)	f_ω	0.05	0.049	0.048	0.046	100,000
	f_α	1.0	0.90	0.058	0.0	100,000
	f_α with SRD	0.9	0.02	0.0001	0.0	100,000

Supplementary Table 1: Model parameters for transition characteristics of different modelling cell types.

parameter	human	mouse
d	1.05	1.07
r	1.1	1.1
$a_{\min}$	0.002	0.01
$a_{\max}$	1.0	1.0
τ_{G1}	32 hours	468 hours
τ_S	8 hours	8 hours
$\tau_{G_2/M}$	8 hours	4 hours
$f_A(0)$	0.5	0.5
$f_A(\frac{\tilde{N}}{2})$	0.45	0.3
$f_A(\tilde{N})$	0.05	0.01
$f_A(\infty)$	0	0
N_A^{norm}	100,000	1300
$f_\Omega(0)$	0.5	0.5
$f_\Omega(\frac{\tilde{N}}{2})$	0.3	0.0075
$f_\Omega(\tilde{N})$	0.1	0.0002
$f_\Omega(\infty)$	0	0
N_Ω^{norm}	100,000	280

Supplementary Table 2: General model parameters. Model parameters for the mouse system were only used to study and compare IFNα related HSC activation in Supplementary Figure 2.

drug combination	normal cells	leukaemic cells	normal cells + SRD	leukaemic cells + SRD
no drugs	type I	type II	type I	type II
TKI	type I	type III	type I	type III
IFNα	type IV	type V	type IV_{SRD}	type V_{SRD}
TKI + IFNα	type IV	type VI	type IV_{SRD}	type VI_{SRD}

Supplementary Table 3: Overview of simulated cell types depending on the particular drug combination. Parameters for the cell types are provided in Supplementary Tables 1 and 2

2.3 „Model-based decision rules reduce the risk of molecular relapse after cessation of tyrosine kinase inhibitor therapy in chronic myeloid leukemia“ (Publikation 3)

Horn M, Glauche I, Müller MC, Hehlmann R, Hochhaus A, Loeffler M, Roeder I; *Blood*. 2013;121(2):378-384

Die dritte eingeschlossene Arbeit erschien Anfang 2013 in der Zeitschrift *Blood* und ist als Hauptpublikation dieser Dissertation anzusehen. Nachdem in vorangegangenen Arbeiten (17) mit Hilfe des ABM in erster Linie die mittlere *BCR-ABL*-Dynamik in einer Patientenkohorte erklärt wurde, steht in dieser Arbeit erstmals explizit die Inter-Patienten-Heterogenität im Mittelpunkt, mit dem Ziel, die prädiktiven Möglichkeiten des dynamischen Stammzellmodells für individuelle Patienten zu nutzen, um eine Optimierung der TKI-Therapie zu erreichen.

Obwohl TKIs in der Mehrzahl der CML-Patienten schnelle molekulare Remissionen induzieren und die Tumorlast bei Abwesenheit von Resistenzmechanismen unter fortgesetzter Therapie weiter fällt, ist ungeklärt, ob diese Medikamente in der Lage sind, den CML-Klon (langfristig) vollständig zu eradizieren. Unter IM-Therapie beobachtet man eine biphasische Abfallkinetik der *BCR-ABL*-Transkriptlevel, wobei sich die Reduktion der Tumorlast nach einem initialen steilen Abfall deutlich abschwächt (43). Es wird angenommen, dass der erste Abfall (Anstieg α) durch rasche Eliminierung proliferativer CML-Zellen verursacht wird, während der moderate Abfall (β) der langsamen Eradikation residualer LSCs geschuldet ist (19). Wenn die Tumorlast unter die Detektionsschwelle von quantitativen PCR-Methoden fällt und die Therapie unter kontrollierten Bedingungen beendet wird, beobachtet man in etwa der Hälfte der Patienten einen molekularen Rückfall (11). Dieser wird vermutlich durch residuale LSCs ausgelöst, welche sich im Knochenmark dem Einfluss von IM, aber auch der Beobachtung entziehen. Basierend auf klinisch verfügbaren Daten ist es derzeit nicht möglich vorherzusagen, welche Patienten nach Therapiestopp einen molekularen Rückfall erleiden.

IM-Therapieeffekte lassen sich im ABM durch zwei Parameter erklären: Transitionscharakteristik f_{ω} (Reduktion der proliferativen Aktivität) und Killrate r_{deg} (Eradikation von CML-Zellen). Modulation dieser Parameter erklärt die beobachtete Patientenheterogenität der *BCR-ABL*-Abfallkinetik. Die kinetischen Parameter α und β lassen sich eindeutig in die Modellparameter f_{ω} und r_{deg} „umrechnen“, so dass jeder Patient mit Hilfe des ABM simuliert werden kann. Damit sind Vorhersagen über die Anzahl residualer LSCs unter Therapie möglich. Basierend auf dieser Modellgröße wird ein Prädiktor vorgeschlagen, der eine Aussage über zu erwartende molekulare Rückfälle nach Therapiestopp geben kann.

Neben dem modellbasierten Prädiktor wird auch eine modellunabhängige Approximation angegeben, die eine Vorhersage des Rückfallrisikos nur mit Hilfe der klinisch bestimmbaren Werte α und β erlaubt. Auch wenn die vorgeschlagene Methode im Paper mit einer unabhängigen Kohorte validiert wurde, muss der Prädiktor seine Überlegenheit verglichen mit anderen Absetzstrategien im Rahmen einer prospektiven randomisierten Studie unter Beweis stellen.

Regular Article

MYELOID NEOPLASIA

Model-based decision rules reduce the risk of molecular relapse after cessation of tyrosine kinase inhibitor therapy in chronic myeloid leukemia

Matthias Horn,[1] Ingmar Glauche,[2] Martin C. Müller,[3] Rüdiger Hehlmann,[3] Andreas Hochhaus,[4] Markus Loeffler,[1] and Ingo Roeder[2]

[1]Institute for Medical Informatics, Statistics and Epidemiology, University of Leipzig, Leipzig, Germany; [2]Institute for Medical Informatics and Biometry, Faculty of Medicine Carl Gustav Carus, Dresden University of Technology, Dresden, Germany; [3]III Medizinische Klinik, Medizinische Fakultät Mannheim, University of Heidelberg, Mannheim, Germany; and [4]Abt Hämatologie/Onkologie, Universitätsklinikum Jena, Jena, Germany

Key Points

- BCR-ABL transcript dynamics in imatinib-treated chronic myeloid leukemia can consistently be described by a mathematical modeling approach.
- Application of the model allows to predict the optimal time point for therapy stop as well as the risk of relapse in individual patients.

Molecular response to imatinib (IM) in chronic myeloid leukemia (CML) is associated with a biphasic but heterogeneous decline of *BCR-ABL* transcript levels. We analyzed this interindividual heterogeneity and provide a predictive mathematical model to prognosticate the long-term response and the individual risk of molecular relapse on treatment cessation. The parameters of the model were determined using 7-year follow-up data from a randomized clinical trial and validated by an independent dataset. Our model predicts that a subset of patients (14%) achieve complete leukemia eradication within less than 15 years and could therefore benefit from discontinuation of treatment. Furthermore, the model prognosticates that 31% of the patients will remain in deep molecular remission ($MR^{5.0}$) after treatment cessation after a fixed period of 2 years in $MR^{5.0}$, whereas 69% are expected to relapse. As a major result, we propose a predictor that allows to assess the patient-specific risk of molecular relapse on treatment discontinuation and to identify patients for whom cessation of therapy would be an appropriate option. Application of the suggested rule for deciding about the time point of treatment cessation is predicted to result in a significant reduction in rate of molecular relapse. (*Blood*. 2013;121(2): 378-384)

Introduction

Chronic myeloid leukemia (CML) is a clonal disorder that is cytogenetically characterized by a translocation of chromosomes 9 and 22, resulting in the formation of the *BCR-ABL* fusion gene on the level of hematopoietic stem cells (HSCs).[1,2] The oncogenic capacity of this gene, which is located on the shortened chromosome 22 (Philadelphia [Ph] chromosome) is well-established. Its product, the BCR-ABL protein, is a constitutively activated tyrosine kinase, which has been shown to be responsible for the pathogenesis of CML.[2]

The current therapy of choice for de novo CML is oral administration of tyrosine kinase inhibitors (TKIs), such as imatinib mesylate (IM),[3] or recently approved second-generation TKIs dasatinib and nilotinib.[4,5] Main mechanism of action of IM (and other TKIs) is inhibition of the oncogenic BCR-ABL tyrosine kinase,[6] resulting in the switching-off of downstream signaling pathways promoting leukemogenesis.[3] It is well-established that IM selectively acts on leukemia cells inducing a proliferation inhibitory effect.[7] Furthermore, it has been reported that the apoptotic rate of actively proliferating leukemia cells is increased under IM therapy.[8,9] Although treatment with IM could still not be demonstrated to be curative, it is suited to achieve a sustained control of the disease in the majority of patients.

Molecular monitoring of tumor load in peripheral blood using quantitative reverse transcriptase polymerase chain reaction (qRT-PCR) revealed that in most patients IM monotherapy induces a biphasic decline of *BCR-ABL* transcript levels, characterized by an initially steep decline, followed by a second moderate decline.[10,11] A sensible explanation for this behavior is the rapid initial depletion of actively cycling *BCR-ABL*–positive cells, followed by the slow elimination of residual leukemic stem cells (LSCs)[11] because of their low turnover.[12,13] Alternatively, this behavior has been interpreted as the result of distinctive IM effects on different hematopoietic cell stages including IM insensitivity of stem cells.[10]

Although molecular IM response in the population of CML patients can be approximated by an average biphasic decline, a large heterogeneity in response patterns between individuals is observed.[11] In the absence of IM resistance, long-term treatment could be shown to be associated with sustained decline of *BCR-ABL* transcript levels.[14] These levels potentially fall below the detection threshold of PCR techniques, which allow for the detection of 1 CML cell in 10^5 nucleated blood cells.[15,16]

Submitted July 5, 2012; accepted November 10, 2012. Prepublished online as *Blood* First Edition paper, November, 21, 2012; DOI 10.1182/blood-2012-07-441956.

The online version of this article contains a data supplement.

The publication costs of this article were defrayed in part by page charge payment. Therefore, and solely to indicate this fact, this article is hereby marked "advertisement" in accordance with 18 USC section 1734.

Side effects of IM therapy as well as economic considerations pose the question whether IM can be safely discontinued after achieving deep molecular remissions (eg, $MR^{5.0}$). Uncertainty arises from the fact that on discontinuation of IM treatment, a heterogeneous picture is obtained: although some patients retain previously achieved molecular responses,[17,18] a molecular recurrence of *BCR-ABL* transcripts is observed in others.[18] Relapses can also be observed in patients lacking any measurable *BCR-ABL* transcripts in peripheral blood.[17]

We sought to predict patient-specific long-term time courses of CML under IM treatment and to support decision-making for potential treatment cessation. We could demonstrate that a statistical description of the disease kinetics is not sufficient to correctly estimate numbers of residual LSCs, which are a critical determinant of relapse after therapy discontinuation. Therefore, we adapted our established mathematical model of HSC and leukemia organization,[11,19,20] which was demonstrated to consistently explain CML genesis and IM treatment on the population level, to predict patient-specific stem cell numbers and long-term treatment outcome. Based on 7-year follow-up data of *BCR-ABL* transcript dynamics from the German cohort of the IRIS trial,[14] we determined model parameters that quantitatively characterize the interindividual heterogeneity of molecular treatment response. Given a patient's *BCR-ABL* transcript kinetics, the adapted model generates predictions for patient-specific long-term response to IM as well as individual times to complete eradication of minimal residual disease (MRD). To test the validity of our approach, we used an independent dataset from the CML IV trial.[21] Furthermore, we derived a model-based predictor for the individual risk of molecular relapse on treatment cessation, which is complemented by a model-independent approximation that can easily be calculated from clinical data. Using a comparative simulation study, we showed that the proposed predictor results in a superior clinical rule to decide on potential discontinuation of therapy compared with relying on a fixed (eg, 2 years) time in sustained deep molecular remission.

Methods

Mathematical model of HSC organization

The mathematical model underlying our results has originally been developed for the HSC system.[19] We previously demonstrated that the model is well-suited to explain clonal dynamics in the human situation.[11,20] In brief, the model assumes CML to be caused by a competition process between malignant (Ph^+) and normal (Ph^-) hematopoietic cells, with quantitative differences in specific model parameters. IM therapy is assumed to induce an apoptotic effect and inhibition of the proliferative activity of Ph^+ stem cells. The stochastic, single cell-based model is implemented in the programming language C++. The source code can be obtained from the authors. A schematic representation and a detailed technical description of the model implementation can be found in supplemental Methods (available on the *Blood* Web site; see the Supplemental Materials link at the top of the online article).

Selection of clinical data

As a training set for model development we used the German cohort of the IRIS trial (n = 69; 400 mg IM daily).[14] Each individual was represented by a time series of *BCR-ABL/ABL* measurements. Six patients (9%) were excluded from the analysis because of insufficient data (defined as less than 5 measurements). Seven patients (10%) suffered from considerable molecular relapse under continued therapy because of IM resistance, whereas 2 (3%) showed treatment failure for unknown reasons (defined as no decline of *BCR-ABL* levels within first year). In 3 individuals (4%) a uniphasic decline was observed. The remaining 51 (74%) patients, who are characterized by a biphasic decline of *BCR-ABL* transcript levels, were used for our modeling analyses.

As independent validation data, we used the 400 mg IM arm of the CML IV trial (n = 280).[21] Because of shorter overall follow-up compared with IRIS, 95 patients (34%) were excluded for reasons of insufficient data. Another 56 (20%) were associated with molecular relapse under IM, whereas 3 (1%) showed treatment failure. In 14 patients (5%) a uniphasic decline was observed. The remaining 112 (40%) showed a biphasic decline of *BCR-ABL* levels. However, only 31 patients had a minimum of 14 qRT-PCR measurements, required for reliable slope estimation (see "Statistical analysis of clinical data"). Hence, only this subset was used for validation.

The selection process described was necessary because our current model version is not able to quantitatively account for treatment failure (eg, because of IM resistance) and uniphasic decline kinetics. Still, the presented model analysis applies to more than 90% of patients who respond to IM without observed relapse. In addition, we confirmed (data not shown) that exclusion of the minority of patients showing a uniphasic decline does not bias the median behavior within the cohorts.

For this analysis, all *BCR-ABL/ABL* ratios were standardized according to the International Scale (IS). Each qRT-PCR measurement was preceded by a plasmid dilution series, that is, the smallest absolute number of *BCR-ABL* transcripts that could be detected in an individual assay was determined. In case of *BCR-ABL* negativity by qRT-PCR, nested PCR was performed. For negative results, *BCR-ABL/ABL* was assumed to be zero. For positive results, *BCR-ABL/ABL* was approximated using the smallest positive *BCR-ABL* copy number from the dilution series (representing an upper bound for the unknown true value).

Statistical analysis of clinical data

On a logarithmic scale, the previously mentioned biphasic decline kinetics of *BCR-ABL* levels in response to IM are sufficiently described by 2 piecewise linear relationships.[10,11] Herein, the slope of the first, steep decline is denoted as α and the slope of the second, moderate decline as β. Patient-specific values for α and β were calculated using a segmented linear regression model (library "segmented," statistical programming environment R). Specifically, we used the Davies test to check the null hypothesis of no slope difference.[22] If the null hypothesis was rejected at the 5% significance level, the breakpoint between first and second slope was estimated by an iterative procedure. As starting value of the iteration, we chose 250 days after therapy initiation based on previous knowledge. For quantification of correlations among slope values and breakpoint, Pearson correlation coefficient was applied.

Results

Statistical analysis of molecular response kinetics

First, we determined the heterogeneity within the patient population of the German IRIS cohort with respect to the biphasic decline of *BCR-ABL* transcript levels (Figure 1). Because of the association of the second decline with long-term treatment success, it would be desirable to predict this decline from the early response. However, we did not find a correlation between strength or duration of the first decline kinetics (characterized by slope and breakpoint, respectively) and the secondary decline (Figure 2). Hence, prediction of long-term outcome is not possible based on early decline kinetics alone, but requires a sufficient number of measurements of the secondary slope. Interestingly, we found a significant correlation between first decline and breakpoint (supplemental Figure 3 and supplemental Results).

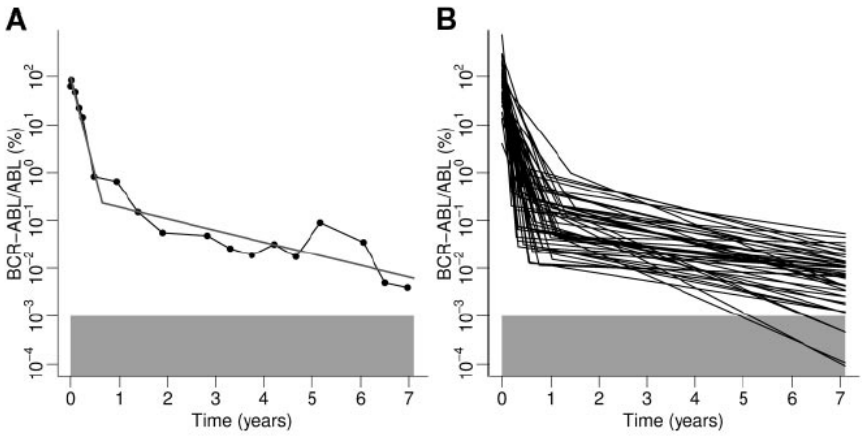

Figure 1. Results of the application of the biphasic regression procedure to clinical data from the German cohort of the IRIS trial. (A) Example of an individual patient. Data points obtained by qRT-PCR are represented by filled circles connected by black lines. The result of the least squares algorithm is depicted by the gray line. (B) Overview of regression results of all 51 patients characterized by a biphasic decline. The gray boxes in panels A and B represent the detection threshold of *BCR-ABL* transcripts levels.

Translating clinical data into the mathematical model

Second, we explored how the estimated kinetic parameters, that is, first (α) and second slope (β) of *BCR-ABL* transcript levels, translate into the parameter space of the dynamic model. Specifically, we used 2 model parameters (degradation rate r_{deg} and transition characteristic f_{ω}, which were previously found to sensitively affect IM therapy effects; see supplemental Methods for details) as patient-specific parameters to account for the heterogeneity in IM response patterns.[11,20] Other model parameters remained unchanged with respect to the values estimated for IM-treated CML (supplemental Table 1). Using an iterative algorithm we calculated model parameters r_{deg} and f_{ω} for each patient based on the observed *BCR-ABL* decline kinetics (see supplemental Results).

Model predictions on long-term treatment

Based on patient-specific parameters of the dynamic model we generated predictions of long-term *BCR-ABL* transcript kinetics for individual patients. Using the example patient from Figure 1A, we demonstrate the application of the procedure: the patient is characterized by slope parameters $\alpha = -4.08$/year and $\beta = -0.24$/year, from which we calculated $r_{deg} = 2.50$ and $f_{\omega} = 0.055$, the parameters of the dynamic model that optimally account for the particular *BCR-ABL* decline kinetics. Using these parameter estimates, we simulated this particular patient in silico, both for the time of available follow-up data (Figure 3A) and, most importantly, thereafter (Figure 3B). The model predicts that after approximately 15 years the *BCR-ABL* transcript levels of this particular patient permanently fall below the detection threshold of qRT-PCR (Figure 3B), which we assume to be MR$^{5.0}$, that is, reduction of *BCR-ABL* transcript levels below 0.001%.[23] After approximately 25 years it can be expected that no *BCR-ABL*–positive cells will be detected in peripheral blood at all, irrespective of the accuracy of the applied measuring method. This is because after this time only very few (mostly quiescent) residual LSCs, which are located in the bone marrow, remain in the system (Figure 3C). Note that the (absolute) stem cell number is not accessible in the clinic, but is a result of the in silico model. For the example patient the model predicts complete eradication of CML cells after 29.4 years of continuing IM therapy, with a standard deviation of 0.78 years.

Table 1 summarizes the model predictions for the considered patients. Even under the ideal circumstances assumed in our model, that is, uninterrupted IM administration and permanent absence of both IM resistance and disease-unrelated complications, the majority of individuals are predicted to require several decades of IM therapy before MRD is completely eradicated. The cumulative rates of complete eradication after 15 and 30 years of treatment are estimated to be 14% and 31%, respectively. In approximately 67% of the patients, residual leukemic cells are predicted throughout the remaining lifetime, assuming life expectancy of 80 years.

As this procedure relies on the full 7-year follow-up data, we examined whether shorter observation times are sufficient for generation of adequate model predictions, that is, whether actual therapeutic predictions can be made after less than 7 years (supplemental Figure 7). We found that in this patient cohort, for obtaining reliable predictions, at least 14 PCR measurements (6-8 per slope) are required, irrespective of follow-up duration.

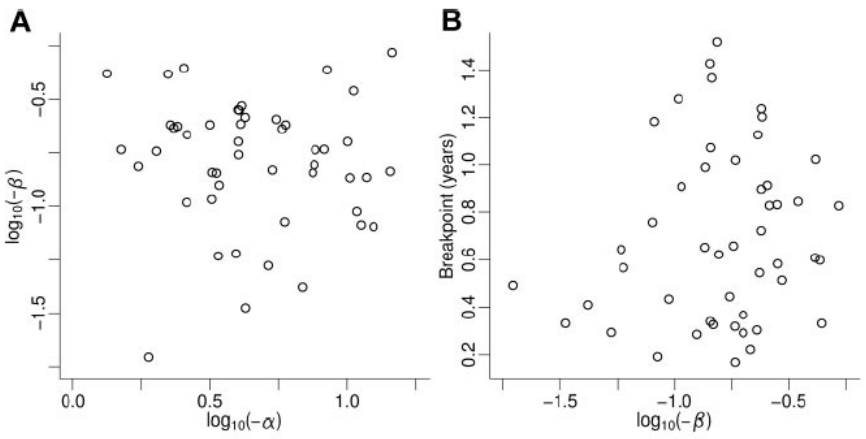

Figure 2. Correlation between kinetic parameters characterizing the molecular response of individual patients with respect to *BCR-ABL* transcript levels. (A) Steep first (α) and moderate second (β) declines of *BCR-ABL* transcript levels are uncorrelated (correlation coefficient $\rho_1 = -0.131$), that is, the second decline cannot be estimated from the first decline. (B) Second decline (ie, long-term response) and breakpoint separating first and second decline are uncorrelated (correlation coefficient $\rho_2 = 0.156$). Variables α and β are log-transformed.

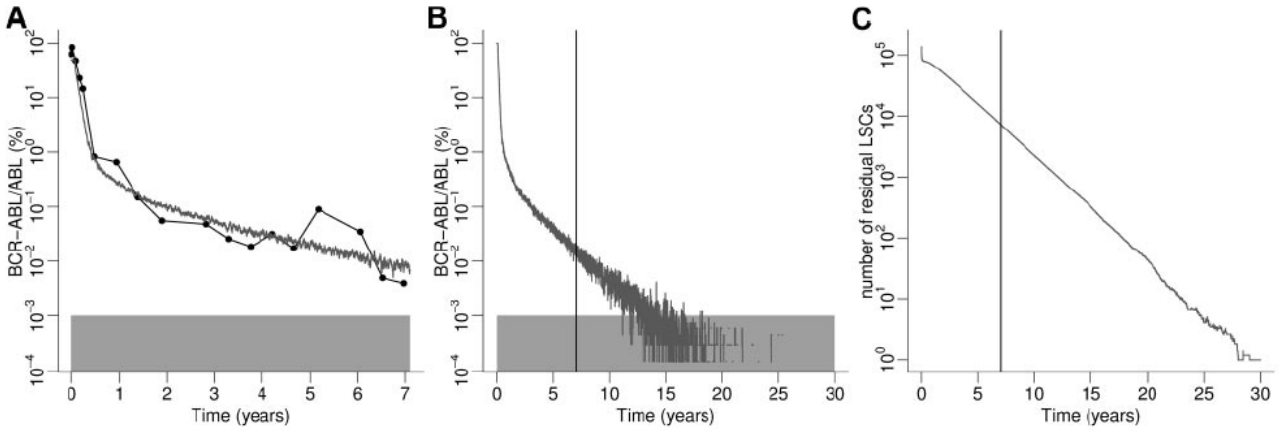

Figure 3. Model predictions for representative individual patient. (A) Data points (*BCR-ABL* transcript levels) obtained by qRT-PCR are represented by filled circles connected by black lines. The corresponding computer simulation is depicted by the gray line. (B) Model prediction from panel A extended to 30 years. The vertical line corresponds to the latest follow-up time point. Gray boxes in panels A and B represent detection threshold of *BCR-ABL* levels. (C) Corresponding absolute number of residual LSCs of the simulation results depicted in panel B. Continuous IM administration is required for approximately 30 years until complete eradication of LSCs is predicted for this particular patient. To account for quantitative differences between simulations because of the model-inherent stochasticity, 5 simulation runs using identical parameter values are performed and averaged.

Consequently, it can be speculated that the accuracy of the predictions for fixed observation times can be enhanced if PCR measurements are performed more frequently (see supplemental Results).

Validation of predictions on long-term IM administration

To validate the described method of calculating parameters of the dynamic model from clinically determined *BCR-ABL* kinetics, we analyzed a second, independent dataset (CML IV trial), which is comparable with the IRIS data with respect to patient characteristics, IM dosage, and response patterns (for selection criteria see "Methods"). We can show that the algorithm derived based on the IRIS data can be applied without changes to the independent dataset. The model results consistently account for the median behavior within the patient population as well as for interpatient heterogeneity of the CML IV cohort (see supplemental Results and supplemental Figures 9 and 10). In addition, we generated model predictions on long-term IM therapy. For the CML IV cohort, the results are summarized in Table 1. The cumulative cure rates after 15 and 30 years of IM treatment (16% and 42%, respectively) are statistically indistinguishable from the predictions generated for the training dataset from the IRIS trial (Table 1).

Model predictions on treatment discontinuation

For the 51 patients from the IRIS trial we simulated the situation of potential IM cessation. In this scenario, each patient was treated with IM in silico until *BCR-ABL* transcript levels fell below the MR$^{5.0}$ detection threshold for 2 consecutive years (assuming trimonthly measurements). For those 42 patients who reached at least a sustained 2-year MR$^{5.0}$ within 20 years or less of simulated IM treatment we generated model predictions for the time to molecular relapse after therapy discontinuation (solid line in Figure 4). It is predicted that the majority of molecular relapses is observed within the first 6 months with only few relapses occurring more than 1 year after treatment cessation. Twelve of 42 patients are predicted not to relapse at all. This model prediction quantitatively resembles recently published clinical results (Figure 4).[17,18] Please note that stopping rules and measurement protocols are not exactly comparable: whereas the simulation and the Australian trial[17] only require (at least) 2 years in MR$^{5.0}$ before IM discontinuation, the French trial[18] also requires a total IM treatment time of at least 3 years. Furthermore, in our simulation and in the Australian trial molecular relapse is defined as detectable *BCR-ABL* transcripts at any level in 2 consecutive PCR measurements, whereas the French trial also requires the *BCR-ABL* to *ABL* ratio to be at least 0.001%.

Table 1. Summary of model predictions for 51 considered patients from the IRIS trial (training set)/31 patients from the CML IV trial (validation set)

Time to complete eradication of MRD	48.9 y (28-112)/ 32.8 y (18-176)
Treatment time to 4.0 log reduction (MR$^{4.0}$)	6.5 y (5.0-9.7)/ 5.3 y (4.5-9.2)
Treatment time to 4.5 log reduction (MR$^{4.5}$)	10.7 y (7.7-13)/ 9.1 y (6.9-13)
Cumulative cure rate after 15 y of treatment	14%/16%
Cumulative cure rate after 30 y of treatment	31%/42%

Time estimates represent medians and, in parentheses, interquartile ranges. Note that "cure" refers to complete eradication of MRD.

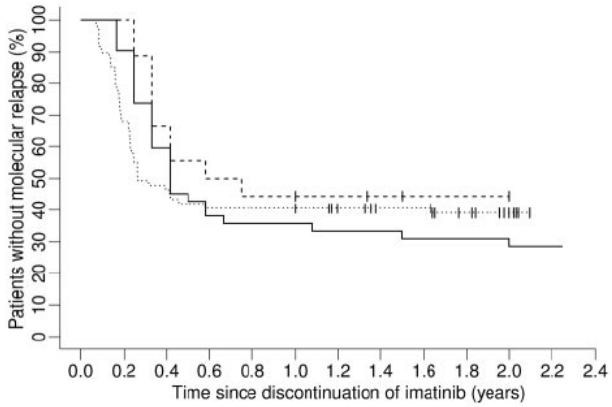

Figure 4. Model prediction on IM treatment cessation after fixed treatment time of 2 years in MR$^{5.0}$ in comparison to survival curves from 2 actual IM discontinuation trials. Shown are Kaplan-Meier estimates of time to molecular relapse after discontinuation of therapy. The solid line shows a model prediction for 42 of 51 patients from the IRIS trial that reached a sustained MR$^{5.0}$ for 2 consecutive years less than 20 years after initiation of IM therapy. Whereas the dotted line corresponds to the results from a French trial,[18] the dashed line shows the survival curve from an Australian trial.[17] For details see "Model predictions on treatment discontinuation."

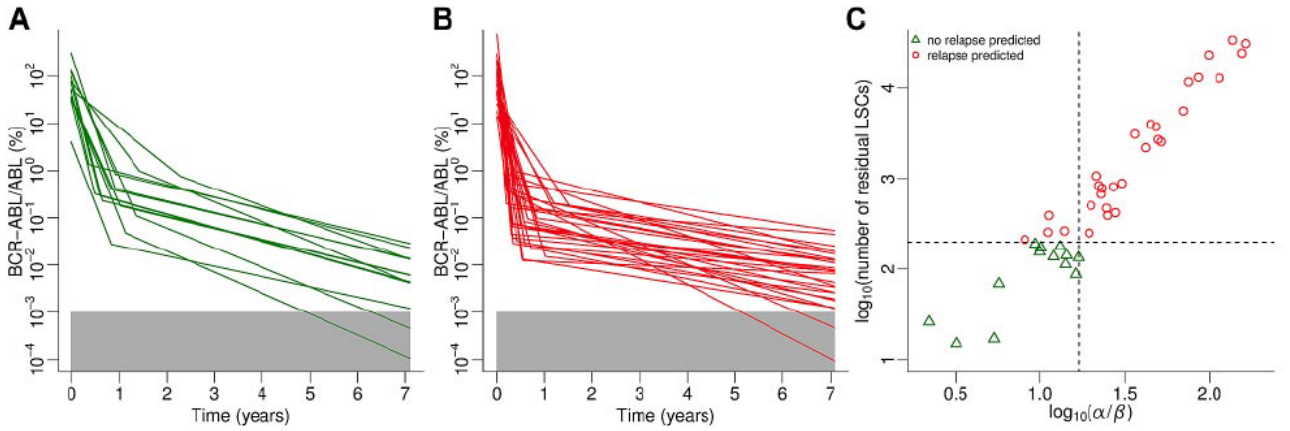

Figure 5. Model predictions on IM treatment cessation. (A) *BCR-ABL* transcript levels under IM treatment of patient subgroup predicted not to relapse after discontinuation of IM therapy. (B) *BCR-ABL* transcript levels under IM treatment of patients predicted to molecularly relapse after treatment cessation. Note that panels A and B divide the kinetics shown in Figure 1B into 2 subsets. (C) Relationship between ratio of first to second declines and number of residual LSCs at the moment of treatment cessation. Data points represent patients who are predicted not to relapse (green triangles) or to relapse (red circles) molecularly. Dashed lines represent predictors that allow for discrimination between patient subgroups (see "Model predictions on treatment discontinuation"). Note that both axes are log-transformed.

Model-predicted relapsing and nonrelapsing subgroups are depicted in Figures 5A and B with respect to IM response kinetics. Qualitatively, a relatively steep second decline is necessary but not sufficient for sustained $MR^{5.0}$ after therapy cessation. In contrast and contrary to intuition, a relatively steep first decline is adverse to achieving this goal. This is because of the fact that a steep first decline is associated with rapid depletion of leukemic cells in peripheral blood (where PCR measurements are performed) but not necessarily in the bone marrow. As a consequence, the treatment time required to substantially reduce MRD is potentially underestimated in the clinic. We found a linear relation (log scale) between the ratio of first and second slopes and the number of residual LSCs at the moment of treatment cessation (Figure 5C). In contrast to relapsing patients (circles), nonrelapsing patients (triangles) are characterized by $\log_{10}$(number of LSCs) ≤ 2.3 (horizontal line). This characteristic, which provides an optimal discrimination of the 2 groups, is based on the prediction of the dynamic model. A good approximation of this classification (approximately 5% misclassifications) can be obtained if the criterion $\alpha/\beta \leq 16$ (vertical line) is applied. We call the latter predictor "model-independent" as it does not require model simulations to be calculated. In contrast to the "model-based" predictor that uses the model-predicted number of residual LSCs, it can directly be calculated from clinically measureable variables.

The "model-independent" predictor, which relates to the condition of 2-year $MR^{5.0}$ before treatment cessation, can be generalized. Let t describe the duration of stable $MR^{5.0}$ under IM treatment until therapy discontinuation (given in years). Then a patient is predicted to remain in $MR^{5.0}$ after treatment cessation if the relation $\alpha/\beta \leq 8 \times t$ holds. That is, the molecularly relapsing subgroup is characterized by a first decline that is more than $8 \times t$ greater than the second decline. This implies that shorter $MR^{5.0}$ times require steeper second declines (given fixed first declines) to predict sustained $MR^{5.0}$ after therapy discontinuation. The predictor based on the number of residual LSCs can be applied in any case, irrespective of $MR^{5.0}$ duration.

Solving the inequality for t, the generalized predictor results in a simple decision rule given as $t \geq \alpha/(8 \times \beta)$. That means the time of sustained $MR^{5.0}$, which is predicted to ensure continuing $MR^{5.0}$ after treatment cessation, can be estimated for each patient individually. Applying this rule to the in silico IRIS cohort, that is, performing computer simulations for each patient and discontinuing IM after the calculated patient-specific time in $MR^{5.0}$, a significantly lower relapse rate ($P < .001$, log-rank test) with approximately 3 times less relapses at 2 years after IM cessation can be observed (solid line in Figure 6A) compared with the fixed time of 2 years in $MR^{5.0}$ (dashed line). Median treatment time in $MR^{5.0}$ before IM cessation resulting from this model prediction is estimated to be 2.8 (range: 0.3-20.5) years (Figure 6B). We also considered a scenario where IM is discontinued after a fixed treatment time of 2.8 years in $MR^{5.0}$, which equals the median treatment time in the individualized stopping regimen. This result, which is depicted by the dotted line in Figure 6A, still represents an inferior outcome with respect to the proposed patient-specific stopping rule.

Discussion

The procedure described here allows for a better appraisal of the individual prognosis of CML patients with direct impact on clinical decision-making. In the clinics, the tumor burden cannot be followed beyond the time point when *BCR-ABL* transcript levels have fallen below the detection threshold of qRT-PCR. In the majority of patients, this threshold is reached only a few years after initiation of IM therapy. However, LSCs, which are believed to drive the disease,[24] reside in the bone marrow and can only be detected in peripheral blood samples if they contribute to blood production in sufficient amounts. There is increasing evidence that primitive HSCs, and probably also LSCs, can "hide" from detection in peripheral blood because of their sustained quiescence.[12,25,26] As the proposed model acts on the level of stem cells, particularly accounting for the duality of stem cell quiescence and active proliferation, it offers a valuable tool to quantitatively complement clinically accessible measures.

With respect to the statistical analysis of the data, taken from the German IRIS cohort,[14] we were able to confirm and extend previous reports of a typical biphasic decline of *BCR-ABL* transcript levels under IM,[10,11] where the first decline probably characterizes initial response to IM and the second decline potentially represents elimination of residual LSCs.[27,28] Furthermore, we observed a strong correlation between steepness of the

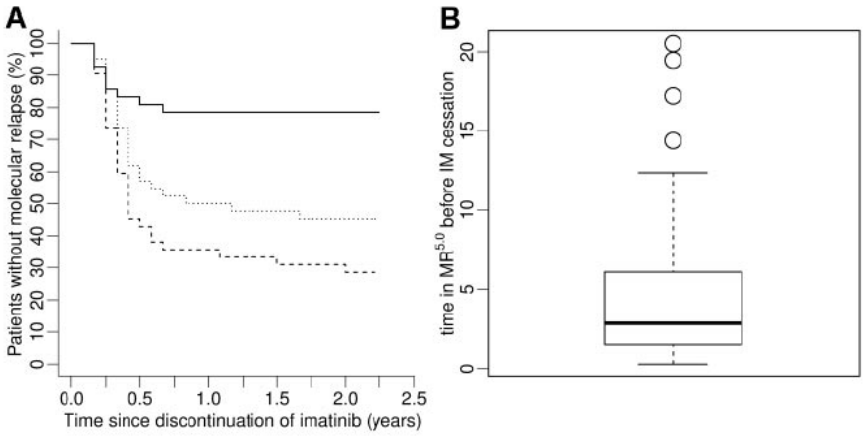

Figure 6. Model prediction on patient-specific IM discontinuation strategy based on individual *BCR-ABL* transcript kinetics. (A) Whereas the standard strategy, that is, fixed 2-year IM treatment in $MR^{5.0}$ before therapy discontinuation, is depicted by the dashed line, the result obtained by the proposed alternative strategy based on a patient-specific stopping rule is shown by the solid line. The dotted line represents a fixed 2.8-year IM treatment in $MR^{5.0}$, motivated by the median treatment time within the cohort in the individualized strategy. In all scenarios, the majority of relapsing patients is predicted to relapse within the first 6 months after IM discontinuation. The relapse rates predict a superior outcome of the personalized predictor-based strategy. (B) Distribution of individual times in $MR^{5.0}$ for the IRIS cohort before treatment cessation is recommended in the in silico patient-specific discontinuation strategy in panel A (solid line). Median treatment time is estimated to be 2.8 (range, 0.3-20.5) years.

first decline and breakpoint separating both declines. This notwithstanding, we found that steepness of the first decline as well as the breakpoint are not sufficient to predict the second slope and thus the time point of MRD eradication. That is, to evaluate the possibility of IM cessation, steepness of the second decline needs to be assessed with sufficient accuracy. Herein, the quality of the estimate sensitively depends on "late" data points, especially in case of few available measurements. Note, however, that follow-up time itself is not the most important parameter in this respect. More important is the number of measurements (6-8 within each of the 2 slope phases). As the *BCR-ABL* transcript levels of the IRIS patients have, in median, been assessed 7 times within the first year of IM therapy but only twice within each year thereafter, the critical number of measurements is reached only after 4 to 5 years. Performing, for example, 2 monthly measurements throughout, 2 to 3 years of follow-up might be sufficient for achieving the same quality of predictions.

The proposed method cannot be applied in case of IM resistance.[29] Furthermore, there are few cases of biphasically declining kinetics where the application of the procedure fails. This applies to "bad responders," that is, patients characterized by a comparatively flat first decline, and consequently by an unusually late breakpoint (after more than 3 years of IM therapy). Still, our model is a valuable tool to estimate the time to complete eradication of the leukemic clone in the majority of CML patients. Model results are consistent with the clinical experience that the majority of patients need to be treated with IM for a very long time period, before (if at all) complete leukemia eradication can be achieved. However, it should be kept in mind that complete eradication might not be necessary before IM therapy can be safely discontinued. Small *BCR-ABL* levels can be detected in healthy volunteers[30] leading to speculations that there exists a critical threshold below which the leukemic clone is small enough to be intrinsically controlled. It is one of our major results that the proposed model is able to identify those patients for whom treatment discontinuation would be a safe option. Along these lines, the model allows to predict the individual outcome in case of treatment stop. We show that patients with no predicted relapse are associated with a relatively steep second decline resulting in low numbers (≤ 200), or complete eradication, of residual LSCs at the moment of discontinuation. Predicted "late" relapses (more than 1 year after IM cessation) are also characterized by relatively small numbers of LSCs. However, in these cases the leukemic clone is still large enough to slowly expand and repopulate the marrow.

In addition to the individual model predictions of long-term *BCR-ABL* levels in peripheral blood as well as of residual LSC numbers in the bone marrow, we propose a simple "model-independent" predictor that allows for discrimination between relapsing and nonrelapsing patients after treatment cessation based on their individual treatment response kinetics. To investigate the quality of the predictor we performed simulation studies comparing an individualized treatment discontinuation strategy versus fixed time periods in sustained deep molecular remission before treatment cessation and found the former to be superior with respect to observed molecular relapse rates after discontinuation. It should be noted that this gain in the nonrelapsing fraction comes at the cost of increasing the median time to IM cessation. However, increasing the time of IM treatment in deep molecular remission uniformly for all patients does not result in comparable benefit because applying this strategy, according to our model analyses, some patients are treated unnecessarily, whereas others require longer TKI therapy to avoid relapsing on treatment discontinuation.

Our model prediction, regarding the strategy that applies a fixed 2-year period in $MR^{5.0}$ before IM discontinuation, closely resembles the outcome from 2 independent clinical trials[17,18] with respect to time to molecular relapse. Although stopping rules and measurement protocols are not identical, it is interesting to note that there are only minor differences between the individual Kaplan-Meier estimates, which we interpret as strong evidence for the validity of our approach. Comparing the 3 scenarios, the highest percentage of events can be observed in the in silico cohort, which is probably because of the fact that the "real" patient cohorts are naturally selected more strongly for good responders, in the sense of patients who reach a sustained deep remission comparatively early. In contrast, the simulation also includes patients reaching the 2-year $MR^{5.0}$ goal relatively late (up to 20 years after initiation of IM therapy), which might increase the relapse probability after therapy discontinuation slightly.

The validity of our model predictions sensitively depends on the underlying assumptions, such as the mechanisms of IM action. However, the predicative power of our model with respect to relapses in discontinuation trials (Figure 4) as well as in previous

settings[11,20] ensures its applicability. Other mathematical CML models did not assume a direct or indirect IM effect on LSCs.[10] However, these assumptions have been modified over time as they could not account for long-term declines of *BCR-ABL* levels in IM treated patients. More recent models[31,32] by those authors can be expected to yield qualitatively similar results to our model as they also assume clonal competition between HSCs and LSCs and a direct effect of IM on LSCs.

As our results were obtained by computer simulations, we recommend testing our strategy in a prospective randomized clinical trial that compares the described discontinuation strategies. The described approach is not limited to IM but can also be applied in an analogous way to first-line second generation TKIs, for example, dasatinib or nilotinib.[4,5] The mechanisms of action of these drugs are similar to IM,[33] and molecular response is also characterized by a biphasic behavior.[27] Currently, decline parameters cannot yet be determined because of insufficient follow-up, but we plan to adapt our approach in due course.

Acknowledgments

This work was supported by the Bundesministerium für Bildung und Forschung (BMBF) grant on Medical Systems Biology "HaematoSys" (BMBF-FKZ 0315452) and grant RO3500/1-2 by the German Research Foundation (DFG). Novartis supported the PCR analysis of the IRIS samples. The CML IV study was supported by Deutsche Krebshilfe, Novartis, BMBF, Deutsche José-Carreras-Leukämiestiftung, Roche, and Essex Pharma.

Authorship

Contribution: M.H., I.R., and M.L. conceived the mathematical model; M.H. conducted the simulations and the model analyses; I.R. and M.L. provided supervision; M.M., A.H., and R.H. provided the clinical data; I.G., I.R., and M.L. provided advice and input for modeling and data analysis; M.H. drafted the paper; I.G., M.M., R.H., A.H., M.L., and I.R. critically reviewed the paper; and all authors read and approved the final version of the paper.

Conflict-of-interest disclosure: A.H. and M.M. receive research support from Novartis, Bristol-Myers Squibb, Pfizer, and Ariad. The remaining authors declare no competing financial interests.

Correspondence: Matthias Horn, Institute for Medical Informatics, Statistics and Epidemiology, University of Leipzig, Haertelstrasse 16-18, 04107 Leipzig, Germany; e-mail: matthias.horn@imise.uni-leipzig.de.

References

1. Hehlmann R, Hochhaus A, Baccarani M. Chronic myeloid leukaemia. *Lancet*. 2007;370(9584):342-350.
2. Melo JV, Barnes DJ. Chronic myeloid leukaemia as a model of disease evolution in human cancer. *Nat Rev Cancer*. 2007;7(6):441-453.
3. Savage DG, Antman KH. Imatinib mesylate: a new oral targeted therapy. *N Engl J Med*. 2002; 346(9):683-693.
4. Kantarjian H, Shah NP, Hochhaus A, et al. Dasatinib versus imatinib in newly diagnosed chronic-phase chronic myeloid leukemia. *N Engl J Med*. 2010;362(24):2260-2270.
5. Saglio G, Kim DW, Issaragrisil S, et al. Nilotinib versus imatinib for newly diagnosed chronic myeloid leukemia. *N Engl J Med*. 2010;362(24): 2251-2259.
6. Buchdunger E, Zimmermann J, Mett H, et al. Inhibition of the Abl protein-tyrosine kinase in vitro and in vivo by a 2-phenylaminopyrimidine derivative. *Cancer Res*. 1996;56(1):100-104.
7. Druker BJ, Tamura S, Buchdunger E, et al. Effects of a selective inhibitor of the Abl tyrosine kinase on the growth of Bcr-Abl positive cells. *Nat Med*. 1996;2(5):561-566.
8. Oetzel C, Jonuleit T, Gotz A, et al. The tyrosine kinase inhibitor CGP 57148 (STI 571) induces apoptosis in BCR-ABL-positive cells by down-regulating BCL-X. *Clin Cancer Res*. 2000;6(5): 1958-1968.
9. Vigneri P, Wang JY. Induction of apoptosis in chronic myelogenous leukaemia cells through nuclear entrapment of BCR-ABL tyrosine kinase. *Nat Med*. 2001;7(2):228-234.
10. Michor F, Hughes TP, Iwasa Y, et al. Dynamics of chronic myeloid leukemia. *Nature*. 2005; 435(7046):1267-1270.
11. Roeder I, Horn M, Glauche I, Hochhaus A, Mueller MC, Loeffler M. Dynamic modeling of imatinib-treated chronic myeloid leukemia: functional insights and clinical implications. *Nat Med*. 2006;12(10):1181-1184.
12. Wilson A, Laurenti E, Oser G, et al. Hematopoietic stem cells reversibly switch from dormancy to self-renewal during homeostasis and repair. *Cell*. 2008;135(6):1118-1129.
13. Glauche I, Moore K, Thielecke L, Horn K, Loeffler M, Roeder I. Stem cell proliferation and quiescence: two sides of the same coin. *PLoS Comput Biol*. 2009;5(7):e1000447.
14. Hochhaus A, O'Brien SG, Guilhot F, et al. Six-year follow-up of patients receiving imatinib for the first-line treatment of chronic myeloid leukemia. *Leukemia*. 2009;23(6):1054-1161.
15. Hochhaus A. Minimal residual disease in chronic myeloid leukaemia patients. *Best Pract Res Clin Haematol*. 2002;15(1):159-178.
16. Goldman J. Monitoring minimal residual disease in BCR-ABL-positive chronic myeloid leukemia in the imatinib era. *Curr Opin Hematol*. 2005;12(1): 33-39.
17. Ross DM, Branford S, Seymour JF, et al. Patients with chronic myeloid leukemia who maintain a complete molecular response after stopping imatinib treatment have evidence of persistent leukemia by DNA PCR. *Leukemia*. 2010;24(10):1719-1724.
18. Mahon FX, Réa D, Guilhot J, et al. Discontinuation of imatinib in patients with chronic myeloid leukaemia who have maintained complete molecular remission for at least 2 years: the prospective, multicentre Stop Imatinib (STIM) trial. *Lancet Oncol*. 2010;11(11):1029-1035.
19. Roeder I, Loeffler M. A novel dynamic model of hematopoietic stem cell organization based on the concept of within-tissue plasticity. *Exp Hematol*. 2002;30(8):853-861.
20. Horn M, Loeffler M, Roeder I. Mathematical modeling of genesis and treatment of chronic myeloid leukemia. *Cells Tissues Organs*. 2008;188(1-2): 236-247.
21. Hehlmann R, Lauseker M, Jung-Munkwitz S, et al. Tolerability-adapted imatinib 800 mg/d versus 400 mg/d versus 400 mg/d plus interferon-α in newly diagnosed chronic myeloid leukemia. *J Clin Oncol*. 2011;29(12):1634-1642.
22. Davies RB. Hypothesis testing when a nuisance parameter is present only under the alternative. *Biometrika*. 1987;74(1):33-43.
23. Cross NCP, White HE, Müller MC, Saglio G, Hochhaus A. Standardized definitions of molecular response in chronic myeloid leukemia. *Leukemia*. 2012;26(10):2172-2175.
24. Sloma I, Jiang X, Eaves AC, Eaves CJ. Insights into the stem cells of chronic myeloid leukemia. *Leukemia*. 2010;24(11):1823-1833.
25. Graham SM, Jørgensen HG, Allan E, et al. Primitive, quiescent, Philadelphia-positive stem cells from patients with chronic myeloid leukemia are insensitive to STI571 in vitro. *Blood*. 2002;99(1): 319-325.
26. Essers MA, Trumpp A. Targeting leukemic stem cells by breaking their dormancy. *Mol Oncol*. 2010;4(5):443-450.
27. Tang M, Gonen M, Quintas-Cardama A, et al. Dynamics of chronic myeloid leukemia response to long-term targeted therapy reveal treatment effects on leukemic stem cells. *Blood*. 2011; 118(6):1622-1631.
28. Stein AM, Bottino D, Modur V, et al. BCR-ABL transcript dynamics support the hypothesis that leukemic stem cells are reduced during imatinib treatment. *Clin Cancer Res*. 2011;17(21):6812-6821.
29. Tauchi T, Ohyashiki K. Molecular mechanisms of resistance of leukemia to imatinib mesylate. *Leuk Res*. 2004;28(Suppl 1):S39-S45.
30. Biernaux C, Loos M, Sels A, Huez G, Stryckmans P. Detection of major BCR-ABL gene expression at a very low level in blood cells of some healthy individuals. *Blood*. 1995;86(8):3118-3122.
31. Foo J, Drummond MW, Clarkson B, Holyoake T, Michor F. Eradication of chronic myeloid leukemia stem cells: a novel mathematical model predicts no therapeutic benefit of adding G-CSF to imatinib. *PLoS Comput Biol*. 2009;5(9):e1000503.
32. Tang M, Foo J, Gonen M, Guilhot J, Mahon FX, Michor F. Selection pressure exerted by imatinib therapy leads to disparate outcomes of imatinib discontinuation trials. *Haematologica*. 2012; 97(10):1553-1561.
33. Sawyers CL. Even better kinase inhibitors for chronic myeloid leukemia. *N Engl J Med*. 2010;362(24): 2314-2315.

Supplemental Materials and Methods

Mathematical model of hematopoietic stem cell (HSC) organization

The mathematical single cell-based model that is underlying the results presented in the paper has originally been developed for the HSC system[1], and has since been extensively validated for animal data, e.g. to describe clonal competition processes and lineage specification[2–4]. Also, we could show that the model is well-suited to explain clonal dynamics in the human situation by applying it to imatinib (IM)-treated chronic myeloid leukemia (CML)[5–8]. A schematic representation of the model can be found in Figure S1.

We assume that HSCs reside in either of two different signaling contexts (**A**, **Ω**), that can be interpreted as adaptations of two different growth environments. Environment **A** represents a stem cell-supporting "niche" within the bone marrow promoting cellular quiescence and regeneration. Environment **Ω**, in contrast, imposes active proliferation. Cells may reversibly switch from one environment to the other. Each model cell has a property a representing its affinity to reside in **A**. A key assumption is that the values of a fluctuate depending on the environment the cell resides in. If a is greater than a given threshold a_{min}, the respective cell is considered as a stem cell. Affinity a can be interpreted as a marker of stemness: the smaller a, the higher the probability that the cell will differentiate into a lineage committed cell and, therefore, lose its stem cell potential. Differentiation (i.e., decrease in a) is considered to be a reversible process until a has reached a_{min}. Whereas cells gradually lose affinity a under the influence of environment **Ω** [$a(t + 1) = a(t) / \mathrm{d}$], they regain it in **A** [$a(t + 1) = a(t) \cdot \mathrm{r}$]. The latter can be interpreted as a regeneration process of the cell. Parameters d and r represent differentiation and regeneration coefficients, respectively. If a falls below a_{min}, it is set to zero. Such a cell has lost its potential to change to **A** and, therefore, to regain a. It is no longer denoted as a stem, but as a differentiated cell, which initiates a clone that amplifies and finally

dies after a fixed lifetime. Whereas cells in **A** are assumed to be quiescent, i.e. in G_0-phase of the cell cycle, cells in **Ω** are actively proliferating with an average generation time τ_c. The transition of cells between the two growth environments is modeled as a stochastic process, i.e. in each time step each cell has a certain probability to migrate from one compartment to the other. The transition probabilities per time (i.e. intensities) depend on the individual cellular affinity a and the transition characteristics f_α and f_ω. These characteristics depend on the current numbers of cells in **A** and **Ω**, respectively (for examples see Figure S2).

Assumptions for modeling CML

The mathematical model (as described in the Materials and Methods section of the paper) assumes CML to be caused by a clonal competition process between malignant (Ph^+) and normal (Ph^-) hematopoietic cells, with quantitative differences in specific model parameters. In order to explain the competitive advantage of leukemic cells compared to normal HSCs, we assume different transition characteristics f_α and f_ω between Ph^+ and Ph^- cells (Figure S2). That means, we assume Ph^+ cells to have an increased and unregulated proliferative activity, modeled by an increased and cell number-independent probability per time step to change to growth environment **Ω** (f_ω), as well as a defective HSC – niche interaction, modeled by an altered probability to migrate to growth environment **A** (f_α).

Motivated by biological evidence, we assume IM therapy to induce an apoptotic effect[9] and an inhibition of the proliferative activity[10] of Ph^+ stem cells. Technically, the apoptotic effect is modeled by a selective kill of a fixed percentage of cycling leukemic cells per time step (degradation rate r_{deg}), while the proliferation inhibition is modeled by a reduction of the activation of leukemic cells into cycle, i.e. altering transition characteristic f_ω. Figure S2 shows that this alteration does not equal a reset back to normal: the reduced transition characteristic f_ω is assumed to remain unregulated, i.e. independent of cell numbers in **Ω**.

This assumption can e.g. be interpreted as a consequence of accrued mutations that remain after *BCR-ABL* activity is suppressed, resulting in continuing loss of control, or by an IM-induced proliferation inhibition that is independent of feedback regulations that can be expected to be present in the normal situation. Thus, in our mathematical model IM therapy effects are characterized by a specific modulation of two parameters (r_{deg}, f_{ω}). These two parameters represent the smallest parameter set required to explain IM therapy effects, i.e. it is possible to include more parameters but not others.

It has been shown previously that the assumptions described above are sufficient to consistently explain average CML emergence, genesis and IM treatment for a population of patients[5,7]. A detailed parameter overview can be found in Table S1. For cessation of IM therapy we assume an instantaneous reduction of r_{deg} to zero, however, transition characteristic f_{ω} remains unchanged under IM treatment.

The model is implemented as a C++ computer program, which can be obtained from the authors. Each cell in the system is simulated according to the above-outlined set of rules. The rules are applied at discrete time steps (Δt = 1h) to simultaneously update the status of all cells.

In order to compare clinically determined *BCR-ABL* transcript levels to the mathematical model, *BCR-ABL/ABL* ratios are approximated using cell numbers in the population of differentiated cells. Let n_1 denote the number of Ph^+ cells and n_2 the number of Ph^- cells, then the relation $BCR\text{-}ABL/ABL \approx n_1 / (n_1 + 2n_2) \cdot 100\%$ is applied. This formula is motivated by the existence of two alleles of each gene within individual cells and by a strong correlation between cytogenetics, assessing the proportion of Ph^+ cells, and real-time quantitative PCR measurements of *BCR-ABL* transcript levels in peripheral blood[11]. Motivated by clinical data, we assume the number of leukemic stem cells (LSCs) at the initiation of IM treatment to be 10^5 (which relates to a *BCR-ABL/ABL* ratio of 99%) for all patients.

Supplemental Results

Relationship between first decline and breakpoint

We found a noteworthy relation between first slope α and breakpoint separating first and second slope (Figure S3). In order to calculate the breakpoint between first and second slope from the estimation of the first slope, the following equation (obtained by a least squares approach) can be used. Applying this relation, the breakpoint can be calculated from the first slope with a median deviation of about five weeks. As a consequence, the breakpoint is interchangeable with the first decline as one can be estimated from the other. However, both require sufficient data on the early response to be estimated properly.

(1) Breakpoint [years] = $1.5078 - 1.2222 \cdot \log_{10}(-\alpha)$

(Note that α (given in 1/year) denotes a decline and is thus a negative number by definition).

Analysis of IM treatment parameters

In order to derive functional relationships between decline kinetics (given by slope parameters α and β) and model parameters that consistently explain IM treatment effects (degradation rate r_{deg} and transition characteristic f_{ω}), we performed computer simulations in which we permitted the two-dimensional (r_{deg}, f_{ω}) parameter space to vary in the intervals [0.05, 4.0] for r_{deg} and [0.005, 0.1] for f_{ω} on a fine-meshed equidistant grid (with step sizes $\Delta r_{deg} = 0.05$ and $\Delta f_{\omega} = 0.005$). The intervals used were motivated by coarse-grained pilot simulations (data not shown). Applying this partitioning, 1600 grid points were considered. Due to the model-inherent stochasticity, small quantitative differences are observed between different simulation runs, even if using identical parameter values. Thus, for each parameter combination $(r_{deg,j}, f_{\omega,j})$, $j \in \{1, \ldots, 1\,600\}$, five individual simulations were performed and averaged. Thereafter, the regression algorithm described in the Materials and Methods section

of the paper was applied to the average simulation results at each grid point. Thereby, each pair $(r_{\mathrm{deg},j}, f_{\omega,j})$ could be uniquely mapped to its corresponding decline parameters (α_j, β_j).

Figure S4 illustrates the results yielded by this procedure. It is evident that the first slope mainly depends on r_{deg}, however, its minor dependence on f_ω must not be neglected. A more complex picture is obtained for the second decline where the observed functional relationship (twisted hyperplane, Figure S4B) is suggesting an interacting effect of both parameters.

Calculation of model parameters from patient data

A continuous functional relationship between, on the one hand, model parameters r_{deg} and f_ω, and, on the other hand, decline estimates α and β can be derived using a nonlinear regression model. We found that for the decline parameters α and β the relations

$$(2)\quad \ln(-\alpha) = c_1 \ln(r_{\mathrm{deg}}) + c_2 f_\omega + c_3 \ln(r_{\mathrm{deg}}) f_\omega + c_4 + \xi$$
$$(3)\quad \ln(-\beta) = c_5 \ln(f_\omega) + c_6 r_{\mathrm{deg}} + c_7 \ln(f_\omega) r_{\mathrm{deg}} + c_8 + \xi$$

can be assumed. Herein, ξ represents a normally distributed random variable with expected value 0 and variance σ^2 that accounts for measurement errors and biological variability. As it was our aim to determine degradation rate r_{deg} and transition characteristic f_ω from the estimated decline parameters α and β, we solved equations (2) and (3) without ξ for r_{deg} and f_ω, respectively, such that they exclusively depend on α and β. Because no closed form exists for the solution, we used an iterative algorithm. This procedure requires a starting point for transition characteristic f_ω, denoted as $\hat{f}_\omega$, which we set to 0.01. Thereafter we calculated

$$(4)\quad \hat{r}_{\mathrm{deg}} = \exp\left(\frac{\ln(-\alpha) - c_2 \hat{f}_\omega - c_4}{c_1 + c_3 \hat{f}_\omega}\right), \text{ and subsequently}$$

$$(5)\quad \hat{f}_\omega = \exp\left(\frac{\ln(-\beta) - c_6\hat{r}_{\deg} - c_8}{c_5 + c_7\hat{r}_{\deg}}\right).$$

Calculation of (4) and (5) was repeated using $\hat{r}_{\deg}$ and $\hat{f}_\omega$ of the previous iteration step until the desired accuracy, measured as the absolute difference between two subsequent steps and denoted as ε, was achieved. We used $\varepsilon = 10^{-5}$. Finally we set $r_{\deg} = \hat{r}_{\deg}$ and $f_\omega = \hat{f}_\omega$.

Applying a least squares approach, we estimated constants $\hat{c}_i$, $i \in \{1, ..., 8\}$, such that first and second declines α and β can be best explained by the IM treatment parameters $r_{\deg}$ and f_ω. We obtained the estimates $\hat{c}_1 = 1.286$, $\hat{c}_2 = -22.39$, $\hat{c}_3 = 17.86$, $\hat{c}_4 = 0.5550$, $\hat{c}_5 = 0.09191$, $\hat{c}_6 = 0.6805$, $\hat{c}_7 = 0.1654$, and $\hat{c}_8 = -1.646$.

Empirical distributions of model parameters

The empirical distributions of $r_{\deg}$ and f_ω obtained by this procedure are depicted in Figure S5. We found that degradation rate $r_{\deg}$ is approximately normally distributed while for transition characteristic f_ω a gamma distribution represents a suitable approximation. Both distributions are characterized by two parameters which we estimated using a maximum likelihood approach. For $r_{\deg} \sim N(\mu, \sigma^2)$ we obtained $\mu = 2.59$ and $\sigma = 0.95$, and for $f_\omega \sim \Gamma(k, \theta)$ we estimated $k = 0.76$ and $\theta = 0.057$. The corresponding probability density functions are also shown in Figure S5. The expected value of the normal distribution is given as $r_{\deg} = \mu = 2.59$, while the expected value of the gamma distribution is calculated by $f_\omega = k \times \theta = 0.044$. The computer simulation corresponding to the theoretical means of the estimated distributions as well as medians and interquartile ranges of the clinical data can be found in Figure S6A. Additionally, 51 numbers were sampled from each of the distributions given above, yielding 51 $(r_{\deg}, f_\omega)$ pairs, which were used to simulate "random patients" *in silico*. Subsequently, the corresponding kinetic parameters α and β were calculated (Figure S6B).

Both distributions given above closely resemble the clinically observed picture; however, they slightly overestimate the median kinetics within the selected cohort of patients, as depicted by the solid line in Figure S6A. Additionally, the variance within the population is slightly overestimated as well (see Figure S6B and cf. Figure 1B in the paper). This is likely due to the fact that the estimations are based on a relatively small set of patients (n = 51).

Restriction of observation time

As the proposed method to generate individual predictions on long-term IM treatment has been developed using full 7-year follow-up data, we examined whether shorter observation times are sufficient for generating adequate model predictions, i.e. whether actual therapeutic predictions can be made after less than seven years. For this purpose, we sequentially restricted the analysis of the available data to shorter follow-up times of, in this order, 1, 2, 3, 4, 5, and 6 years. The maximum in this sequence is reduced accordingly for cases with less than 7 years observation time. The analysis is demonstrated using the example patient from Figure 1A: Due to insufficient number of measurements, the regression algorithm is unable to reliably estimate decline parameters after a follow-up of 1 and 2 years. As shown in Figure S7A, at years 3, 4, and 5 the second decline can be obtained but is overestimated, i.e. as depicted in Figure S7B, the time to MRD eradication is underestimated. Only at year 6 the model prediction reflects the estimations for the latest available follow-up time point.

For the population of all 51 patients, the results are as follows: In 71% of the cases, a follow-up of 5 years or less (with a majority of 37% at 4 years) is sufficient to predict the time to a complete eradication of LSCs as it is obtained with seven-year follow-up data. At this time a median of 14 PCR measurements has been performed, irrespective of follow-up duration.

Validation by CML IV patient data

As mentioned in the paper, a second, independent data set (31 patients from the CML IV trial) was used to validate the model predictions on long-term IM treatment outcome and therapy cessation. As a first step and similarly to the IRIS training set, the patient kinetics were approximated by two piecewise linear relationships using a biphasic regression procedure (as described in the Materials and Methods section in the paper), yielding estimations of the slopes of both the first steep and the second moderate decline (see Figure S8 and cf. Figure 1 in the paper). Based on these estimations, we calculated the corresponding model parameters r_{deg} and f_{ω} for each of the considered patients using the iterative algorithm derived and explained above. Note that the calculations were performed without changing any of the parameters of the two response surfaces (Figure S4) that have been determined using the IRIS data. As a result of the individual estimations we obtained the empirical distributions of r_{deg} and f_{ω}, which are depicted in Figure S9 and closely resemble the distributions obtained for the IRIS data (cf. Figure S5). More precisely, for $r_{\mathrm{deg}} \sim N(\mu, \sigma^2)$ we estimated $\mu = 2.80$ and $\sigma = 0.80$, and for $f_{\omega} \sim \Gamma(k, \theta)$ we obtained $k = 0.96$ and $\theta = 0.056$, resulting in expected values $r_{\mathrm{deg}} = \mu = 2.80$ and $f_{\omega} = k \times \theta = 0.053$. Using these values as model parameters *in silico*, which can be interpreted as simulation of the "median" patient, the results depicted in Figure S10A are obtained. Additionally 31 "random patients" were simulated using random numbers sampled from the empirical distributions (see Figure S10B). Evidently, the clinical picture (cf. Figure S8B) was qualitatively well reproduced by the procedure. However, similarly to the IRIS training set, both the median kinetics and the variance within the patient population were slightly overestimated by the empirical distributions.

Supplemental References

1. Roeder I, Loeffler M. A novel dynamic model of hematopoietic stem cell organization based on the concept of within-tissue plasticity. *Exp Hematol*. 2002;30(8):853–861.

2. Roeder I, Kamminga LM, Braesel K, Dontje B, de Haan G, Loeffler M. Competitive clonal hematopoiesis in mouse chimeras explained by a stochastic model of stem cell organization. *Blood*. 2005;105(2):609–616.

3. Roeder I, Horn K, Sieburg HB, Cho R, Muller-Sieburg C, Loeffler M. Characterization and quantification of clonal heterogeneity among hematopoietic stem cells: a model-based approach. *Blood*. 2008;112(13):4874–4883.

4. Glauche I, Moore K, Thielecke L, Horn K, Loeffler M, Roeder I. Stem cell proliferation and quiescence – two sides of the same coin. *PLoS Comput Biol*. 2009;5(7):e1000447.

5. Roeder I, Horn M, Glauche I, Hochhaus A, Mueller MC, Loeffler M. Dynamic modeling of imatinib-treated chronic myeloid leukemia: functional insights and clinical implications. *Nat Med*. 2006;12(10):1181–1184.

6. Glauche I, Horn M, Roeder I. Leukaemia stem cells: hit or miss? *Br J Cancer*. 2007;96(4):677–678.

7. Horn M, Loeffler M, Roeder I. Mathematical modeling of genesis and treatment of chronic myeloid leukemia. *Cells Tissues Organs*. 2008;188(1–2):236–247.

8. Roeder I, Glauche I. Pathogenesis, treatment effects, and resistance dynamics in chronic myeloid leukemia – insights from mathematical model analyses. *J Mol Med*. 2008;86(1):17–27.

9. Vigneri P, Wang JY. Induction of apoptosis in chronic myelogenous leukemia cells through nuclear entrapment of BCR-ABL tyrosine kinase. *Nat Med*. 2001;7(2):228–234.

10. Holtz MS, Slovak ML, Zhang F, Sawyers CL, Forman SJ, Bhatia R. Imatinib mesylate (STI571) inhibits growth of primitive malignant progenitors in chronic myelogenous leukemia through reversal of abnormally increased proliferation. *Blood*. 2002;99(10):3792–3800.

11. Branford S, Hughes TP, Rudzki Z. Monitoring chronic myeloid leukaemia therapy by real-time quantitative PCR in blood is a reliable alternative to bone marrow cytogenetics. *Br J Haematol*. 1999;107(3):587–599.

Parameter	Ph^- cells	Ph^+ cells
a_{min}	0.002	0.002
a_{max}	1.0	1.0
d	1.05	1.05
r	1.1	1.1
τ_c	48 h	48 h
τ_S	8 h	8 h
$\tau_{G_2/M}$	8 h	8 h
$\tilde{\tau}_c$	24 h	24 h
λ_p	20 d	20 d
λ_m	8 d	8 d
$f_\alpha(0)$	0.5	1.0
$f_\alpha(\tilde{N}_A/2)$	0.45	0.9
$f_\alpha(\tilde{N}_A)$	0.05	0.058
$f_\alpha(\infty)$	0.0	0.0
$\tilde{N}_A$	10^5	10^5
$f_\omega(0)$	0.5	1.0 (0.05)
$f_\omega(\tilde{N}_\Omega/2)$	0.3	0.999 (0.0499)
$f_\omega(\tilde{N}_\Omega)$	0.1	0.998 (0.0498)
$f_\omega(\infty)$	0.0	0.996 (0.0496)
$\tilde{N}_\Omega$	10^5	10^5
r_{deg}	(0.0)	(2.8)

Table S1. Parameter values used in the computer simulations. The parameters are as follows: (a_{min}, a_{max}) = range of affinity a that characterizes the propensity of a cell to reside in **A**; d = differentiation coefficient; r = regeneration coefficient; τ_c = cell cycle duration of stem cells; $\tau_S, \tau_{G_2/M}$ = durations of S- and G_2/M-phase; $\tilde{\tau}_c$ = average generation time of proliferating differentiated cells; λ_p = transition time for proliferating precursor cell stages; λ_m = life time of nonproliferating precursor cell stages and mature, terminally differentiated cells; f_α, f_ω = transition characteristics for transitions from growth environment **Ω** to **A** and **A** to **Ω**; $f_\alpha(\cdot), f_\omega(\cdot)$ = function values of transition characteristics at given argument; $\tilde{N}_A, \tilde{N}_\Omega$ = scaling factors of transition characteristics. Values in brackets represent IM treatment parameters of the "median" patient. For further details see text.

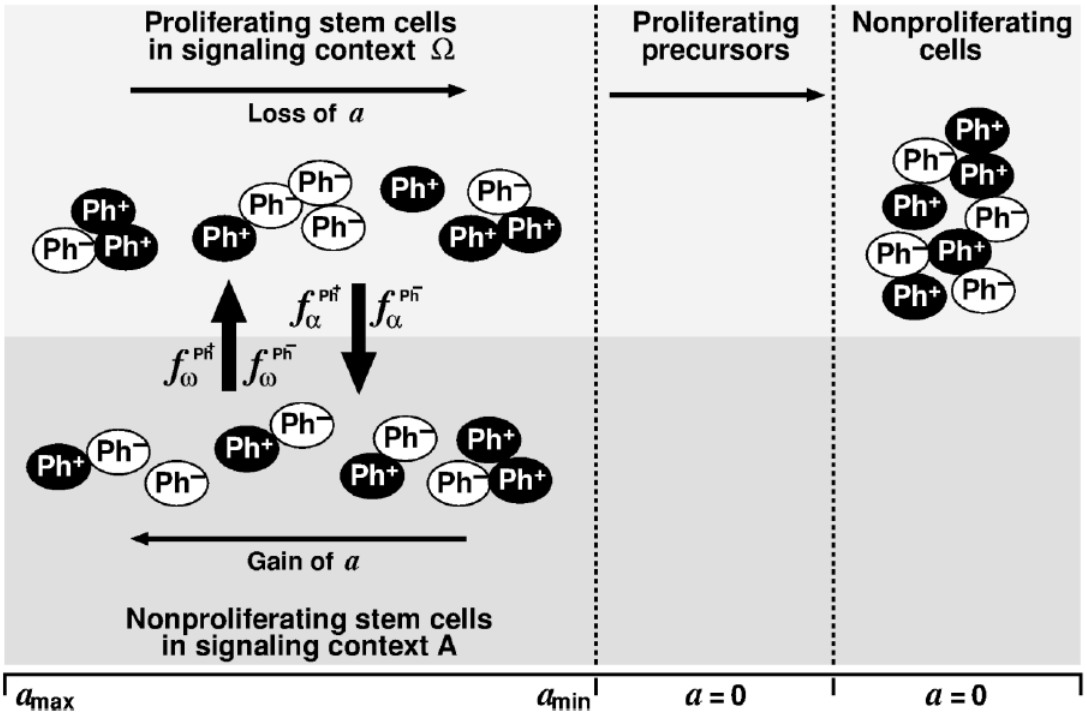

Figure S1. Schematic representation of the mathematical model. Normal (Ph^-) and malignant (Ph^+) stem cells are assumed to coexist within two common signaling contexts (**A**, **Ω**) and can reversibly switch from one context to the other. For a model description, see text.

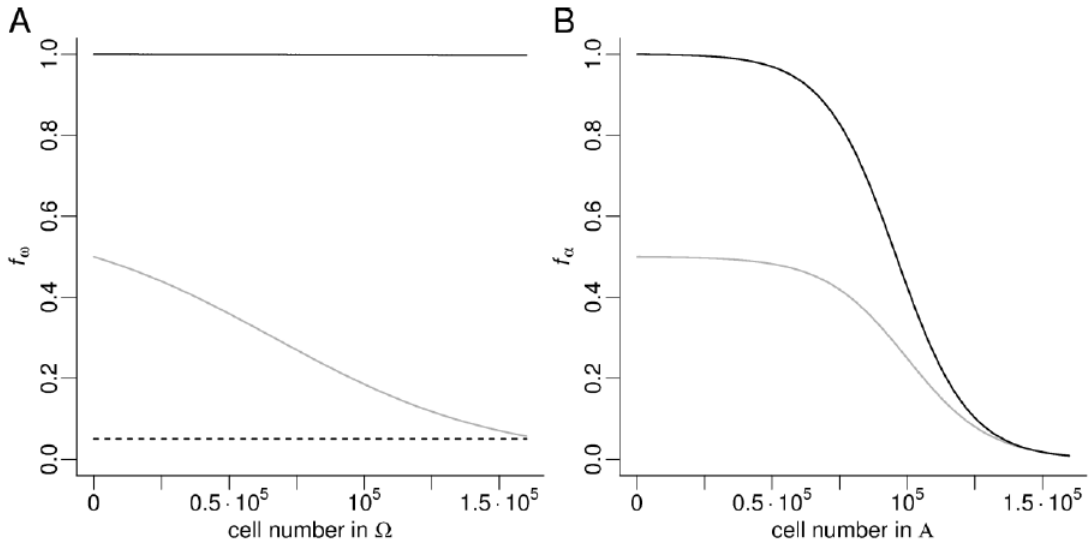

Figure S2. **Schematic representation of transition characteristics**. Shown are examples of f_ω (A) and f_α (B) of normal (gray) and malignant (black) stem cells for the situation of untreated (solid lines) and IM-treated (dashed line) CML. Note that f_α of leukemic cells is assumed to be identical for the treated and untreated situation. Please also note that the dashed line represents treatment of the "median" patient. For the adequate description of individual patients, f_ω is potentially shifted along the y-axis, which can be interpreted as either a relatively elevated (increased f_ω) or reduced (decreased f_ω) activation rate of leukemic stem cells into cell cycle compared to the median situation.

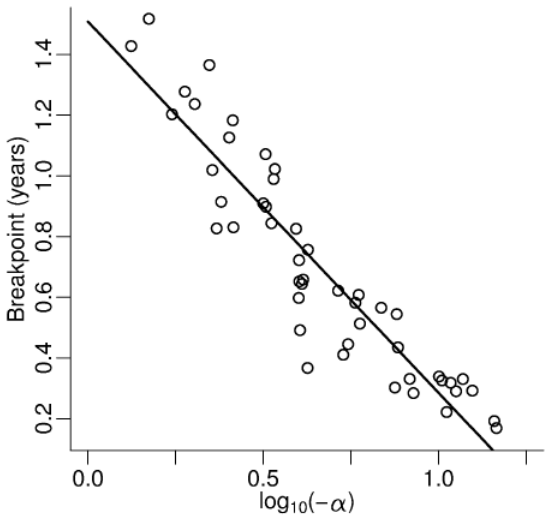

Figure S3. Correlation between first decline (α) and breakpoint separating first and second decline of *BCR-ABL* transcript levels. A linear relationship between first decline and breakpoint can be assumed (Pearson's correlation coefficient $\rho = -0.93$). For details we refer to the Supplemental Results. Note that variable α is log-transformed.

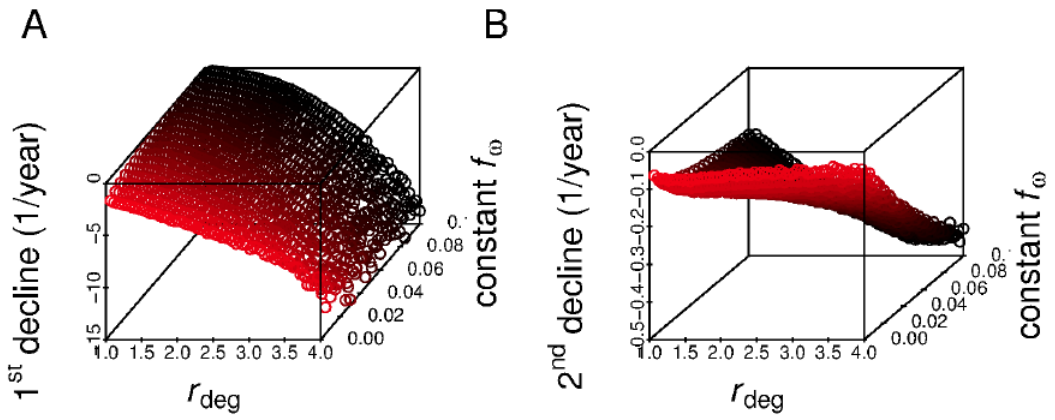

Figure S4. **Results of parameter space screening utilizing computer simulations**. Each point corresponds to one (r_{deg}, f_ω) parameter configuration out of 1600. Performing computer simulations (average of five simulation runs, respectively) each such pair yields a biphasic decline of *BCR-ABL* levels, characterized by the first (steep) and second (moderate) decline. For each case, decline parameters α and β are determined using a piecewise regression procedure (see text). (A) The first decline mainly depends on r_{deg} and, not surprisingly, increases with increasing apoptotic rates. (B) The shape of the hyperplane suggests a more complicated relationship between model parameters r_{deg} and f_ω and the second decline.

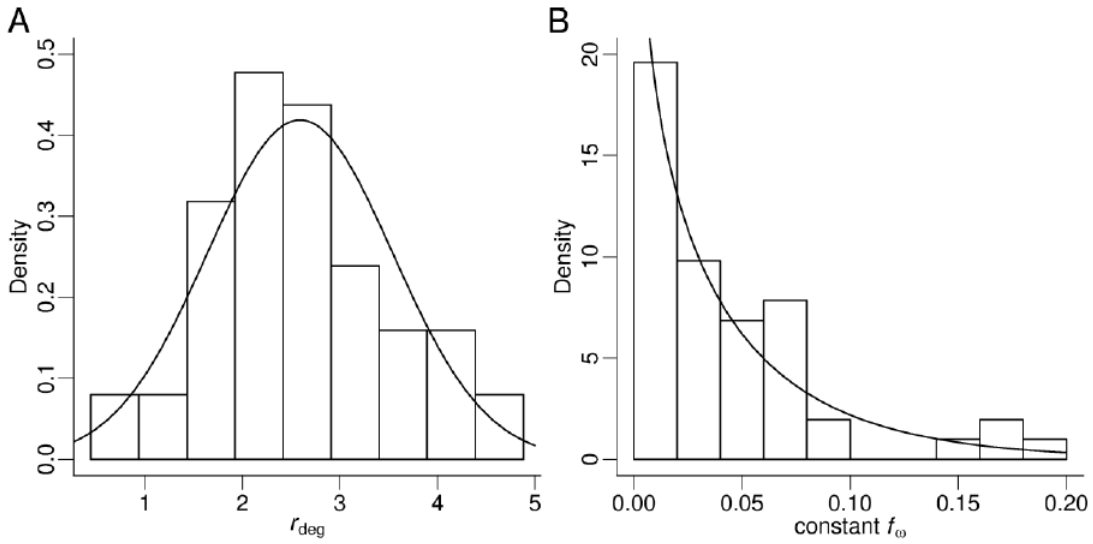

Figure S5. Parameter distributions (degradation rate r_{deg}, transition characteristic f_ω) for IRIS cohort. Shown are estimated distributions of model parameters that consistently explain the observed patient heterogeneity within the IRIS trial with respect to the decline of *BCR-ABL* transcript levels. (A) Empirical density function of degradation rates r_{deg} is depicted by the histogram. A normal distribution is fitted to the data (solid line), yielding $\mu = 2.59$ and $\sigma = 0.95$. (B) The histogram shows the empirical density function of transition characteristic f_ω. A gamma distribution, characterized by shape parameter $k = 0.76$ and scale parameter $\theta = 0.057$, is found to represent a suitable approximation (solid line). For details see text.

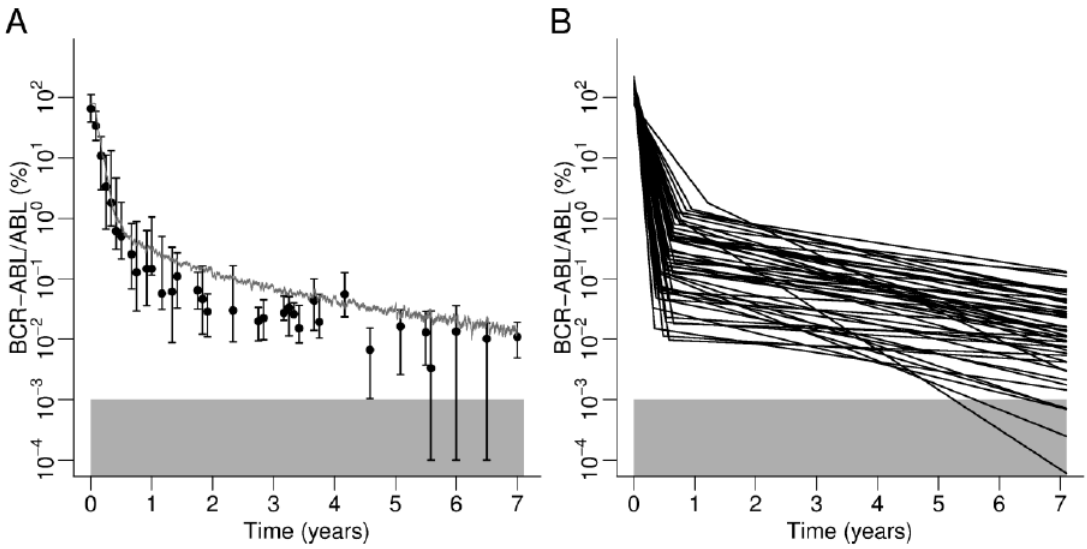

Figure S6. Validation of parameter distributions for degradation rate r_{deg} and transition characteristic f_ω estimated from the IRIS data. (A) The clinical data (n = 51 selected patients with biphasic decline of *BCR-ABL* transcript levels) is represented by medians (filled circles) and interquartile ranges. The solid line corresponds to a computer simulation (average of five individual simulation runs) using the theoretical mean values of the estimated distributions, which can be interpreted as IM treatment of the "median patient". Note that 10^{-4} % denotes zero, i.e. zero values are plotted on the lowermost value of the y-axis. (B) First and second declines estimated from the simulation of 51 "random patients". Random numbers were generated from the distributions estimated for r_{deg} and f_ω (Figure S5). The gray boxes in panels A and B represent the detection threshold of *BCR-ABL* transcripts.

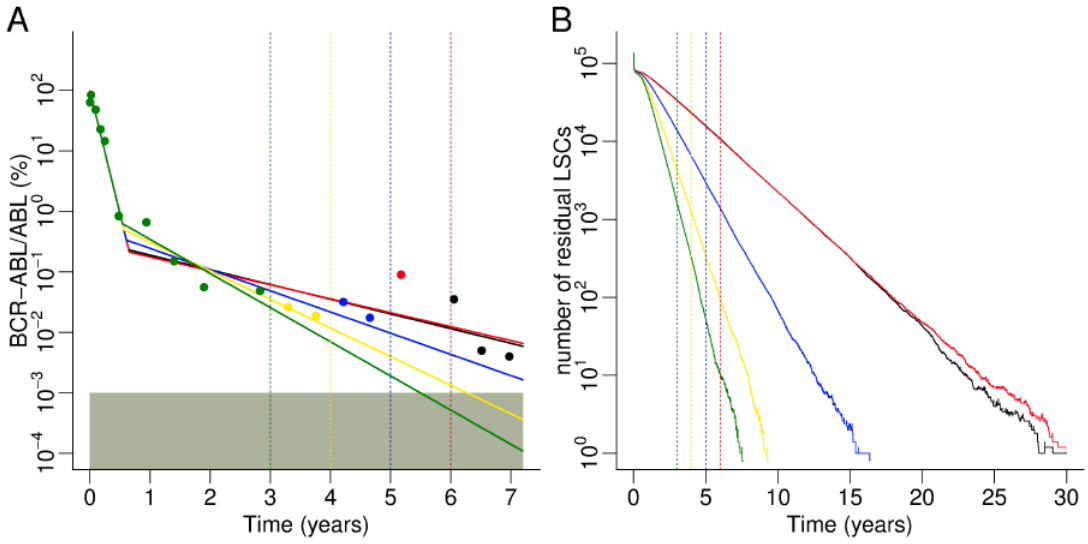

Figure S7. Restriction of observation time for example patient. (A) Calculation of decline parameters α and β from first 3 (green), 4 (orange), 5 (blue), and 6 (red) years of IM therapy. Full seven-year follow-up is depicted in black. Clinical data is represented by filled circles, results of the least-squares algorithm are depicted by solid lines. (B) Corresponding predictions of residual LSCs obtained by computer simulation (average of five simulation runs). Colors correspond to panel A. Vertical lines represent cut-off time points, respectively.

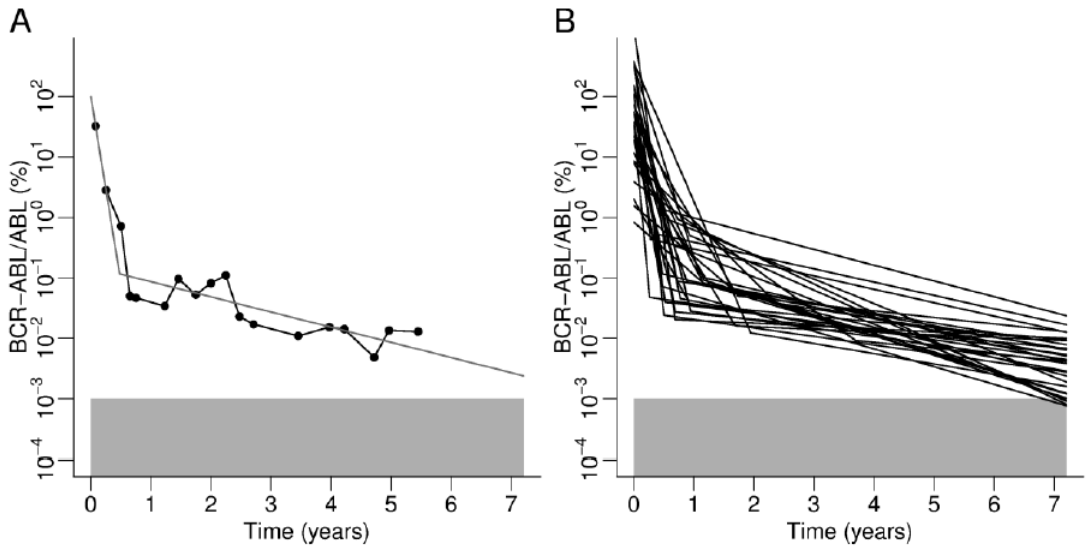

Figure S8. **Application of biphasic regression procedure to clinical data from the CML IV trial**. (A) Example of an individual patient. Data points obtained by qRT-PCR are represented by filled circles connected by black lines. The result of the least squares algorithm is depicted by the gray line. (B) Overview of regression results for 31 selected patients from the CML IV trial characterized by a biphasic decline.

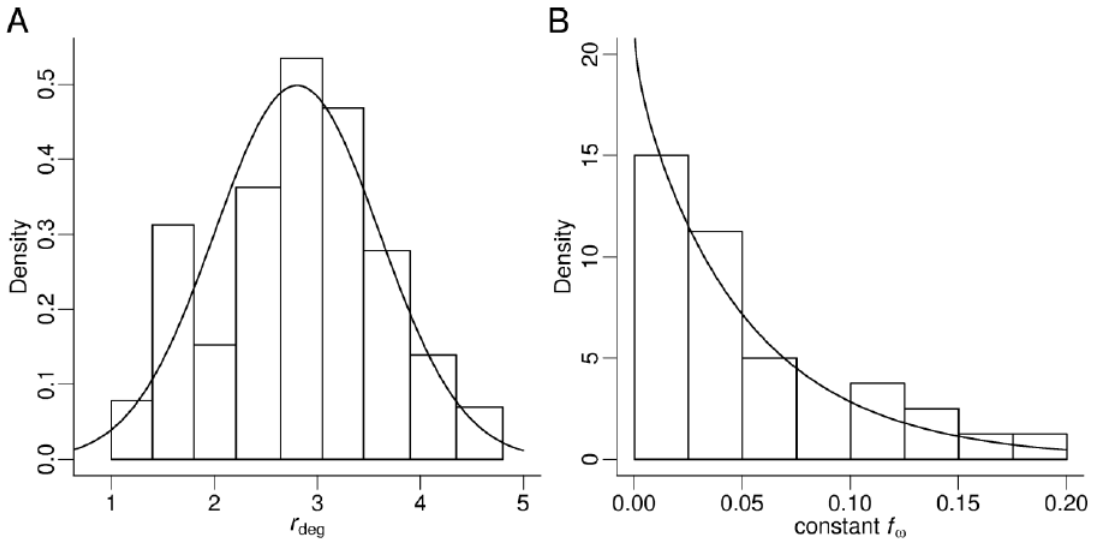

Figure S9. **Parameter distributions (degradation rate r_{deg}, transition characteristic f_ω) for CML IV cohort**. Shown are estimated distributions of model parameters that explain the observed patient heterogeneity within the CML IV trial with respect to the decline of *BCR-ABL* transcript levels. (A) Empirical density function of degradation rates r_{deg} is depicted by the histogram. A normal distribution is fitted to the data (solid line), yielding $\mu = 2.80$ and $\sigma = 0.80$. (B) The histogram shows the empirical density function of transition characteristic f_ω. A gamma distribution, characterized by shape parameter $k = 0.96$ and scale parameter $\theta = 0.056$, is found to represent a suitable approximation (solid line). For details see text.

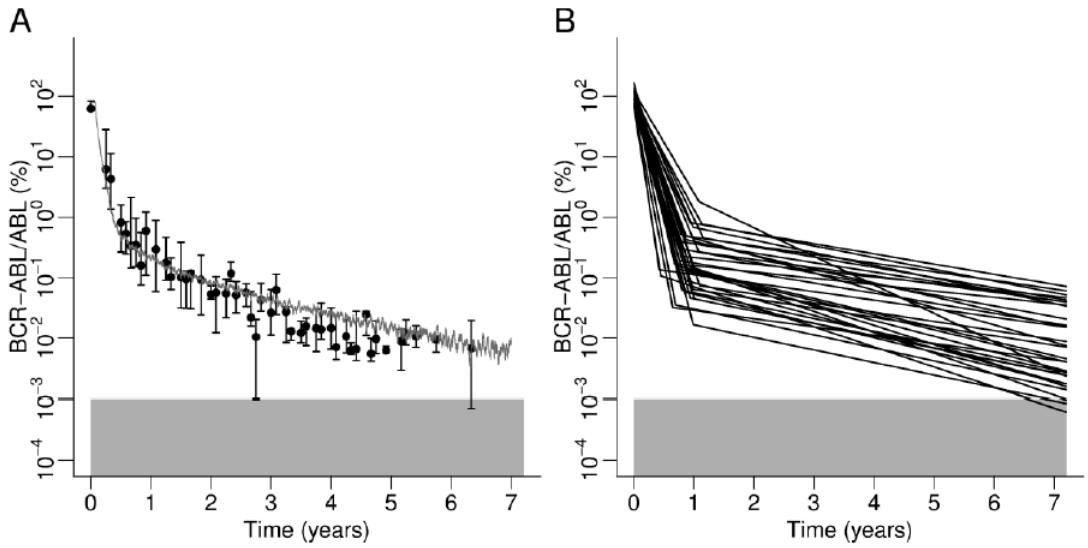

Figure S10. Validation of parameter distributions for degradation rate r_{deg} and transition characteristic f_{ω} estimated from CML IV patient data. (A) Clinical data (n = 31 selected patients with biphasic decline of *BCR-ABL* levels) is represented by medians (filled circles) and interquartile ranges. The solid line corresponds to a computer simulation (average of five simulations) using the theoretical mean values of the estimated distributions. (B) First and second declines estimated from the simulation of 31 "random patients". Random numbers were generated from the distributions estimated for r_{deg} and f_{ω} (Figure S9).

2.3.1 Zusätzliche Resultate

Im folgenden Abschnitt werden die Modellergebnisse betreffs Patientenheterogenität unter IM-Behandlung im Vergleich zum in Abschnitt 2.3 angefügten *Blood*-Paper vertieft.

Wie im Paper erläutert, folgen die klinisch messbaren Verläufe der *BCR-ABL*-Transkriptlevel bei der überwiegenden Mehrzahl der Patienten einer biphasischen Abfallkinetik. Die eindeutige Charakterisierung einer solchen Kinetik erfordert die Betrachtung eines Ausgangslevels (Zeitpunkt null), der Steilheit des ersten Abfalls, des Bruchpunkts zwischen beiden Abfällen (ersatzweise des *BCR-ABL*/*ABL*-Wertes am Bruchpunkt) sowie der Steilheit des zweiten Abfalls. Da die meisten Patienten der IRIS-Kohorte ein Ausgangslevel von 80% *BCR-ABL*/*ABL* oder mehr aufweisen, wurde modellseitig vereinfachend ein festes Ausgangslevel von 99% Ph-positiven Zellen angenommen (siehe auch Abschnitt 1.3.2). Aufgrund der beschriebenen starken Korrelation zwischen erstem Abfall und Bruchpunkt wird der Bruchpunkt bei der Charakterisierung der biphasischen Kinetik vernachlässigt. Folglich wird jede Kinetik allein durch die beiden Parameter α und β charakterisiert. Hierbei bezeichnet α den ersten (steilen) und β den zweiten (moderaten) Abfall der Tumorlast. Aus diesen beiden Werten lassen sich mit Hilfe einer Iterationsformel eindeutig zugehörige Modellparameter f_{ω} und r_{deg} berechnen, die eine Simulation der IM-Therapie des jeweiligen Patienten gestatten (Abbildung 10).

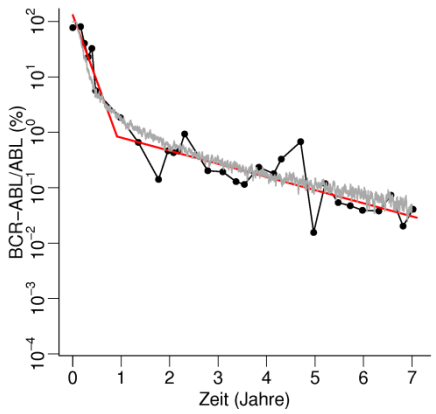

Abbildung 10: Modellanpassung eines Beispielpatienten (optimaler Fit). Schwarze Punkte repräsentieren Datenpunkte, die roten Linien stellen eine biphasische Least-Squares-Anpassung dar. Die korrespondierende Modellsimulation (Einzelsimulation) ist grau dargestellt.

Die beschriebenen Vereinfachungen wirken sich nachteilig auf die Güte aus, mit der das Modell die klinisch beobachteten Kinetiken beschreiben kann. Kinetiken, bei denen das Ausgangslevel entgegen der Annahme deutlich unter 100% liegt, können vom Modell nur dahingehend reproduziert werden, dass der erste Abfall leicht (nach oben) parallel verschoben ist.

Ähnliches gilt für Fälle, wo der klinisch beobachtete Bruchpunkt vom erwarteten Zeitpunkt (siehe Gleichung (1) in den „Supplemental Results“) abweicht. In diesem Fall beginnt der zweite Abfall in der Modellsimulation zum falschen Zeitpunkt, was sich ebenfalls in einem (bezüglich optimalem Fit) parallel verschobenen zweiten Abfall äußert (Abbildung 11). Dies hat potenziell zur Folge, dass die PCR-Detektionsschwelle (bzw. $MR^{5,0}$) in der Simulation zu einem anderen Zeitpunkt erreicht wird als in der korrespondierenden klinischen Abfallkinetik. Für die Ermittlung der Zeit in $MR^{5,0}$ bis zum empfohlenen Therapiestopp ist dies jedoch unerheblich, da nur die Zeit ab dem Unterschreiten der entsprechenden Schwelle betrachtet wird.

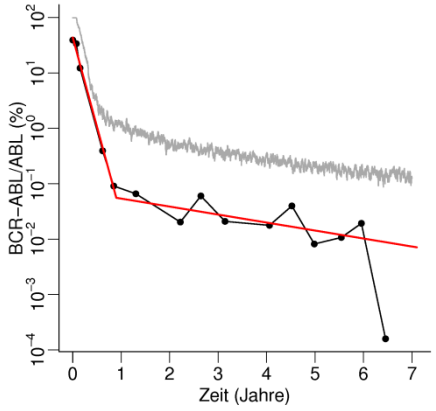

Abbildung 11: Modellanpassung eines Beispielpatienten (parallelverschobene Abfälle).

Darüber hinaus gibt es einige wenige (3 der ausgewählten 51) Fälle, in denen die Modellsimulation auch hinsichtlich der Parallelität der Abfälle die klinische Kinetik nicht reproduzieren kann (Abbildung 12). Hierbei handelt es sich um schlecht auf IM ansprechende Patienten, die durch einen verhältnismäßig flachen ersten Abfall und somit durch einen ungewöhnlich späten Bruchpunkt (nach mehr als dreijähriger Therapie) gekennzeichnet sind.

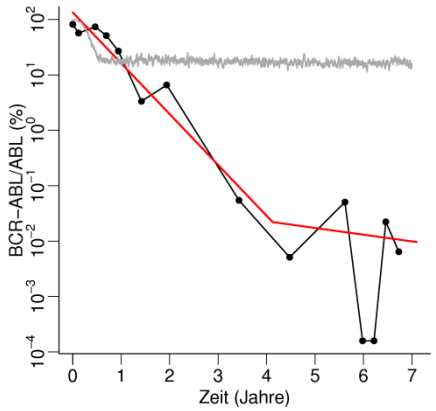

Abbildung 12: Modellanpassung eines Beispielpatienten (äußerst später Bruchpunkt).

2.4 Kennzeichnung des Eigenanteils

Im folgenden Abschnitt sind die wichtigsten geleisteten Eigenanteile für alle eingeschlossenen Publikationen stichpunktartig zusammengefasst. Bei gemeinsamer Bearbeitung einer Aufgabe sind die daran beteiligten Koautoren mit Initialen angegeben.

Publikation 1:

- inhaltliche Konzeption des „Letter to the Editor“ (mit IG und IR)
- Anpassung des ABM an die klinischen Daten aus der IRIS-Studie
- kritische Diskussion des Brieftextes (mit IG und IR)

Publikation 2:

- Mitarbeit an der Durchführung der Modellsimulationen (mit KH)
- kritische Diskussion des Manuskripttextes (mit allen Koautoren)

Publikation 3:

- Konzeption der Modellstudie (mit IR und ML)
- (statistische) Aufbereitung der klinischen Daten aus IRIS- und CML-IV-Studie
- Adaption des ABM an die Fragestellungen des Papers inklusive Programmierung
- Durchführung der Modellsimulationen
- Auswertung und Interpretation der Modellergebnisse (mit IR und ML)
- Ableitung der Prädiktoren aus den Simulationsergebnissen
- grafische Aufbereitung der Ergebnisse sowie Anfertigen der Abbildungen
- Schreiben von Manuskript und Supplement

3. Zusammenfassung

3.1 Wesentliche Ergebnisse der Arbeit

Das dieser Arbeit zugrunde liegende dynamische Modell erlaubt eine konsistente Beschreibung zahlreicher klinischer und biologischer Beobachtungen im Zusammenhang mit CML, sowohl während der Entstehung der Krankheit als auch unter verschiedenen medikamentösen Therapien. Das Modell geht von einer Dualität von proliferativen und ruhenden Stammzellen aus, die ihren Proliferationsstatus reversibel ändern können. Basierend auf diesen Annahmen liefert das Modell eine Erklärung sowohl für den biphasischen Abfall der *BCR-ABL*-Transkriptlevel unter IM-Therapie als auch die fortgesetzte Reduktion der Tumorlast bei langjähriger Behandlung: Demnach wirkt IM auch auf Ebene der Stammzellen, allerdings sind nur proliferativ aktive Zellen (entsprechend Modellkompartiment Ω) der Zytotoxizität des Medikaments ausgesetzt (vgl. Publikation 1). Der steile initiale Abfall der Tumorlast wird dabei durch die schnelle Eradikation proliferativer leukämischer Zellen erklärt, während sich der Abfall anschließend durch den deutlich geringeren Turnover der ruhenden LSCs erheblich abschwächt. Die Annahme vollständiger Insensitivität von LSCs gegenüber IM ist mit der klinischen Beobachtung einer kontinuierlichen Reduktion der Tumorlast nicht kompatibel. Die Modellresultate liefern aus theoretischer Sicht starke Argumente dafür, dass TKI-Therapie auch leukämische Stammzellen eradizieren kann und prinzipiell (langfristig) eine vollständige Eliminierung des leukämischen Klons möglich ist.

Da „langfristig“ laut Modellvorhersage eine IM-Therapie von bis zu mehreren Jahrzehnten bedeutet, könnte ein Therapieziel darin bestehen, die residualen LSCs durch Gabe zusätzlicher Substanzen in den Zyklus zu aktivieren, wo sie der TKI-Wirkung ausgesetzt sind. Unter der Annahme, dass IFN-α die Fähigkeit zur Stammzellaktivierung nicht nur in der Maus, sondern auch im Menschen besitzt, wird in Publikation 2 ausführlich untersucht, unter welchen Bedingungen eine solche Kombinationsstrategie potenziell Synergieeffekte hervorbringen könnte. Es zeigt sich, dass eine Kombination mit TKIs dann einen Vorteil bringt, wenn IFN-α normale und maligne Zellen mit gleicher Effektivität in den Zyklus aktivieren kann. Ist der Effekt für maligne LSCs geringer als für HSCs, erhöht sich die Zeit bis zur Eradikation des malignen Klons, ein Vorteil gegenüber TKI-Monotherapie ist aber immer noch zu beobachten. Falls IFN-α nur auf normale Stammzellen wirkt, geht der Vorteil der Kombinationstherapie vollständig verloren oder wird sogar zu einem Nachteil, wenn die Stimulation mit

IFN-α bei den betroffenen Zellen zusätzlich eine Störung im Selbsterneuerungspotenzial induziert. Am ausgeprägtesten ist der Vorteil der Kombination von TKI und IFN-α, wenn beide Substanzen zu jedem Zeitpunkt gemeinsam im System vorhanden sind. Muss IFN-α z.B. aufgrund von Nebenwirkungen gepulst verabreicht werden, ist jedoch immer noch mit einer (wenn auch weniger starken) Überlegenheit der Kombinationsstrategie zu rechnen.

Auch ohne Kombination mit anderen Substanzen sind TKI bei vielen Patienten in der Lage, tiefe molekulare Remissionen zu induzieren. Oft fällt der *BCR-ABL*-Transkriptlevel unter die Detektionsschwelle von qRT-PCR. Aufgrund von erheblichen Nebenwirkungen der TKI und ökonomischen Erwägungen geht man in solchen Fällen vermehrt dazu über, in kontrollierten Studien die TKI-Therapie abzubrechen. Zwar gibt es im Rahmen solcher Studien klare Kriterien, wann der Therapieabbruch frühestens erfolgen darf (z.B. unter Therapie zwei Jahre in kompletter molekularer Remission), aber eine Vorhersage, ob ein Patient nach Therapiestopp von einem molekularen Rückfall betroffen sein wird, ist nicht möglich. In der Praxis rezidivieren auch unter oben genannten Absetzkriterien etwa die Hälfte der Patienten.

In Publikation 3 wird vorgeschlagen, das ABM als Werkzeug zur Vorhersage des Rückfallrisikos bei individuellen Patienten zu verwenden. Hierzu muss aus der biphasischen Abfallkinetik der *BCR-ABL*-Transkriptlevel die Steilheit der zwei Phasen (α, β) bestimmt werden. Die beobachtete Patientenheterogenität im Abfall der Tumorlast lässt sich durch Modulation der Modellparameter f_ω und r_{deg} erklären. Es kann gezeigt werden, dass sich die kinetischen Parameter α und β eindeutig in die Modellparameter f_ω und r_{deg} „übersetzen“ lassen. Damit ist eine Simulation der Hämatopoese des entsprechenden Patienten *in silico* möglich.

Neben einer Vorhersage des Langzeittherapieerfolgs kann für den individuellen Patienten die Anzahl residualer LSCs über die Zeit verfolgt werden. Diese Größe ist klinisch nicht bestimmbar. Basierend auf diesem Wert wird vorhergesagt, dass kein molekularer Rückfall zu erwarten ist, wenn die Beziehung $\log_{10}(\text{Anzahl LSCs}) \leq 2.3$ gilt. Da die Anwendung des Modells zeit- und rechenaufwändig ist, wird approximativ zusätzlich ein modellunabhängiger Prädiktor angegeben. Dieser ist abhängig von der Zeit t (in Jahren), die sich ein Patient vor Therapieabbruch in stabiler $MR^{5,0}$ befand. Es wird vorhergesagt, dass der Patient seine Remission nach TKI-Stopp behält, wenn die Relation $\alpha/\beta \leq 8 \cdot t$ erfüllt ist. Die vorgeschlagene Methode wurde auf Basis der Daten der IRIS-Studie entwickelt, konnte aber in Modellsimulationen mit den Daten der CML-IV-Studie validiert werden. Die im Modell gezeigte Überlegenheit des individuellen Absetzkriteriums im Vergleich zu anderen Strategien muss sich jedoch in der klinischen Praxis im Rahmen von prospektiven randomisierten Studien beweisen.

3.2 Diskussion und Ausblick

Mathematische Modelle wie das in dieser Arbeit angewendete ABM stellen wertvolle Werkzeuge zur Unterstützung der klinischen Entscheidungsfindung dar. Unter der Voraussetzung, dass die vereinfachenden Modellannahmen die zugrunde liegenden biologischen Mechanismen hinreichend abbilden, ist es möglich, experimentelle Hypothesen und neuartige Behandlungsstrategien *in silico* zu testen und klinische Limitationen zu identifizieren. Basierend auf den Simulationsergebnissen können klinisch nachprüfbare Vorhersagen getroffen werden.

Eine solche neuartige Behandlungsstrategie stellt unter anderem die Kombinationstherapie von TKI und IFN-α dar. Mit Hilfe des Modells lassen sich hierfür verschiedene potenzielle Wirkmechanismen postulieren und Bedingungen ableiten, welche erfüllt sein müssen, damit die Kombinations- der TKI-Monotherapie hinsichtlich MRD-Eradikation überlegen ist. Eine der Hauptannahmen in Publikation 2 ist, dass IFN-α im Menschen eine Aktivierung ruhender HSCs in den Zellzyklus bewirkt. Diese Eigenschaft konnte bislang nur in der Maus gezeigt werden (14), allerdings gibt es keine Evidenz für grundlegend unterschiedliche Wirkmechanismen von IFN-α zwischen beiden Spezies. Selbst wenn IFN-α die postulierte Eigenschaft auch in der humanen Situation besitzt, garantiert sie noch keinen Erfolg der Kombinationstherapie. Mögliche Limitationen, welche das Modell identifizieren konnte, liegen in einem durch IFN-α induzierten temporären Selbsterneuerungsdefizit der aktivierten Zellen, sowie im Verabreichungsregime. Demnach ist eine kontinuierliche einer gepulsten Gabe von IFN-α vorzuziehen. Letzteres könnte auch eine Ursache dafür sein, dass frühere Kombinationsstudien mit hinsichtlich Stammzellaktivierung ähnlich wirkenden Substanzen wie G-CSF (53) keine Überlegenheit im Vergleich zu TKI-Monotherapie zeigen konnten (54).

Klinisch limitierend wirken sich bezüglich kontinuierlicher Gabe von IFN-α allerdings starke Nebenwirkungen aus, die oft Dosisreduktionen oder Absetzen von IFN-α zur Folge haben, mit entsprechenden Konsequenzen für mögliche Synergien. Einige Studien, in denen die Kombination von TKI und IFN-α untersucht wurde, wie z.B. IM und IFN-α im Rahmen der CML-IV-Studie, verwenden das „normale“ (gentechnisch hergestellte) Zytokin, da es für die CML-Therapie bereits zugelassen war. Eine Überlegenheit des Kombinationsarmes konnte nicht demonstriert werden (49). Um die Nebenwirkungen zu reduzieren und damit die Einhaltung der vorgesehenen IFN-α-Dosis zu gewährleisten, wird in aktuellen Studien auf pegyliertes IFN-α zurückgegriffen. Die Ergebnisse, etwa der französischen SPIRIT-Studie, zeigen, dass die Kombination dieser Substanz mit IM eine signifikante Überlegenheit

hinsichtlich des Erreichens einer $MR^{4,0}$ nach 12 Monaten bewirkt, verglichen mit IM-Monotherapie (37). Es bleibt abzuwarten, ob sich die Resultate in anderen Studien bestätigen.

Der Fokus der aktuell laufenden Kombinationsstudien liegt auf den immunologischen Wirkmechanismen von IFN-α (35). Die Tatsache, dass Patienten in molekularer Remission (aber mit detektierbarer MRD) nur mit IFN-α-Erhaltungstherapie viele Jahre in Remission bleiben (55), liefert einen Hinweis darauf, dass in diesen Patienten Immunmechanismen wirken, die während der CML-Entstehung den initial sehr kleinen leukämischen Klon noch nicht kontrollieren konnten. Es gibt Berichte, dass Remissionen bei zuvor erfolgter IFN-α-Therapie selbst nach vollständigem Therapiestopp erhalten bleiben (56). In diesem Zusammenhang wird der Einfluss spezieller T-Zellen diskutiert (57). Die Beobachtungen legen nahe, dass die immunologischen Effekte im Falle sehr weniger residualer Leukämiezellen einen wesentlichen Mechanismus darstellen und in zukünftigen Modellversionen berücksichtigt werden sollten.

Ein weiterer Bereich, in dem das ABM zur Unterstützung klinischer Entscheidungsfindung beitragen kann, sind Abbruchstudien. Dabei wird die TKI-Therapie nach Erreichen tiefer molekularer Remissionen kontrolliert beendet und im Falle molekularer Rückfälle wieder aufgenommen. Die in Publikation 3 vorgeschlagenen Prädiktoren zur Vorhersage des individuellen Risikos eines molekularen Rückfalls nach Abbruch der IM-Therapie sind zwar im Rahmen der Simulationsstudien anderen Absetzkriterien überlegen, ob sich die Ergebnisse auch in der Praxis bestätigen, muss sich in prospektiven randomisierten Studien zeigen. Hinsichtlich TKI-Abbruchstudien wäre zusätzlich eine Prognosefaktoranalyse hilfreich. Bei Vorliegen hinreichend großer Datensätze bezüglich einer zweijährigen kompletten molekularen Remission vor Therapieabbruch ließe sich zum Beispiel prüfen, ob der beste Prädiktor für den Erhalt der Remission die Geschwindigkeit ist, diese Remission zu erreichen.

In der CML-V-Studie („TIGER“) der Deutschen CML-Studiengruppe, deren Rekrutierung am 1. August 2012 begann, werden die zwei oben diskutierten Hauptaspekte dieser Dissertation, TKI in Kombination mit IFN-α sowie vollständiger Therapieabbruch, gemeinsam untersucht (Abbildung 13). Konkret wird dabei ein TKI der zweiten Generation (Nilotinib) mit einer Kombinationstherapie aus Nilotinib und pegyliertem IFN-α verglichen. Nach mindestens zweijähriger Therapie wird bei bestätigter MMR im Kombinationsarm auf eine reine IFN-α-Erhaltungstherapie umgestellt. Der Monotherapie-Arm läuft in der Erhaltung unverändert weiter. Nach insgesamt wenigstens dreijähriger Therapie, davon wenigstens die letzten 12 Monate in kontinuierlicher $MR^{4,0}$, wird die Therapie in beiden Armen unter strenger Kontrolle vollständig abgebrochen und nur bei einem molekularen Rückfall wieder aufgenommen.

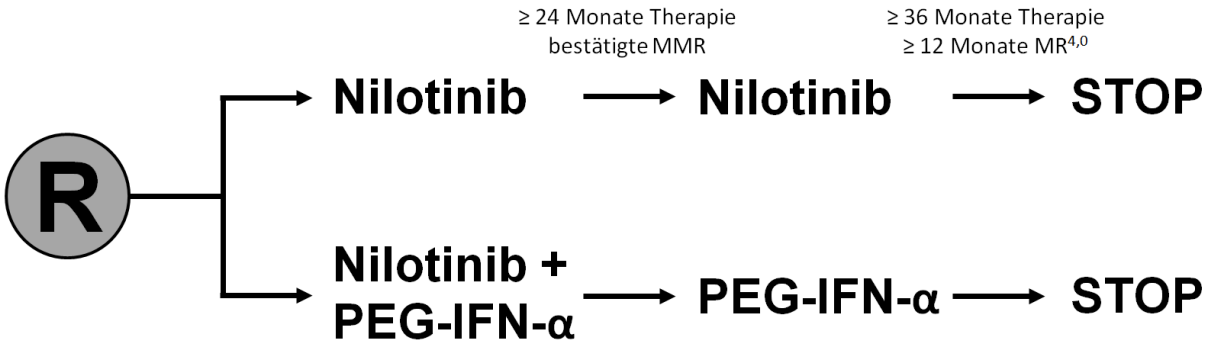

Abbildung 13: Design der CML-V-Studie. In der zweiarmigen prospektiven randomisierten „TIGER"-Studie wird Nilotinib-Monotherapie mit einer Kombination aus Nilotinib und pegyliertem IFN-α verglichen. Nach einer Erhaltungsphase ist geplant, die Therapie im Fall einer mindestens ein Jahr andauernden $MR^{4,0}$ vollständig abzubrechen.

Auch wenn mit Hilfe des obigen Designs sowohl die Frage möglicher Synergien einer Kombinationstherapie aus TKI und IFN-α als auch einer möglichen Heilung der CML beantwortet werden soll, sind hierzu aus Sicht der präsentierten Modellanalysen einige Anmerkungen naheliegend. Zum einen lässt sich mit dem Studiendesign die Abhängigkeit der Effektgröße einer IFN-α-Erhaltung von der Induktionstherapie nicht klären. Eine Beantwortung dieser Frage wäre vor dem Hintergrund verschiedener postulierter Wirkmechanismen von IFN-α (immunologischer Effekt, Aktivierung von HSCs in den Zellzyklus) relevant. Zum anderen sagt das Modell voraus, dass das gewählte feste Absetzkriterium suboptimal ist, da die Therapie bei einigen Patienten zu früh abgesetzt wird, während andere unnötig lange therapiert werden. Ein modellbasiertes patientenindividuelles Absetzkriterium wie in Publikation 3 vorgeschlagen könnte die Rate rezidivierender Patienten verringern.

In dieser Dissertation wurde der Aspekt der TKI-Resistenzen infolge von Mutationen der *BCR-ABL*-Kinasedomäne nicht betrachtet. So könnte eine Kombination aus TKI und IFN-α bei Vorliegen von Sekundärmutationen sogar nachteilig sein, wenn die TKI-resistenten Klone von IFN-α in den Zellzyklus aktiviert und dadurch verstärkt selektiert werden. Außerdem ist die in Publikation 3 vorgeschlagene patientenindividuelle Prädiktion des Rezidivrisikos nach Therapieabbruch explizit nur möglich, wenn keine IM-resistenten Klone die Kompetition normaler und maligner Zellen beeinflussen.

Im Rahmen einer von mir mit betreuten Diplomarbeit, in welcher das ABM zur Erklärung der Kinetiken therapieresistenter Klone unter TKI der zweiten Generation (Nilotinib, Dasatinib) eingesetzt wurde, konnten aufgrund zu geringer Fallzahlen der klinisch gemessenen Mutanten

und großer interindividueller Heterogenität der Kinetiken keine eindeutigen Resultate abgeleitet werden (58). Dadurch, dass bei etwa 20% aller Patienten unter TKI *BCR-ABL*-Mutationen nachweisbar und fast immer mit Therapieresistenz assoziiert sind (59), ist für zukünftige Modellanalysen eine Berücksichtigung von Resistenzmechanismen erforderlich.

Das verwendete Modell ist einzelzellbasiert, das heißt, jedes individuelle Zellobjekt wird separat betrachtet und muss in jedem Zeitschritt gemäß der definierten Regeln einzeln aktualisiert werden. Aufgrund der großen Anzahl von Stammzellen im System sind Modellsimulationen daher sehr rechenaufwändig. So dauert die Simulation eines einzelnen Patienten für einen Behandlungszeitraum von etwa sieben Jahren mit modernsten Prozessoren einige Stunden. Da aufgrund der stochastischen Elemente des Modells selbst bei identischen Parameterwerten quantitativ unterschiedliche Modellresultate erzielt werden können, werden oft mindestens fünf Simulationen mit identischen Parametern durchgeführt und das arithmetische Mittel der Ergebnisse berechnet. Bei Verwendung eines einzelnen Prozessors vervielfacht sich die Rechenzeit hierdurch zusätzlich, was aber durch Parallelisierung wieder ausgeglichen werden kann. Eine Parallelisierung des Modellalgorithmus selbst bringt hingegen kaum Zeitgewinn, da zu jedem Zeitpunkt im Modell die Anzahl aller Zellen bekannt sein muss, was eine Synchronisierung sämtlicher paralleler Threads nach jedem Zeitschritt erfordert.

Abhilfe könnte eine Beschreibung des Modells mit Hilfe von Differenzengleichungen schaffen. Nach Unterteilung der Signalumgebungen A und Ω in zahlreiche Subkompartimente, deren Ein- und Ausströme durch entsprechende Gleichungen beschrieben werden, lässt sich zeigen, dass die Resultate des Differenzengleichungsmodells und des mittleren ABM-Verhaltens im Wesentlichen identisch sind. Die Rechenzeit einer Einzelsimulation ist bis zu 80 mal niedriger als beim ABM. Allerdings geht in der deterministischen Beschreibung der stochastische Aspekt vollständig verloren (60). Klonale Fluktuationen im Fall sehr kleiner Zellzahlen, welche zum Aussterben eines Klons führen können, sind mit dem Differenzengleichungsmodell nicht abbildbar, in der klinischen Praxis hingegen bedeutsam. Dennoch stellt eine deterministische Beschreibung des Modells in einigen Fällen eine hinreichende Approximation des ABM dar, die möglicherweise auch die Praktikabilität der Anwendung des Modells für Ärzte im Rahmen klinischer Entscheidungsfindung verbessert.

Mit dem Ziel der einfacheren Anwendbarkeit des Modells für Mediziner und andere Wissenschaftler wurde im Rahmen dieser Arbeit eine Implementation des ABM in der statistischen Programmierumgebung R angefertigt. Die bisher verfügbare Implementation in der Programmiersprache C++ setzt Fähigkeiten im Kompilieren von Quellcode voraus. Die R-Ver-

sion des Modells erfordert hingegen lediglich die Installation des frei verfügbaren Open-Source-Programms R (http://www.r-project.org/) sowie das implementierte Modell, welches ich nach Kontaktaufnahme jedem Interessierten zur Verfügung stelle. Anschließend lassen sich Modellsimulationen durch Eingabe einfacher Befehle in der R-Umgebung starten. Leider sind die Rechenzeiten deutlich höher als in vergleichbaren C++-Simulationen, was unter anderem dem Fehlen geeigneter Datenstrukturen (z.B. pointerbasierte Listen) in R geschuldet ist.

Das in dieser Arbeit verwendete ABM ist Grundlage der in Publikation 3 vorgeschlagenen Absetzkriterien bei IM-Therapie. Diese stellen ein Paradebeispiel für eine modellbasierte, individualisierte Therapie dar. Das bedeutet, mit Hilfe eines mathematischen Modells wird ein Entscheidungsalgorithmus vorgeschlagen, der für alle Patienten einheitlich, aber durch patientenindividuell unterschiedliche Parameter gekennzeichnet ist. Dadurch wird eine auf den jeweiligen Patienten zugeschnittene und verglichen mit bisherigen Strategien optimierte Therapie ermöglicht. Eine Evolvierung der patientenindividuellen Parameter kann erfolgen, wenn zusätzliche klinische Informationen einbezogen werden, z.B. durch genauere Charakterisierung der Abfallkinetik der *BCR-ABL*-Transkriptlevel oder Betrachtung immunologischer Effekte im Fall sehr geringer residualer LSCs. Hierdurch ist eine Verbesserung der Prädiktion zum Beispiel hinsichtlich eines molekularen Rückfalls nach Therapieabbruch zu erwarten.

Die vorgeschlagene Strategie kann nicht nur bei IM angewendet, sondern in ähnlicher Form auch auf Erstlinientherapien mit TKIs der zweiten Generation wie Dasatinib oder Nilotinib übertragen werden. Hierzu kann eine analoge „Umrechnung“ der individuellen *BCR-ABL*-Transkriptlevel in Modellparameter mit anschließender Simulation des jeweiligen Patienten vorgenommen werden. Bei hinreichender Fallzahl wird hierdurch eventuell eine modellbasierte Vergleichbarkeit der Medikamente, zum Beispiel hinsichtlich des Erreichens tiefer Remissionen und Rezidivwahrscheinlichkeiten, ermöglicht. Diese Resultate könnten außerdem einen Beitrag zur Abschätzung der Kosteneffektivität der verwendeten Substanzen liefern. Aus jetziger Sicht muss jedoch festgestellt werden, dass das verfügbare Follow-up bezüglich Einsatz der Zweitgenerations-TKIs in der Erstlinie noch nicht genügt, um die Prozedur, insbesondere hinsichtlich Bestimmung der kinetischen Parameter α und β, anwenden zu können.

Abschließend soll darauf hingewiesen werden, dass das verwendete Modell über die Jahre, insbesondere auch in seiner Anwendung auf CML-Daten, immer weiter verfeinert und weiterentwickelt wurde. Mittlerweile ist ein Grad der Vollständigkeit erreicht, der einen Einsatz des Modells bei der Entwicklung von Studiendesigns rechtfertigt. Inwieweit sich das Modell im Rahmen von prospektiven klinischen Studien bewährt, wird abzuwarten bleiben.

4. Literaturverzeichnis

1. **Hehlmann R, Hochhaus A, Baccarani M.** Chronic myeloid leukaemia. *Lancet.* 2007;370(9584), pp. 342-350.

2. **Bacher U, Schnittger S, Haferlach T.** Molecular genetics in acute myeloid leukemia. *Curr Opin Oncol.* 2010;22(6), pp. 646-655.

3. **An X, Tiwari AK, Sun Y, Ding PR, Ashby CR Jr, Chen ZS.** BCR-ABL tyrosine kinase inhibitors in the treatment of Philadelphia chromosome positive chronic myeloid leukemia: A review. *Leuk Res.* 2010;34(10), pp. 1255-1268.

4. **Buchdunger E, Zimmermann J, Mett H, Meyer T, Müller M, Druker BJ, Lydon NB.** Inhibition of the Abl protein-tyrosine kinase in vitro and in vivo by a 2-phenylaminopyrimidine derivative. *Cancer Res.* 1996;56(1), pp. 100-104.

5. **Oetzel C, Jonuleit T, Götz A, van der Kuip H, Michels H, Duyster J, Hallek M, Aulitzky WE.** The tyrosine kinase inhibitor CGP 57148 (STI 571) induces apoptosis in BCR-ABL-positive cells by down-regulating BCL-X. *Clin Cancer Res.* 2000;6(5), pp. 1958-1968.

6. **Melo JV, Barnes DJ.** Chronic myeloid leukaemia as a model of disease evolution in human cancer. *Nat Rev Cancer.* 2007;7(6), pp. 441-453.

7. **Hehlmann R, Heimpel H, Hasford J, Kolb HJ, Pralle H, Hossfeld DK, Queisser W, Löffler H, Hochhaus A, Heinze B.** Randomized comparison of interferon-alpha with busulfan and hydroxyurea in chronic myelogenous leukemia. *Blood.* 1994;84(12), pp. 4064-4077.

8. **Druker BJ, Guilhot F, O'Brien SG, Gathmann I, Kantarjian H, Gattermann N, Deininger MW, Silver RT, Goldman JM, Stone RM, Cervantes F, Hochhaus A, Powell BL, Gabrilove JL, Rousselot P, Reiffers J, Cornelissen JJ, Hughes T, Agis H, et al.** Five-year follow-up of patients receiving imatinib for chronic myeloid leukemia. *N Engl J Med.* 2006;355(23), pp. 2408-2417.

9. **O'Brien SG, Guilhot F, Larson RA, Gathmann I, Baccarani M, Cervantes F, Cornelissen JJ, Fischer T, Hochhaus A, Hughes T, Lechner K, Nielsen JL, Rousselot P, Reiffers J, Saglio G, Shepherd J, Simonsson B, Gratwohl A, Goldman JM, Kantarjian H, et al.** Imatinib compared with interferon and low-dose cytarabine for newly diagnosed chronic-phase chronic myeloid leukemia. *N Engl J Med.* 2003;348(11), pp. 994-1004.

10. **Hochhaus, A.** Minimal residual disease in chronic myeloid leukaemia patients. *Best Pract Res Clin Haematol.* 2002;15(1), pp. 159-178.

11. **Mahon FX, Réa D, Guilhot J, Guilhot F, Huguet F, Nicolini F, Legros L, Charbonnier A, Guerci A, Varet B, Etienne G, Reiffers J, Rousselot P.** Discontinuation of imatinib in patients with chronic myeloid leukaemia who have maintained complete

molecular remission for at least 2 years: the prospective, multicentre Stop Imatinib (STIM) trial. *Lancet Oncol.* 2010;11(11), pp. 1029-1035.

12. **Graham SM, Jørgensen HG, Allan E, Pearson C, Alcorn MJ, Richmond L, Holyoake TL.** Primitive, quiescent, Philadelphia-positive stem cells from patients with chronic myeloid leukemia are insensitive to STI571 in vitro. *Blood.* 2002;99(1), pp. 319-325.

13. **Essers MA, Trumpp A.** Targeting leukemic stem cells by breaking their dormancy. *Mol Oncol.* 2010;4(5), pp. 443-450.

14. **Essers MA, Offner S, Blanco-Bose WE, Waibler Z, Kalinke U, Duchosal MA, Trumpp A.** IFNalpha activates dormant haematopoietic stem cells in vivo. *Nature.* 2009;458(7240), pp. 904-908.

15. **Roeder I, Loeffler M.** A novel dynamic model of hematopoietic stem cell organization based on the concept of within-tissue plasticity. *Exp Hematol.* 2002;30(8), pp. 853-861.

16. **Horn, M.** Mathematical modeling of genesis and treatment of chronic myeloid leukemia (Diplomarbeit, Universität Leipzig). 2006.

17. **Roeder I, Horn M, Glauche I, Hochhaus A, Mueller MC, Loeffler M.** Dynamic modeling of imatinib-treated chronic myeloid leukemia: functional insights and clinical implications. *Nat Med.* 2006;12(10), pp. 1181-1184.

18. **Morrison SJ, Uchida N, Weissman IL.** The biology of hematopoietic stem cells. *Annu Rev Cell Dev Biol.* 1995;11, pp. 35-71.

19. **Wilson A, Laurenti E, Oser G, van der Wath RC, Blanco-Bose W, Jaworski M, Offner S, Dunant CF, Eshkind L, Bockamp E, Lió P, Macdonald HR, Trumpp A.** Hematopoietic stem cells reversibly switch from dormancy to self-renewal during homeostasis and repair. *Cell.* 2008;135(6), pp. 1118-1129.

20. **Uchida N, Fleming WH, Alpern EJ, Weissman IL.** Heterogeneity of hematopoietic stem cells. *Curr Opin Immunol.* 199;5(2), pp. 177-184.

21. **Loeffler M, Roeder I.** Tissue stem cells: definition, plasticity, heterogeneity, self-organization and models - a conceptual approach. *Cells Tissues Organs.* 2002;171(1), pp. 8-26.

22. **Goldman JM, Melo JV.** Chronic myeloid leukemia - advances in biology and new approaches to treatment. *N Engl J Med.* 2003;349(15), pp. 1451-1464.

23. **Ichimaru M, Tomonaga M, Amenomori T, Matsuo T.** Atomic bomb and leukemia. *J Radiat Res.* 1991;32 Suppl 1, pp. 162-167.

24. **Sessarego M, Fugazza G, Bruzzone R, Ballestrero A, Miglino M, Bacigalupo A.** Complex chromosome rearrangements may locate the bcr/abl fusion gene sites other than 22q11. *Haematologica.* 2000;85(1), pp. 35-39.

25. **Ernst T, Hochhaus A.** Chronic myeloid leukemia: clinical impact of BCR-ABL1 mutations and other lesions associated with disease progression. *Semin Oncol.* 2012;39(1), pp. 58-66.

26. **Kreuzer KA, Le Coutre P, Landt O, Na IK, Schwarz M, Schultheis K, Hochhaus A, Dörken B.** Preexistence and evolution of imatinib mesylate-resistant clones in chronic myelogenous leukemia detected by a PNA-based PCR clamping technique. *Ann Hematol.* 2003;82(5), pp. 284-289.

27. **Yeung DT, Parker WT, Branford S.** Molecular methods in diagnosis and monitoring of haematological malignancies. *Pathology.* 2011;43(6), pp. 566-579.

28. **Cross, NC.** Standardisation of molecular monitoring for chronic myeloid leukaemia. *Best Pract Res Clin Haematol.* 2009;22(3), pp. 355-365.

29. **Goldman, J.** Monitoring minimal residual disease in BCR-ABL-positive chronic myeloid leukemia in the imatinib era. *Curr Opin Hematol.* 2005;12(1), pp. 33-39.

30. **de Lima PD, Cardoso PC, Khayat AS, Bahia Mde O, Burbano RR.** Evaluation of the mutagenic activity of hydroxyurea on the G1-S-G2 phases of the cell cycle: an in vitro study. *Genet Mol Res.* 2003;2(3), pp. 328-333.

31. **Hehlmann R, Heimpel H, Hasford J, Kolb HJ, Pralle H, Hossfeld DK, Queisser W, Löffler H, Heinze B, Georgii A, et al.** Randomized comparison of busulfan and hydroxyurea in chronic myelogenous leukemia: prolongation of survival by hydroxyurea. *Blood.* 1993;82(2), pp. 398-407.

32. **Parmar S, Platanias LC.** Interferons: mechanisms of action and clinical applications. *Curr Opin Oncol.* 2003;15(6), pp. 431-439.

33. **Bhatia R, Wayner EA, McGlave PB, Verfaillie CM.** Interferon-alpha restores normal adhesion of chronic myelogenous leukemia hematopoietic progenitors to bone marrow stroma by correcting impaired beta 1 integrin receptor function. *J Clin Invest.* 1994;94(1), pp. 384-391.

34. **Verma A, Platanias LC.** Signaling via the interferon-alpha receptor in chronic myelogenous leukemia cells. *Leuk Lymphoma.* 2002;43(4), pp. 703-709.

35. **Talpaz M, Hehlmann R, Quintás-Cardama A, Mercer J, Cortes J.** Re-emergence of interferon-α in the treatment of chronic myeloid leukemia. *Leukemia.* 2013;27(4), pp. 803-812.

36. **Simonsson B, Gedde-Dahl T, Markevärn B, Remes K, Stentoft J, Almqvist A, Björeman M, Flogegård M, Koskenvesa P, Lindblom A, Malm C, Mustjoki S, Myhr-Eriksson K, Ohm L, Räsänen A, Sinisalo M, Själander A, Strömberg U, Bjerrum OW, Ehrencrona H, et al.** Combination of pegylated IFN-α2b with imatinib increases molecular response rates in patients with low- or intermediate-risk chronic myeloid leukemia. *Blood.* 2011;118(12), pp. 3228-3235.

37. **Preudhomme C, Guilhot J, Nicolini FE, Guerci-Bresler A, Rigal-Huguet F, Maloisel F, Coiteux V, Gardembas M, Berthou C, Vekhoff A, Rea D, Jourdan E, Allard C, Delmer A, Rousselot P, Legros L, Berger M, Corm S, Etienne G, Roche-Lestienne C, et al.** Imatinib plus peginterferon alfa-2a in chronic myeloid leukemia. *N Engl J Med.* 2010;363(26), pp. 2511-2521.

38. **Savage DG, Antman KH.** Imatinib mesylate - a new oral targeted therapy. *N Engl J Med.* 2002;346(9), pp. 683-693.

39. **Druker BJ, Tamura S, Buchdunger E, Ohno S, Segal GM, Fanning S, Zimmermann J, Lydon NB.** Effects of a selective inhibitor of the Abl tyrosine kinase on the growth of Bcr-Abl positive cells. *Nat Med.* 1996;2(5), pp. 561-566.

40. **Vigneri P, Wang JY.** Induction of apoptosis in chronic myelogenous leukemia cells through nuclear entrapment of BCR-ABL tyrosine kinase. *Nat Med.* 2001;7(2), pp. 228-234.

41. **Hochhaus A, O'Brien SG, Guilhot F, Druker BJ, Branford S, Foroni L, Goldman JM, Müller MC, Radich JP, Rudoltz M, Mone M, Gathmann I, Hughes TP, Larson RA.** Six-year follow-up of patients receiving imatinib for the first-line treatment of chronic myeloid leukemia. *Leukemia.* 2009;23(6), pp. 1054-1061.

42. **Hughes TP, Kaeda J, Branford S, Rudzki Z, Hochhaus A, Hensley ML, Gathmann I, Bolton AE, van Hoomissen IC, Goldman JM, Radich JP.** Frequency of major molecular responses to imatinib or interferon alfa plus cytarabine in newly diagnosed chronic myeloid leukemia. *N Engl J Med.* 2003;349(15), pp. 1423-1432.

43. **Michor F, Hughes TP, Iwasa Y, Branford S, Shah NP, Sawyers CL, Nowak MA.** Dynamics of chronic myeloid leukaemia. *Nature.* 2005;435(7046), pp. 1267-1270.

44. **Tauchi T, Ohyashiki K.** Molecular mechanisms of resistance of leukemia to imatinib mesylate. *Leuk Res.* 2004;28 Suppl 1, pp. S39-S45.

45. **Kantarjian H, Shah NP, Hochhaus A, Cortes J, Shah S, Ayala M, Moiraghi B, Shen Z, Mayer J, Pasquini R, Nakamae H, Huguet F, Boqué C, Chuah C, Bleickardt E, Bradley-Garelik MB, Zhu C, Szatrowski T, Shapiro D, Baccarani M.** Dasatinib versus imatinib in newly diagnosed chronic-phase chronic myeloid leukemia. *N Engl J Med.* 2010;362(24), pp. 2260-2270.

46. **Saglio G, Kim DW, Issaragrisil S, le Coutre P, Etienne G, Lobo C, Pasquini R, Clark RE, Hochhaus A, Hughes TP, Gallagher N, Hoenekopp A, Dong M, Haque A, Larson RA, Kantarjian HM.** Nilotinib versus imatinib for newly diagnosed chronic myeloid leukemia. *N Engl J Med.* 2010;362(24), pp. 2251-2259.

47. **Shah, NP.** Ponatinib: targeting the T315I mutation in chronic myelogenous leukemia. *Clin Adv Hematol Oncol.* 2011;9(12), pp. 925-926.

48. **Deininger M, O'Brien SG, Guilhot F, Goldman JM, Hochhaus A, Hughes TP, Radich JP, Hatfield AK, Mone M, Filian J, Reynolds J, Gathmann I, Larson RA, Druker BJ.** International Randomized Study of Interferon vs. STI571 (IRIS) 8-year follow

up: sustained survival and low risk for progression or events in patients with newly diagnosed chronic myeloid leukemia in chronic phase (CML-CP) treated with imatinib. *ASH abstract #1126.* 2009.

49. **Hehlmann R, Lauseker M, Jung-Munkwitz S, Leitner A, Müller MC, Pletsch N, Proetel U, Haferlach C, Schlegelberger B, Balleisen L, Hänel M, Pfirrmann M, Krause SW, Nerl C, Pralle H, Gratwohl A, Hossfeld DK, Hasford J, Hochhaus A, Saussele S.** Tolerability-adapted imatinib 800 mg/d versus 400 mg/d versus 400 mg/d plus interferon-α in newly diagnosed chronic myeloid leukemia. *J Clin Oncol.* 2011;29(12), pp. 1634-1642.

50. **Biernaux C, Loos M, Sels A, Huez G, Stryckmans P.** Detection of major bcr-abl gene expression at a very low level in blood cells of some healthy individuals. *Blood.* 1995;86(8), pp. 3118-3122.

51. **Roeder I, Kamminga LM, Braesel K, Dontje B, de Haan G, Loeffler M.** Competitive clonal hematopoiesis in mouse chimeras explained by a stochastic model of stem cell organization. *Blood.* 2005;105(2), pp. 609-616.

52. **Branford S, Hughes TP, Rudzki Z.** Monitoring chronic myeloid leukaemia therapy by real-time quantitative PCR in blood is a reliable alternative to bone marrow cytogenetics. *Br J Haematol.* 1999;107(3), pp. 587-599.

53. **Jørgensen HG, Copland M, Allan EK, Jiang X, Eaves A, Eaves C, Holyoake TL.** Intermittent exposure of primitive quiescent chronic myeloid leukemia cells to granulocyte-colony stimulating factor in vitro promotes their elimination by imatinib mesylate. *Clin Cancer Res.* 2006;12(2), pp. 626-633.

54. **Drummond MW, Heaney N, Kaeda J, Nicolini FE, Clark RE, Wilson G, Shepherd P, Tighe J, McLintock L, Hughes T, Holyoake TL.** A pilot study of continuous imatinib vs pulsed imatinib with or without G-CSF in CML patients who have achieved a complete cytogenetic response. *Leukemia.* 2009;23(6), pp. 1199-1201.

55. **Burchert A, Müller MC, Kostrewa P, Erben P, Bostel T, Liebler S, Hehlmann R, Neubauer A, Hochhaus A.** Sustained molecular response with interferon alfa maintenance after induction therapy with imatinib plus interferon alfa in patients with chronic myeloid leukemia. *J Clin Oncol.* 2010;28(8), pp. 1429-1435.

56. **Veneri D, Tecchio C, De Matteis G, Paviati E, Benati M, Franchini M, Pizzolo G.** Long-term persistence of molecular response after discontinuation of interferon-alpha in two patients with chronic myeloid leukaemia. *Blood Transfus.* 2012;10(2), pp. 233-234.

57. **Molldrem JJ, Lee PP, Wang C, Felio K, Kantarjian HM, Champlin RE, Davis MM.** Evidence that specific T lymphocytes may participate in the elimination of chronic myelogenous leukemia. *Nat Med.* 2000;6(9), pp. 1018-1023.

58. **Knechtel, A.** Mathematische Modellierung der Wachstumsdynamiken therapieresistenter Zellklone in Patienten mit chronischer myeloischer Leukämie (Diplomarbeit, HTWK Leipzig). 2011.

59. **Branford S, Rudzki Z, Walsh S, Parkinson I, Grigg A, Szer J, Taylor K, Herrmann R, Seymour JF, Arthur C, Joske D, Lynch K, Hughes T.** Detection of BCR-ABL mutations in patients with CML treated with imatinib is virtually always accompanied by clinical resistance, and mutations in the ATP phosphate-binding loop (P-loop) are associated with a poor prognosis. *Blood.* 2003;102(1), pp. 276-283.

60. **Kim PS, Lee PP, Levy D.** Modeling imatinib-treated chronic myelogenous leukemia: reducing the complexity of agent-based models. *Bull Math Biol.* 2008;70(3), pp. 728-744.

61. **Abbott LH, Michor F.** Mathematical models of targeted cancer therapy. *Br J Cancer.* 2006;95(9), pp. 1136-1141.

5. Eigene Publikationen (nur peer-reviewed)

Roeder I, Horn M, Glauche I, Hochhaus A, Mueller MC, Loeffler M. Dynamic modeling of imatinib-treated chronic myeloid leukemia: functional insights and clinical implications. *Nat Med*. 2006 Oct;12(10):1181-1184.

Glauche I, Horn M, Roeder I. Leukaemia stem cells: hit or miss? *Br J Cancer*. 2007 Feb 26;96(4):677-678.

Horn M, Loeffler M, Roeder I. Mathematical modeling of genesis and treatment of chronic myeloid leukemia. *Cells Tissues Organs*. 2008;188(1-2):236-247.

Roeder I, Herberg M, Horn M. An "age"-structured model of hematopoietic stem cell organization with application to chronic myeloid leukemia. *Bull Math Biol*. 2009 Apr;71(3): 602-626.

Glauche I, Horn K, Horn M, Thielecke L, Essers MA, Trumpp A, Roeder I. Therapy of chronic myeloid leukaemia can benefit from the activation of stem cells: simulation studies of different treatment combinations. *Br J Cancer*. 2012 May 22;106(11):1742-1752.

Horn M, Glauche I, Müller MC, Hehlmann R, Hochhaus A, Loeffler M, Roeder I. Model-based decision rules reduce the risk of molecular relapse after cessation of tyrosine kinase inhibitor therapy in chronic myeloid leukemia. *Blood*. 2013 Jan 10;121(2):378-384.

6. Konferenzbeiträge (Auswahl)

Vortrag. European Conference on Mathematical and Theoretical Biology; Dresden (07/2005)

Poster. 4th Leipzig Research Festival for Life Sciences; Leipzig (12/2005) (**Posterpreis**)

Vortrag. 51. Jahrestagung der Deutschen Gesellschaft für Medizinische Informatik, Biometrie und Epidemiologie (GMDS); Leipzig (09/2006)

Poster. International Conference: Embryonic and Somatic Stem Cells – Regenerative Systems for Cell and Tissue Repair; Dresden (09/2006) (**Posterpreis**)

Vortrag und Poster. Jahrestagung der Deutschen, Österreichischen und Schweizerischen Gesellschaften für Hämatologie und Onkologie; Leipzig (11/2006)

Poster. Society for Hematology and Stem Cells (ISEH), 36th Annual Scientific Meeting; Hamburg (09/2007)

Vortrag. 4th International Workshop on Concepts and Mathematical Models of Stem Cell Organization: Stem Cells and Leukaemia – Concepts, Models, Simulations; London (04/2008)

Poster. 9th Leipzig Research Festival for Life Sciences; Leipzig (12/2010) (**Posterpreis**)

Poster. 12th International Conference on Systems Biology (ICSB); Mannheim (08/2011)

Vortrag. Jahrestagung der Deutschen, Österreichischen und Schweizerischen Gesellschaften für Hämatologie und Onkologie; Basel (10/2011)

Poster. Conference on Systems Biology of Mammalian Cells (SBMC); Leipzig (07/2012)

7. Erklärung

Hiermit erkläre ich, dass ich die vorliegende Arbeit selbstständig und ohne unzulässige Hilfe oder Benutzung anderer als der angegebenen Hilfsmittel angefertigt habe. Ich versichere, dass Dritte von mir weder unmittelbar noch mittelbar geldwerte Leistungen für Arbeiten erhalten haben, die im Zusammenhang mit dem Inhalt der vorgelegten Dissertation stehen, und dass die vorgelegte Arbeit weder im Inland noch im Ausland in gleicher oder ähnlicher Form einer anderen Prüfungsbehörde zum Zweck einer Promotion oder eines anderen Prüfungsverfahrens vorgelegt wurde. Alles aus anderen Quellen und von anderen Personen übernommene Material, das in der Arbeit verwendet wurde oder auf das direkt Bezug genommen wird, wurde als solches kenntlich gemacht. Insbesondere wurden alle Personen genannt, die direkt an der Entstehung der vorliegenden Arbeit beteiligt waren.

17.01.2014

Datum Unterschrift

8. Curriculum vitae

PERSÖNLICHE DATEN

Name	Matthias Horn
Anschrift	Saalecker Str. 13 04229 Leipzig
Geburtstag	5. März 1980
Geburtsort	Leipzig
Staatsangehörigkeit	deutsch
Familienstand	verheiratet, zwei Kinder

SCHULBILDUNG

09/1986 – 07/1992	Polytechnische Oberschule „Palmiro Togliatti“ Leipzig
09/1992 – 07/1998	Gymnasium „Robert-Koch-Schule“ Leipzig Abschluss: Allgemeine Hochschulreife

STUDIUM UND BERUF

10/1999 – 08/2000	Zivildienst
10/1998 – 06/2006	Studium der Medizininformatik an der Universität Leipzig
01/2005 – 06/2006	Diplomarbeit “Mathematical modeling of genesis and treatment of chronic myeloid leukemia”, Institut für Medizinische Informatik, Statistik und Epidemiologie (IMISE), Universität Leipzig Abschluss: Diplominformatiker (Dipl.-Inf.)
07/2006 – 05/2007	wissenschaftlicher Mitarbeiter am IMISE, Universität Leipzig
06/2007 – 12/2007	wissenschaftlicher Mitarbeiter am Interdisziplinären Zentrum für Bioinformatik (IZBI), Universität Leipzig
01/2008 – 08/2012	wissenschaftlicher Mitarbeiter am IMISE, Universität Leipzig
09/2012 – 12/2012	wissenschaftlicher Mitarbeiter am Leipziger Forschungszentrum für Zivilisationserkrankungen (LIFE), Universität Leipzig
seit 01/2013	wissenschaftlicher Mitarbeiter am IMISE, Universität Leipzig